THE INFLUENCE OF MOBILE MACROALGAE ON THE EROSION OF COHESIVE SEDIMENTS

by

Alexander L. Levy

B.Sc.H, Acadia University, 1998

Thesis

submitted in partial fulfillment of the

requirements for the Degree of

Master of Science (Biology)

Acadia University

Fall, 2000

TABLE OF CONTENTS

LIST OF TABLES

LIST OF FIGURES

LIST OF PLATES

LIST OF APPENDICES

ABSTRACT

The influence of mobile fragments of macroalgae of the species *Chondrus crispus* and *Furcellaria lumbricalis* on the erosion of prepared artificial cohesive beds was investigated in a Mini Flume. The purpose of the study was to describe how mobile fragments of macroalgae were transported at varying current velocities, and to determine whether their transport had the potential to significantly alter the erosion of cohesive beds. Algal fronds were divided into three sizes and abundances and each trial was replicated three times to determine intrinsic variability and to allow for statistical analysis. There was a high degree of variability in the suspended sediment concentrations and erosion rates within treatments. This was attributed to: (1) variation of the average settling rates of algae used in the trials; (2) variation of algal velocities with respect to current velocity; (3) variability of the morphologies and structural rigidities of the algae used; (4) variation in percent contact of the algae with the bed; and (5) interactions between algal fronds. Results showed that mobile algal fragments significantly increased erosion rates and suspended sediment concentrations over those of the control experiments, in which there was no apparent fluid induced erosion of the bed, and that erosion rates and suspended sediment concentrations varied directly with respect to algal size and abundance. Mode of algal transport varied with current velocity and species; however, a general trend was observed: motion began by sliding and rolling, followed by a mixture of suspension and sliding and then by continuous suspension of the macroalgae. The study concluded that mobile macroalgae moving as bedload have the potential to significantly increase erosion rates and suspended sediment concentrations of cohesive sediments within the lagoon of Venice, Italy.

LIST OF ABBREVIATIONS AND SYMBOLS

(i) SSC = Mass Suspended Sediment Concentration (mg L^{-1})

(ii) OBS = Optical Backscatter Sensor

(iii) Ua = Algal Velocity (m s^{-1})

(iv) Uy = Current Velocity (m s^{-1})

(v) U_* = Friction Velocity (m s^{-1})

(vi) [Suspended Sediment] = Suspended Sediment Concentration (mg L^{-1})

ACKNOWLEDGEMENTS

The study was carried out under the supervision of Dr. Carl Amos (Senior Lecturer at the Southampton Oceanography Centre, U.K.) and Dr. Graham Daborn (Professor of Biology at Acadia University and Director or the Acadia Center of Estuarine Research). Dr. Daborn devoted a great deal of time discussing various issues and proofreading the text, and for that I am grateful. I would like to thank Dr. Amos for providing me with the opportunity to go to Venice, Italy and be involved in such a wonderful research program. Furthermore, thank you Dr. Amos and Richard Pickrill (Geological Survey of Canada – Atlantic) for supplying equipment, time and financial support to ensure the success of the project.

Patrick Farell and Valerie Partridge, of the Acadia Statistical-Consulting Center, were extremely helpful with the experimental design and the statistical analysis of the data. I would also like to thank Mogens Flindt for providing useful background information and field observations of macroalgae within the lagoon of Venice.

In addition, I would like to thank Lisa Langille for her support and proofreading of the text and Iain Hollis for helping me search for and collect specimens.

INTRODUCTION TO STUDY

1.0 INTRODUCTION AND PURPOSE

Muddy sediments show an increased resistance to erosion over that which would be expected from the analysis of size and weight of the constituent sediment particles alone. This added erosion resistance is the result of interparticle surface attractions (Paterson & Underwood, 1990; Boggs, 1995) induced by flocculation in sea water and by the organic binding of sediments by marine phytobenthos (Neumann *et al.*, 1970; Holland *et al.*, 1974; Grant *et al.*, 1986; Vos *et al.*, 1988). Thus, muddy sediments are generally referred to as cohesive sediments.

It was long believed that the erosion of cohesive sediments resulted from the release of particles into suspension when the shear stress (τ_o) exceeded some threshold stress (τ_c). However, later studies have shown this explanation to be an oversimplification of the process (Mehta & Partheniades, 1982). Mehta and Partheniades (1982) revealed that two predominant forms of erosion exist within laboratory experiments; they were entitled Type I and Type II erosion. Type I erosion exponentially decays to zero with time and involves the release of flocs into suspension under low Reynolds numbers. Type II erosion is continuous over time and involves the release of rip-up clasts, which form mobile aggregates that move as surface creep and in saltation (Amos *et al.*, 1997; Amos *et al.*, 1998a). In addition, Amos *et al.* (1998a) showed that there was a bed load component to the transport of sediment over cohesive beds. It is believed that the incorporation of shell fragments as well as organic and inorganic detritus increases the erosion rates of cohesive sediments over those of the fluid induced erosion (Amos *et al.*, 1998a; Amos *et al.*, in press).

It is known that extremely high growths of macroalgae, triggered by eutrophication, and their drift, have had serious environmental impacts in marine environments (Sfriso *et al.*, 1989; McComb and Davis, 1993; Bach *et al.*, 1993; Runca *et al.*, 1993; Morand and Briand, 1996). Morand and Briand (1996) suggest that examples of excessive growth of macroalgae (particularly the chlorophytes *Ulva* and *Enteromorpha* and the rhodophyte *Gracilaria*) are becoming more widespread as a result of increasing eutrophication of coastal waters, and now occur in at least 25 countries around the world. Lagoons, bays and shallow estuaries located near agricultural, industrial and urban areas appear to be most affected by these increases in macroalgal growth (Morand and Briand, 1996). Negative impacts of these excessive growths include problems such as anoxic conditions (Sfriso, 1987; Sfriso *et al.*, 1987; Tagliapietra *et al.*, 1988; McComb and Davis, 1993; Bach *et al.*, 1993; Runca *et al.*, 1993; Sfriso *et al.*, 1993; Sfriso and Pavoni, 1994; Den Hartog *et al.*, 1996; Flindt *et al.*, 1997ab), decline in the aesthetic appearance of coasts (McComb and Davis, 1993; Bach *et al.*, 1993; Morand and Briand, 1996), and the elimination of sea grasses (Sfriso, 1987; Sfriso *et al.*, 1989; Bach *et al.*, 1993; McComb and Davis, 1993; Runca *et al.*, 1993; Den Hartog ,1996; Sfriso and Marcomini, 1996; Tagliapietra *et al.*, 1998).

Despite the mention of altered sediment characteristics (Morand and Briand, 1996) and decreased resuspension of sediments correlated with high *Ulva* densities (Sfriso and Marcomini, 1997), no research has focused on the direct sediment impacts of algal drift at the sediment-water interface. Flindt *et al.* (1997b) determined that advective transport of macroalgae, at varying heights in the water column, represented the major loss process for this material from the lagoon of Venice, Italy. Moreover, some species of

macroalgae have fairly high settling rates and are transported as bed load within the lagoon of Venice (e.g. *Chondrus crispus* and *Gracilaria* sp.) (Flindt M., personal communication, 1998). However, Flindt *et al.* (1997b) also mentioned that little is known about the quantitative aspects of advective transport of macroalgae within coastal ecosystems.

The purpose of my study was to describe how mobile fragments of the macroalgae *Chondrus crispus* and *Furcellaria lumbricalis* were transported at varying current velocities, and to determine whether their transport had the potential to significantly alter the erosion process of artificial cohesive beds in a Mini Flume. Furthermore, this study was designed to assess the effects (if any) of size and abundance of the two species on the erosion process.

1.1 BACKGROUND

a. *Outline*

This project was carried out under the supervision of Dr. Carl L. Amos and Dr. Graham Daborn and was part of the Geological Survey of Canada's (GSC) component for F-ECTS (Feed-backs of Estuarine Circulation and Transport of Sediments on Phytobenthos).

The main focus of F-ECTS is to examine feed back loops involving phytobenthos, hydrodynamics, nutrient cycling, and sediment transport in estuarine ecosystems (THETIS, 1997). F-ECTS considered the lagoon of Venice to be a pilot case study and it was designed to allow the parameterization of the main physical and biological processes of the ecosystem, which would provide a specific background for the comparative assessment to two different European estuarine ecosystems: Laguna della Ria Formosa

(Portugal) and Roskilde Fjord (Denmark) using the same techniques. Based on these parameterized biophysical interactions, linked models for the simulation of the feed-back between the physical processes and the phytobenthic habitat will be set up.

The GSC worked as a sub-contractor to the University of Wales Cardiff, UK in order to achieve the goals defined in the European Community's proposal F-ECTS (Amos C.L., personal communication, 1998). The work presented in this thesis is a constituent of the GSC's component to examine the impact of ballistic momentum flux (i.e. erosion and deformation of a bed caused by the energy transfer from saltating material to the bed via its impact) of macroalgae on the lagoon of Venice sediments.

b. *Lagoon of Venice*

The lagoon of Venice (Plate 1) is a shallow coastal embayment located in the northern end of the Adriatic Sea in northeastern Italy (45°30'N, 12°21'E). Its origin dates back to approximately 6000 years ago when a rising sea level flooded the upper Adriatic Wurmian Paleoplain (Gatto & Carbognin, 1981). The present lagoon is 50 km long and between 10 to 15 km in width, covering a total area of 550 km^2 (THETIS, 1997; Day *et al.*, 1998). 75 % of the lagoon consists of relatively shallow water (less than 1 m deep) with an average depth of 1.1 m and a tidal range of 0.6 to 1.1 m (THETIS, 1997; Day *et al.*, 1998). Shallow areas are separated by tidal channels that can reach depths up to 20 m (THETIS, 1997). It is classified as a restricted lagoon, as the three seaward entrances (Lido, Malamocco, and Chioggia) are relatively narrow and open at all times (Calvo *et al.*, 1991).

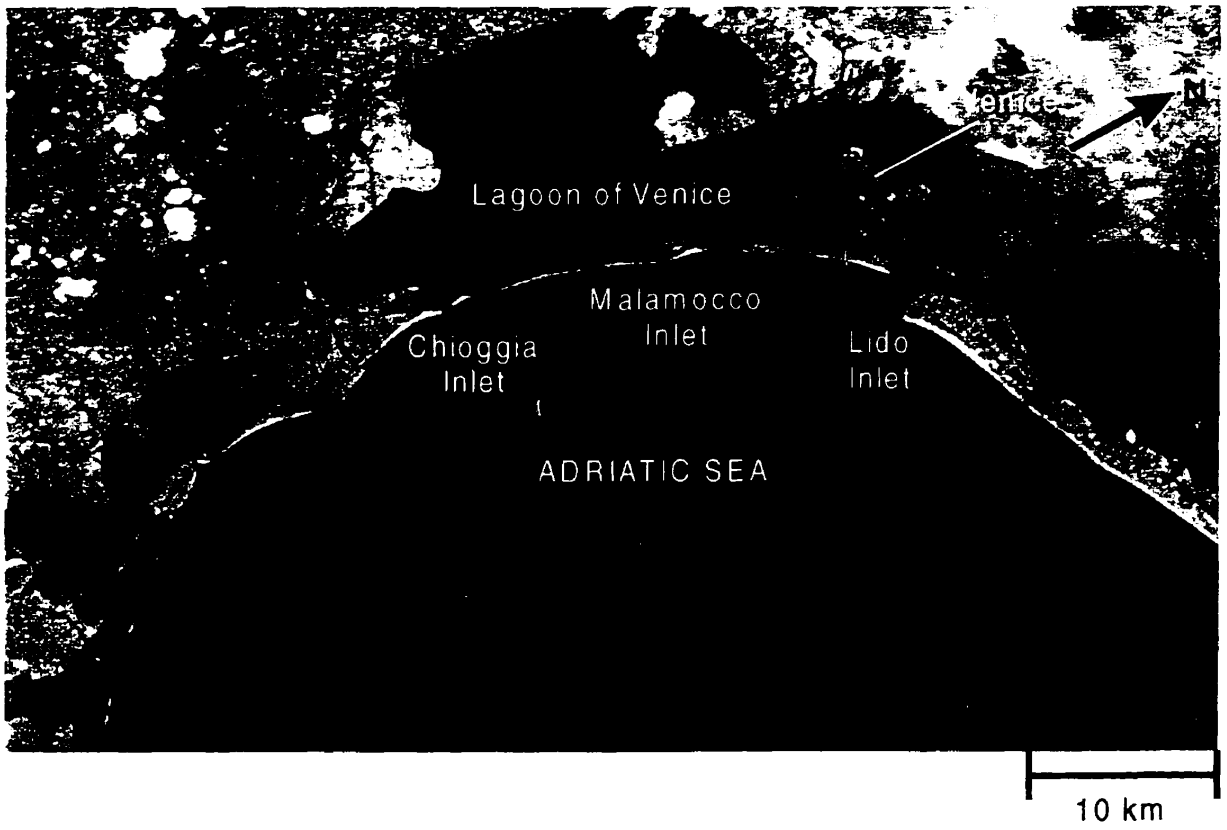

Plate 1. Aerial view of Venice and its lagoon.

The tidal currents flowing through these entrances can reach velocities up to 2.69 m/s at 1 m from the bottom sediments (Calvo *et al.*, 1991). Freshwater and nutrients are predominately supplied to the lagoon by its 1830 km^2 drainage basin (THETIS, 1997). This drainage basin is heavily influenced by human activity, which in turn, affects the morphology, productivity and relative "health" of the lagoon. It is estimated that 7-9 million kg of nitrogen and 1 million kg of phosphorous enter the lagoon per year from agricultural and urban effluents along with civil and industrial point sources (Bach *et al.*, 1993; Flindt *et al.*, 1997a; THETIS, 1997). In the lagoon these nutrients serve as fertilizers for macroalgal growth, allowing blooms to occur when favorable environmental conditions correspond with the high nutrient concentrations (Bach *et al.*, 1993). Five major rivers and 20 minor tributaries discharge fresh water to the lagoon (Flindt *et al.*, 1997a). Salinity varies both spatially and temporally and can range from 5 to 40 $^{o}/_{oo}$ (THETIS, 1997). Surface sediments consist primarily of fine-grained sediments, with clay and silt size particles dominating the substrate (Calvo *et al.*, 1991).

c. *Macroalgae within the Lagoon of Venice*

The intense eutrophication of the lagoon of Venice (as mentioned above) has caused the increase in biomass of macroalgae, especially green opportunistic species, such as *Ulva rigida*. As a result, macroalgae are the predominant primary producers found within the lagoon (Runca *et al.*, 1993; Sfriso *et al.*, 1994). This dominance has caused serious environmental problems for the ecosystem and has consequently reduced the quality of the ecosystem through anoxia, reduced light penetration to the bed, competition, reduced species diversity, and aesthetic degradation.

Populations of macroalgae within the lagoon are subject to change. Anthropogenic alterations (e.g. pollution, changes in nutrient concentrations, hydrodynamic alterations, etc.) and adverse meteorological conditions (e.g. temperature, winds, cloudiness, etc.) are thought to impact the distribution, diversity and abundance of the lagoon's macroalgae. Sfriso's (1987) comparison with previous studies (e.g Schiffner and Vatova (1938) and Pignatti (1962)) showed an increase in the biomass of Chlorophyceae from 25 to 34 % accompanied with a reduction in Rhodophyceae from 62 – 51 %. Furthermore, environmental changes occurred within the central part of the lagoon by which *Enteromorpha* sp., *Ulva rigida*, *Punctuaria latifolia*, *Cladophora* sp., and *Gracilaria verrucosa* had replaced the sea grasses *Cymodocea nodosa*, and *Zostera noltii*. In addition to changes in macroalgae abundance, Sfriso (1987) observed a vertical rising of deeper vegetational zones, consequently resulting in the present species growing in shallower water than they had grown in before.

Before the mid to late 1980s *Gracilaria* was the second largest population of macroalga in the lagoon of Venice in terms of biomass production (mean standing crop of 36 000 t and an annual production rate of 132 000 t (wet weight)) (Sfriso *et al.*, 1994). During the 1980s, when *Ulva rigida* dominated the macroalgae biomass, growth of *Gracilaria* sp. was restricted; it predominately grew in areas containing low *Ulva* densities (e.g. canal edges and areas with high currents and high suspended particulate matter). In the lagoon of Venice, *Gracilaria* is represented by at least five species, with the predominant species being *Gracilaria verrucosa* and *Gracilaria longa* (together they represent > 95 % of the *Gracilaria* biomass of the lagoon) (Sfriso *et al.*, 1993). Calculations of biomass and net production over the entire lagoon for 1993 showed that

Gracilaria had a mean standing crop of approximately 16 000 t and a net annual production rate of approximately 70 000 t (wet weight). *Gracilaria* is a seasonal species with peak biomass being achieved between June and September, depending upon the location within the lagoon. Decline of this species was attributed to the increased anthropogenic harvesting for agar and the increased competition with *U. rigida.* (Sfriso *et al.*, 1994).

Since the 1980s *U. rigida* has been the predominant macroalga within the lagoon of Venice. Production of this species was high between early spring and late autumn, and biomass peaks reached up to 20 kg m^{-2} (Sfriso *et al.*, 1987). Biomass peaks were generally followed by an anoxic crisis, due to the respiratory demands for oxygen exceeding that produced by photosynthesis, which in turn led to the accumulation of hydrogen sulphide (Sfriso and Pavoni, 1994). More recently, Sfriso and Marcomini (1996) mentioned that *Ulva* has progressively decreased in abundance and distribution, since 1990, over the entire lagoon. This decline was attributed to unfavorable weather conditions, increased resuspension of particulate matter, increased grazing pressure, harvesting by the Venice Municipality, and the disruptive actions of *Tapes* fishing (Sfriso and Marcomini, 1996). Furthermore, Sfriso and Marcomini (1996) believe that other seasonal macroalgae, such as *Gracilaria* and *Enteromorpha*, and submersed macrophytes are progressively spreading to the areas previously covered by the dense populations of *Ulva rigida.*

d) General Flume Application and Design

Flumes have been used extensively in sedimentary geology and civil engineering over the last century to examine modes and rates of sediment transport (Nowell and

Jumars, 1987). Nowell and Jumars (1987) state that there is no universally applicable flume and that flume design and operation must be developed with the specific objective of the study in mind. Amos *et al.* (1992) mentioned that annular flumes have many attributes that make them appropriate for studying bed erosion. Their constant channel geometry and infinite flow length allow them to fully develop a benthic boundary layer above the sediment surface (Amos *et al.*, 1992). Furthermore, annular flumes eliminate the problems associated with entrance and exit conditions as mentioned by Nowell and Jumars (1987) and Widdows *et al.* (1998). In addition, substrate problems associated with consolidation times and bed stratification induced by settling, as well as edge effects and artifacts created by transporting and placing a sample in the flume were reduced/eliminated by using an artificial cohesive bed (Amos *et al.*, in press).

1.2 PREVIOUS WORK

Sfriso and Marcomini's (1997) study on the macrophyte production within the lagoon of Venice, revealed that large densities of *Ulva* significantly influence nutrient concentrations, oxygenation of the sediment and the sediment resuspension process. Moreover, their study showed that high densities of *Ulva* inhibit sediment resuspension due to the high sediment coverage by the *Ulva* fronds.

During a summer field campaign Flindt *et al.* (1997b) studied the growth and losses by grazing, sporulation and advective transport of benthic macroalgae in the lagoon of Venice. From their study it was determined that the transport of *Ulva* sp. and *Chaetomorpha* sp. were linearly related with current velocity and that different species of macroalgae were transported at different depths within the water column. Furthermore,

Flindt *et al.* (1997b) concluded that the main loss process, for these aquatic species, was due to the advective transport of the material from the lagoon.

Amos *et al.* (1998a) mention that large particles that contact a bed have the potential to contribute to the erosion threshold and the erosion rates of that bed. Furthermore, the study by Amos *et al.* (1998a) showed that the shape of an aggregate was important in the erosion process. An additional study performed by Amos *et al.* (in press) showed that saltating shells increased the erosion rate over the fluid induced erosion by a factor of twenty. Furthermore, their study revealed that the shell erosion rate was affected by the mode of transport of the shells and the erosion rate increased with shell diameter and shell number. Consequently they deduced that the littorinid shells scattered over the mudflat of Annapolis Basin had the potential to significantly increase the erosion of the bed (Amos *et al.*, in press).

This study was based on the above conclusions of Flindt *et al.* (1997b), Amos *et al.* (1998a) and Amos *et al.*, (in press), and was designed to assess the impacts (if any) of macroalgae on the erosion of cohesive beds and to describe how the macroalgal fragments were transported with respect to current velocity.

METHODOLOGY

2.0 GENERAL METHODOLOGY

Two species of macroalgae (*Chondrus crispus* and *Furcellaria lumbricalis*) were collected and used for experimentation in a laboratory settling tube and Mini Flume. Experiments were conducted at the Bedford Institute of Oceanography, Nova Scotia, to determine the impact of abundance and size of the two algal species on the erosion of artificial cohesive beds. Each species of macroalga was divided into three abundance (e.g. 2, 4 and 6 pieces) and three size categories. Settling rates for all of the algal pieces were measured and recorded prior to erosion experiments. Erosion experiments were performed inside a Mini Flume, which was capable of creating a range of current velocities and detecting changes in mass suspended sediment concentration (SSC) of the water column at different current velocities. Erosion experiments were performed in triplicate to help determine the intrinsic variability of the erosion process and to allow for statistical analysis of the effects of the macroalgae on the erosion of the muddy sediments.

2.1 ALGAE PREPARATION

a. *Choice of Macroalgae*

Originally the experiments were designed to study the impacts of macroalgae (e.g. *Chondrus crispus* and *Gracilaria* sp.) collected from the lagoon of Venice, Italy. However, local specimens had to be used due to unforeseen delays with the transport of macroalgae from Venice to Nova Scotia and the limited availability of the Mini Flume.

Chondrus crispus (Plate 2), commonly known as Irish Moss, and *Furcellaria lumbricalis* (Plate 3) were chosen because they could be easily classified into different size categories, had fairly high settling rates, were easily collected locally in Prince Edward Island (P.E.I.) and resembled the morphology of species that were readily transported in the lagoon of Venice (Flindt, M., personal communication, 1998). Furthermore, based on preliminary settling experiments in Venice, Italy and a personal communication from Mogens Flindt, these species were chosen as they were thought to be transported near the bottom of the water column. These observations suggested that *C. crispus* and *F. lumbricalis* may have more impact on the erosion of benthic sediments than macroalgae and/or macrophytes that are transported within the upper layers of the water column (e.g. *Zostera* sp., *Ulva* sp.) (Flindt *et al.*, 1997b).

Both *C. crispus* and *F. lumbricalis* are red algae and belong to the Phylum Rhodophyta. Bird and McLachlan (1992) describe attached *C. crispus* plants as bushy, loose to dense clumps of fronds arising from a crustose holdfast. They vary in form depending upon the environment in which they grow (e.g level of turbulence) and can reach heights up to 32 cm tall. The basic anatomy consists of repeated, widely divergent, dichotomous branching in one plane above a tapered, stipe-like lower portion, which is compressed to flattened throughout except at the terete (i.e. cylindrical) base. This species is known to occur in the low intertidal zone and mid-tidal pools as well as subtidally up to 16-18 m in depth (Bird and McLachlan, 1992).

Attached plants of *F. lumbricalis* are described as being bushy, consisting of slender, regularly dichotomously branched fronds arising from a fibrous holdfast of tangled branched stolons. The plants are generally 10-15 cm tall and occur subtidally,

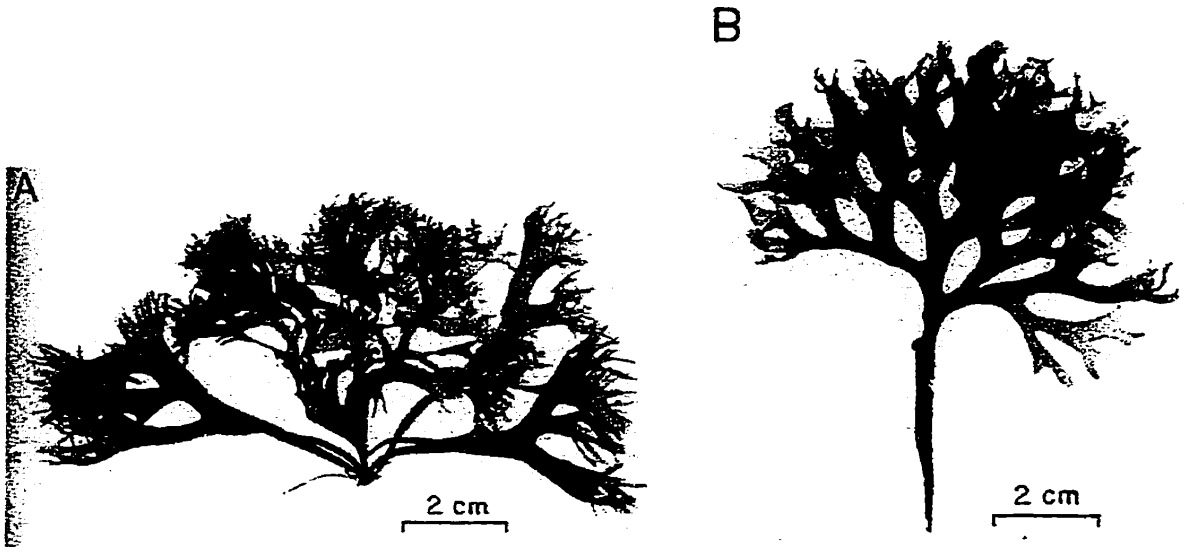

Plate 2. Photographs of a *Chondrus crispus* plant with moderately broad fronds (A) and an individual frond showing typical compact, regularly dichotomous branches above the stipe. (Bird and McLachlan, 1992)

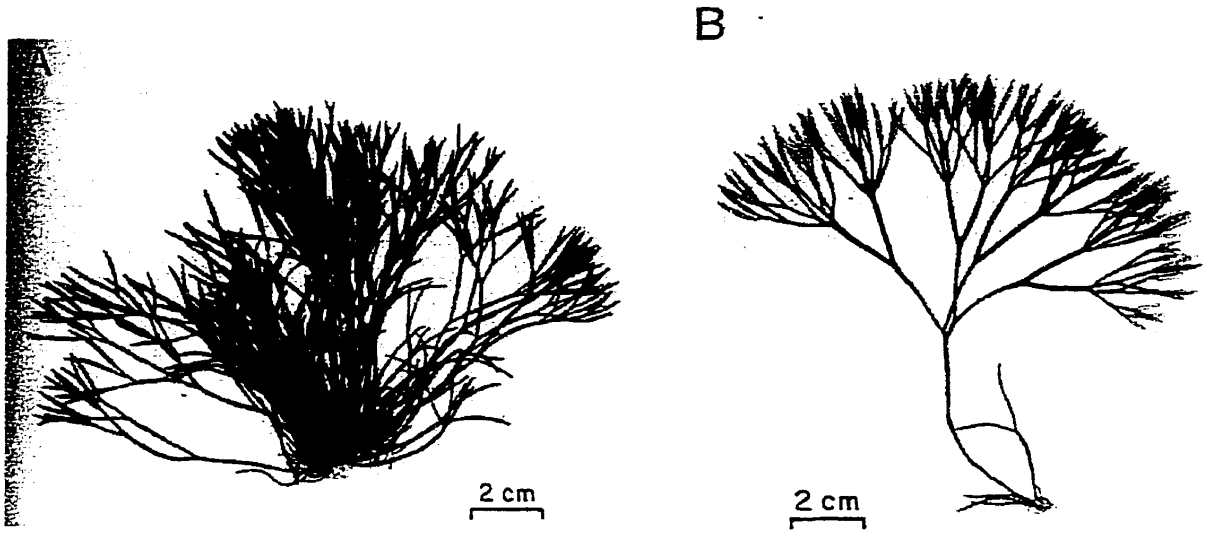

Plate 3. Photographs of a *Furcellaria lumbricalis* plant (A) and an individual frond (B). (Bird and McLachlan, 1992)

primarily in depths ranging between 2 –12 m deep in the Maritimes. This species has been known to occur in great numbers on local beaches as driftweed and is harvested for carrageenan (Bird and McLachlan, 1992). *F. lumbricalis* was chosen for these experiments as it superficially resembles the morphology of *Gracilaria tikvahiae*, whose distribution is known to some degree within the lagoon of Venice (Sfriso *et al.*,1994). It grows in similar water depths to *G. tikvahiae*, and both *F. lumbricalis* and *G. tikvahiae* are known to occur as drift weed/free living populations (Bird and McLachlan, 1992). Bird and McLachlan (1992) describe the alga, which was formerly known as *Gracilaria foliifera* and *Gracilaria verrucosa*, as being between 30-40 cm tall, freely and irregularly branched plants with fronds that range from terete to flattened which may be highly variable on a single thallus. They can occur as attached or free living populations. Attached individuals generally grow in the subtidal zone in water depths of approximately 2 m and are held to the substrate by a discoid holdfast. Free living populations may occur at greater depths; they tend to form large bushy clumps and are thought to originate from a shallower habitat.

b. *Collection and Preparation of the Macroalgae*

Both species of macroalgae used for the settling and erosion experiments were collected from the southern shore of P.E.I, Canada. Sediment and organisms living on the algae were cleaned from the material by gently rubbing the thalli and rinsing them with water. This was done to ensure that their settling rates and impact on erosion were solely attributable to the macroalgae. After cleaning, the macroalgae were preserved in a 5 % formalin and seawater solution.

Specimens of both species of algae were divided into three size categories (small, medium, and large) according to mass, and were chosen so that they were morphologically smaller representative pieces of the whole. For example, the size categories were achieved by removing algal branches, while maintaining similar morphologies to the original piece. Furthermore, care was taken to ensure that these size categories were small enough so that they would not readily interact with the walls of the Mini Flume (i.e. they were smaller than the flume width). Small, medium and large pieces of *C. crispus* had average ($\pm$ 1 sd) wet weights of 0.46 ± 0.01, 1.26 ± 0.03, 1.86 ± 0.04 grams respectively; *F. lumbricalis* pieces had average ($\pm$ 1 sd) wet weights of 0.25 ± 0.01, 0.76 ± 0.02, and 2.04 ± 0.03 grams respectively. Care was also taken to ensure that pieces of the macroalgae did not dry out during the weighing procedure. For example, after the water was removed from the surface of the macroalgae, by blotting with paper towel, and the weights were determined, the pieces were submerged in a seawater container to prevent them from drying.

2.2 SETTLING EXPERIMENTS

a. *Settling Procedure and Description of the Settling Tube*

The range of algal masses that were used in the Nova Scotian settling experiments was smaller than that of the mass range used in Venice. It was believed that some of the larger specimens that were settled in Venice were too large for the Mini Flume and would make too much contact with the walls. Therefore, a smaller mass range (as mentioned above) was used for the settling and erosion experiments.

All Nova Scotian settling experiments were performed in a 168 cm long acrylic settling tube (Plate 4) with a diameter of 11.90 cm. A measuring tape was attached to one

Plate 4. The settling tube that was used to determine algal still water settling velocities.

side of the tube so that accurate measurements of settling rates could be determined. Seawater with a salinity of ~ 32 $^{o}/_{oo}$ was warmed to the room temperature (20.5 to 21.5 ^{o}C) and then filtered through a Tyler Equivalent 150 mesh sieve (opening = 106 μm) to remove suspended particulate matter. The filtered seawater was then poured into the tube and filled to the 160 cm level. After filling the tube, air bubbles from the inner wall were removed by scraping the surface with plastic hosing. Removal of the air bubbles ensured that the settling time of the algae would not be altered by trapping air beneath them as they settled.

After the settling tube preparation was complete, a piece of alga was carefully placed in the first few centimeters of the water column and gently moved to ensure that no air was trapped between branches. Following release, each piece was allowed to settle for 20 cm before the timing began. This allowed the aggregate to achieve its characteristic settling orientation before timing began. The settling alga was timed using a Timex® stopwatch for a distance of 100 cm. Still water settling rates were determined by dividing the distance settled by the time required to settle that distance. A representative portion of all settling experiments was video taped using a SONY® Handycam video camera. The above procedure was carried out for every piece of alga used in the erosion experiments. Settling experiments in Venice were carried out in the same procedure as outlined above using a similar settling tube with slightly larger dimensions (e.g. diameter = 12 cm, length = 2 m).

2.3 EROSION EXPERIMENTS

a. *Description of the Mini Flume*

The Mini Flume (Plate 5 and Fig. 1) is a smaller version of the Lab Carousel (Amos *et al.*, 1998b) and was designed to examine the erosion and settling rates of marine sediments under controlled conditions. It is an annular flume with a diameter of 30.5 cm and an annulus width of 4.5 cm. The flume is constructed of transparent acrylic to allow for clear visual observations of erosion and settling. Flow within the annulus is induced by a rotating circular lid containing four equidistantly placed square paddles. Lid rotation is driven by an OEM® series stepper motor (model # OEM 83-135-MO), which is powered by a Xantrex 1000 watt power supply. The flume contains three D & A Instruments® optical backscatter sensors (OBS), which are installed at heights of 4 cm, 10 cm and 20 cm above the bed. Data from the sensors were logged at 1 Hz on a Campbell Scientific® CR 10 data logger and stored on diskette. The flume also contains three sampling ports (located at the same heights as the OBS) which are used for collecting water samples and for filling/emptying the flume.

The flow field, the height of the boundary layer, turbulent intensity, and the wall effects of the Mini Flume were examined using a Laser Doppler Velocimeter. These results showed that a benthic boundary layer existed approximately 1 cm above the bed regardless of the water speed. Velocity increased rapidly, upward from the bed, within the boundary layer and remained constant above this level (Fung, 1997).

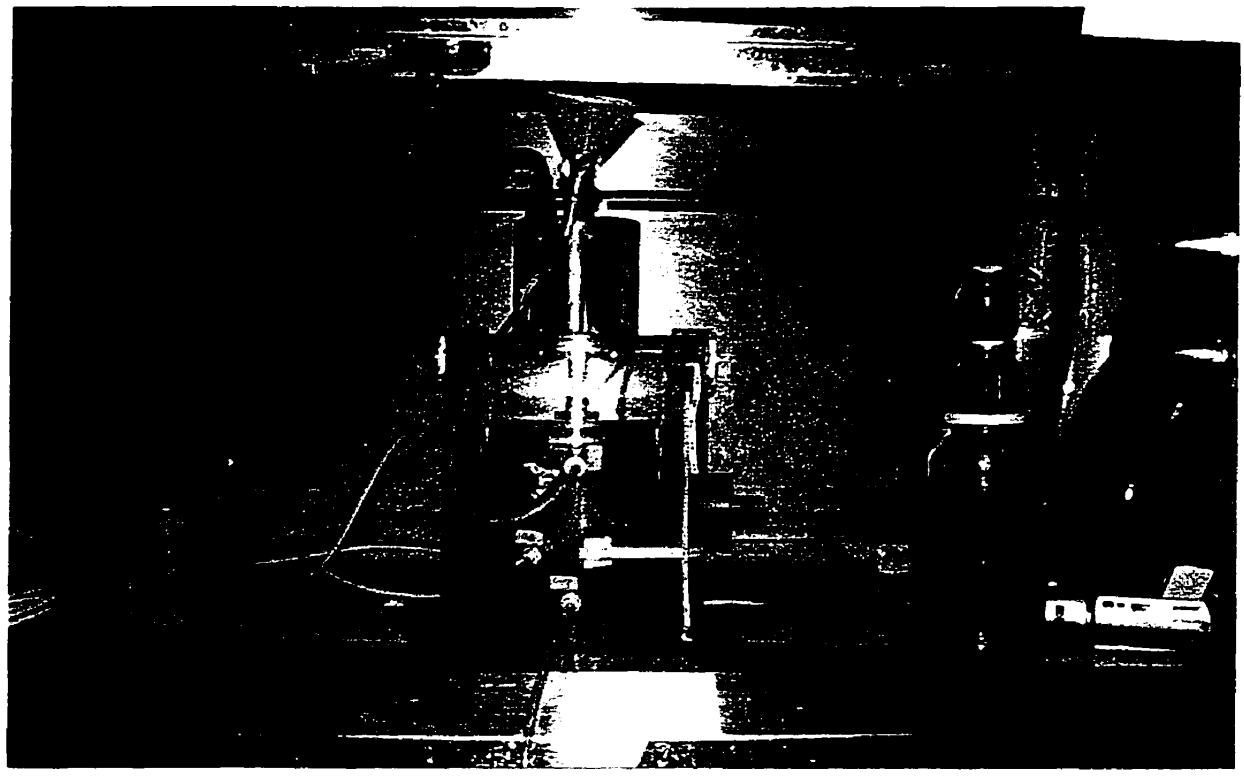

Plate 5. The Mini Flume that was used for all of the erosion experiments.

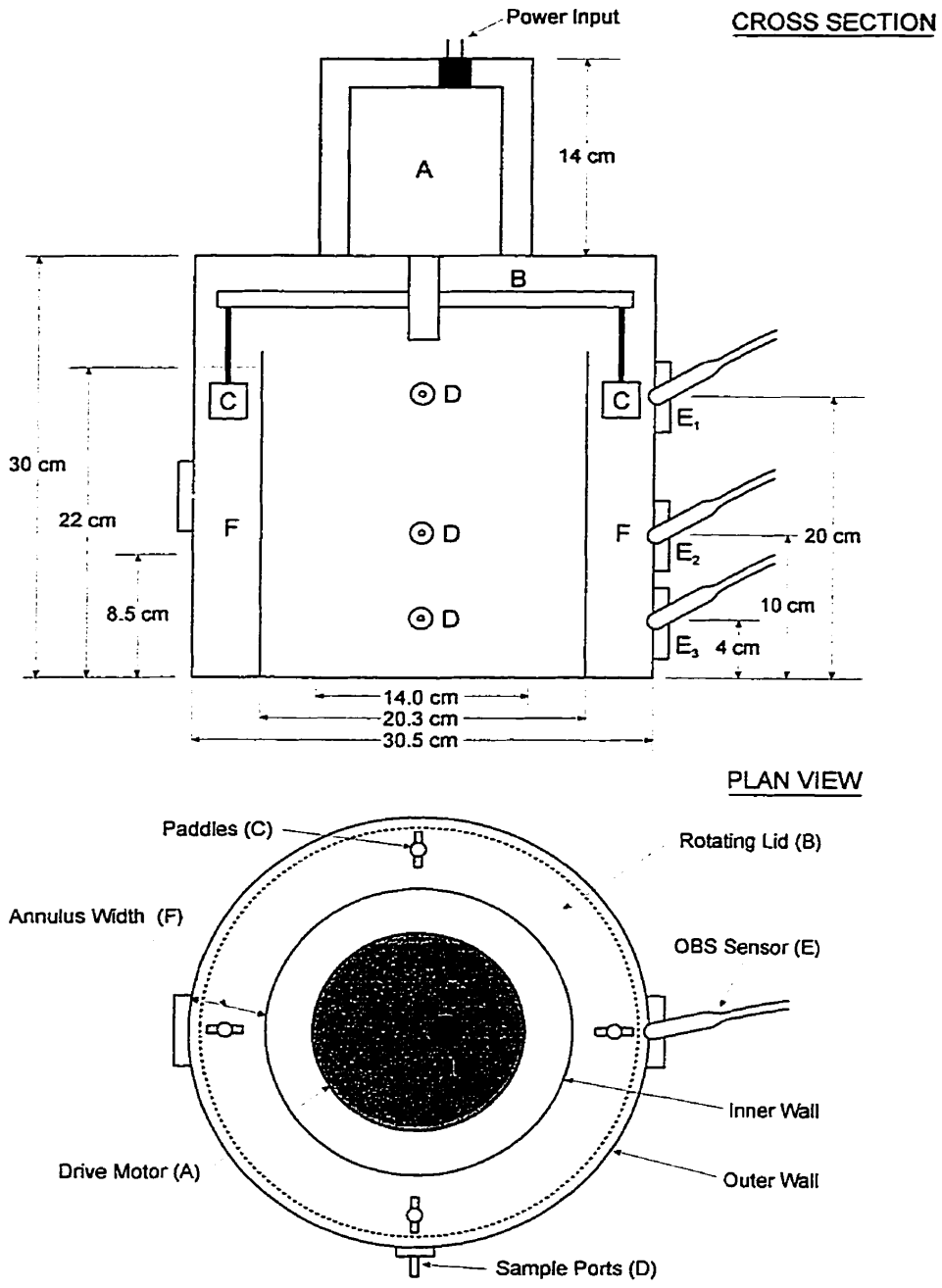

Figure 1. Technical diagram of the Mini Flume showing flume constituents (e.g. Drive motor (A), rotating lid (B), paddles (C), sample ports (D), OBS sensors (E_1 - E_3), and annulus (F)) and their dimensions. (Amos *et al.*, in press)

b. *Description of the Clay Beds and Bed Preparation*

The clay bed used in the erosion experiments was formed with Tucker's PHB non-grog® pottery clay. The clay is an industrial mixture of glacial clays from Kentucky, USA and is classified as a soft silty clay (after Terzaghi and Peck, 1967). It contains 4 % very fine sand, 56 % silt and 40 % clay and consists of quartz, kaolinite, and illite with no organic matter (Amos *et al.*, in press). The pottery clay had a mean water content of 20 % and a mean wet bulk density of 2470 kg/m^3. Preparation of the clay bed for the experiments was based on Amos *et al.* (in press). One third of a clay pug was rolled out, using a rolling pin (Plate 6 a,b,c), to produce a flat disc approximately 36 cm in diameter and 1.5 cm thick. This served as an erodible substrate for the experiments and also acted as a watertight seal for the base of the Mini Flume.

It is realized that this artificial bed is not representative of natural sediments occurring within the lagoon of Venice. However, this bed was chosen for experimentation as it was easily prepared and eliminated problems associated with settling natural sediments in laboratory flumes (Amos *et al.*, in press). It is thought that the erodibility of this bed is lower than that of the natural sediments from the lagoon of Venice; hence, the erosion results would be conservative. However, it was assumed that the overall process of erosion and the various modes of transport of the algae would be similar in the flume as in the lagoon of Venice.

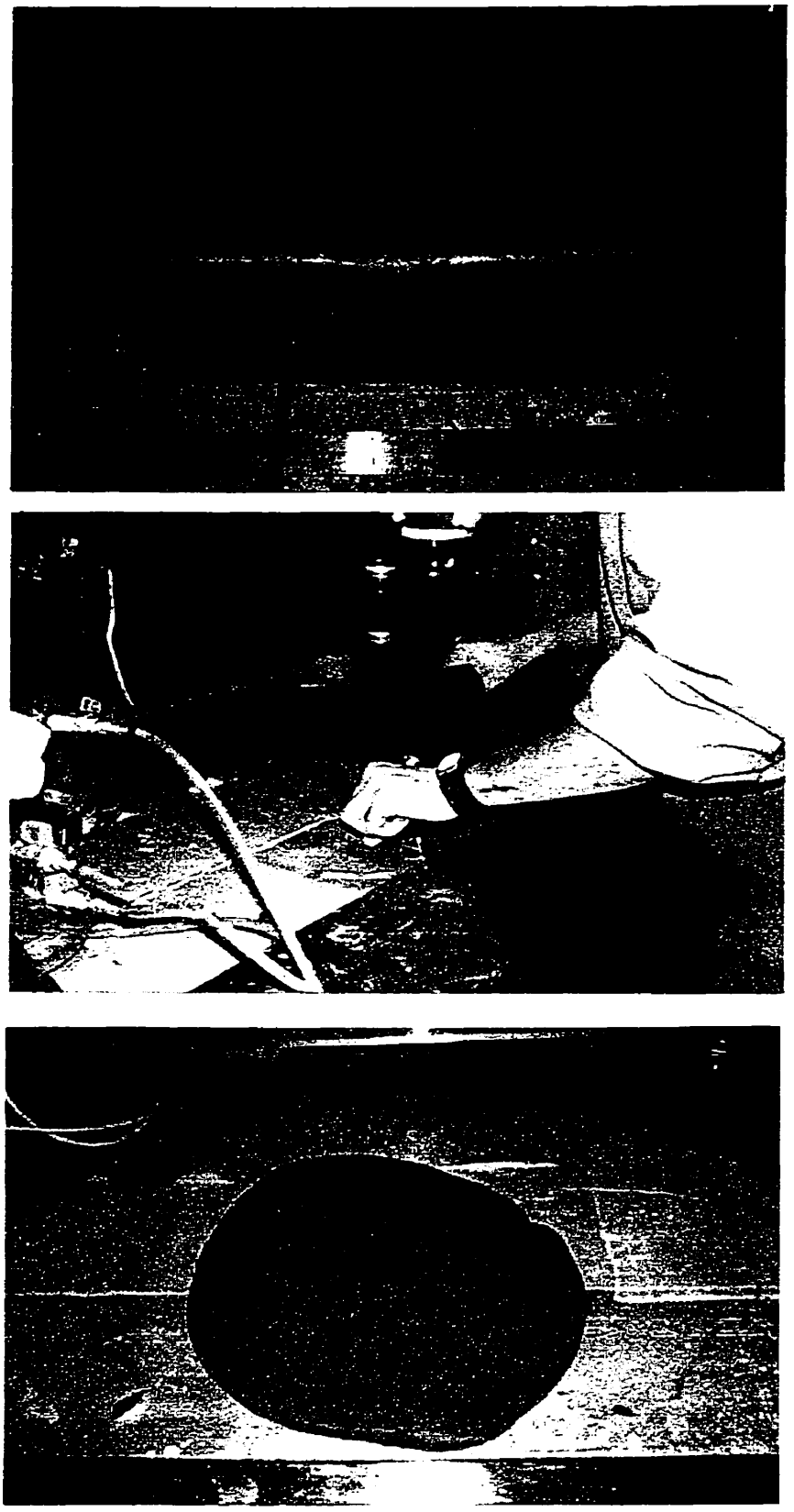

Plate 6 a,b,c. Procedure for preparing the clay bed.

c. *Motor Program and Sampling Protocol*

The OEM® series stepper motor was programmed to rotate the lid at seven different velocities (Table 1). Each velocity was maintained at a constant value for a period of 20 minutes before increasing to the next velocity increment. The azmithual current velocity (U_y) was related to lid rotation (ROT) by the equation:

(1) $U_y = 0.56$ (ROT) (Amos *et al.*, in press).

Time (min)	Step #	ROT (m/s)	U_y (m/s)
0	-	0	0
0-20	1	0.13	0.075
20-40	2	0.27	0.15
40-60	3	0.40	0.22
60-80	4	0.53	0.30
80-100	5	0.67	0.37
100-120	6	0.80	0.45
140-160	7	0.94	0.52
160	-	0	0

Table 1. Time (min), step number and the corresponding lid rotation speed (ROT) and azmithual current velocity (U_y).

The suspended sediment concentration at each step was determined by taking a 60 ml water sample from the middle sampling port ten minutes after each velocity increase. Water samples were then filtered through pre-weighed and dried, 25 mm Whatman GF/B® glass fiber filters to determine the mass concentration of sediment in suspension in mg L^{-1}; this was used to calibrate the OBS. OBS calibration was performed by regressing the measured mass concentrations of sediment (mg L^{-1}) against the OBS voltages (mV). OBS voltages for each experiment were then transformed to suspended sediment concentrations (mg L^{-1}) by substituting the OBS mV values into the corresponding regression equation calculated above. The overall OBS output data versus suspended sediment concentration was strong and the data from experiments overlapped;

therefore, a single calibration curve could have been used (Appendix A). However, separate calibrations were performed for the individual experiments to increase the accuracy of the conversion. Individual calibrations for erosion experiments had an average ($\pm$ 1sd) r-squared value of 0.940 $\pm$ 0.118 and an average ($\pm$ 1sd) p-value of 0.003 $\pm$ 0.010. However, the overall relationship for the control experiments was not as strong (Appendix B) and the calibrations for the individual erosion experiments had an average ($\pm$ 1sd) r-squared of 0.328 $\pm$ 0.078 and an average ($\pm$ 1sd) p-value of 0.146 $\pm$ 0.064.

d. *Erosion Experiments*

After the bed was rolled out into a uniform disc, the frame of the Mini Flume was pushed into the clay forming a donut-shaped pattern (annulus width = 4.5 cm) in the sediment (Plate 7). The flume was then carefully filled with filtered seawater, at room temperature, to a height of approximately 22 cm above the bed (volume = 7.9 L). The varying numbers and sizes of algal pieces were added (depending on the experiment and with the exception of control experiments) so that they were spaced equidistantly from one another. Finally, the lid was secured to the frame and the data logging began. Data were logged at still water conditions for approximately 15 minutes to allow the OBS sensors to stabilize at ambient suspended sediment concentrations before initiating the experiment. Ten minutes after logging at 0 velocity the first SSC sample was taken and filtered. After an additional 5 minutes the motor program was initiated and the SONY® Handycam video camera was started to record the experiment. Initial observations of the mode of transport of the algae and their erosional impact were noted; however, more detailed observations were made later by reviewing the videotapes of the experiments.

Plate 7. Flume "footprint" left in the clay bed after an experiment.

Erosion experiments were performed in triplicate for each of the three size categories and the three abundance categories for both species of macroalgae. In addition, six control experiments were performed (4 with water samples used to calibrate OBS), yielding a total of 42 erosion experiments. Experiment order was randomized to reduce any effects that might be attributed to increasing skill at preparing the clay bed. Furthermore, experiments were redone when difficulties arose (infrequent) during the flume operation (e.g. problems with OBS, power failure, algae getting caught on OBS, etc.).

2.4 DATA ANALYSIS

a. *Video Analysis*

Individual video experiments were analyzed using a Sony® SVO-1450 VHS VCR. Video tapes were analyzed to determine the duration that the algal pieces spent in motion for each velocity step, how the algal pieces interacted with one another and the bed, algal velocity, percent contact time with the bed, and the mode of transport.

Algal interactions were further quantified by recording the times that the algae spent as individual pieces or as aggregates during each of the seven velocity steps. Algal velocities were determined for the individual pieces and respective clumps for each velocity step of all of the trials. This velocity was calculated by dividing the distance the alga traveled (e.g. 5 times the circumference at the center of the paddles in most cases) by the time required for the number of revolutions measured. This procedure was averaged for three subsets within each velocity step (when possible). Furthermore, the difference between algal velocity (U_a) and current velocity (U_y) was calculated along with percent energy transfer (Amos *et al.*, in press). Percent energy transfer was estimated by dividing

the algal velocity by the current velocity and converting this number to a percent energy transmitted to the bed as shown in equation 2:

(2) % Energy Transfer = $100 - ((U_a/U_y)* 100)$.

Percent energy transfer was calculated under the assumption that the majority of the algal fragment/aggregate protruded out of the boundary layer and into the constant flow above the boundary layer, as it was in this layer that current velocity was measured. Furthermore, percent energy transfer was only used for relative comparisons for the purposes of this study.

Percent contact was calculated for both individual pieces and aggregates for each velocity step by dividing the distance that the algal pieces were in contact with the bed (D_c) by the total distance traveled (D_t) as shown in equation 3:

(3) % Contact = $(D_c/D_t) * 100$.

Distances over which the alga was in contact with the bed were accurately measured using the grid that was taped to one side of the Mini Flume and by watching the videos in slow motion. Each algal piece/aggregate was observed over the course of 50 flume revolutions (when possible) in order to get a representative percent contact subset for each velocity step.

Mode of transport was determined by observing how the alga contacted the bed as it traveled around in the flume. These transport modes were further simplified into the predominant modes observed in each step (e.g. rolling/sliding, sliding/brushing, mixture between suspension and sliding and continuous suspension).

b. *Erosion Rates*

Erosion rates (mg m^{-2} s^{-1}) for each experiment were derived from suspended sediment concentration versus U_y graphs (Fig. 4-14) by calculating the rate of change in the suspended sediment concentrations and converting this to an erosion rate using equation 4:

$$(4) \quad Erosion\ \ Rate = \frac{(SSC_{t+\Delta t} - SSC_t) \times V}{\Delta t \times \alpha}$$

Where: $SSC_{t+\Delta t} - SSC_t$ = the rate of change of the SSC (mg L^{-1})

V = the flume volume (7.9 L)

Δt = time span over which that the rate of change of SSC was determined (s)

α = flume bed area (3.24×10^{-2} m^{-2}) (Amos *et al.*, in press).

Thus, an erosion rate was produced for each velocity step in the experiment. Plots of erosion rate versus current velocity were then produced to show the differences between the different size and abundance treatments.

The erosion threshold was estimated by the extrapolation method described by Sutherland *et al.* (1998). The SSC was regressed against log U_* and the critical shear velocity (U_{*crit}) was found by solving the regression equation for a SSC of 0 mg L^{-1}. The critical shear velocity was then transformed to bed shear stress (τ_o) using equation 5 and 6:

(5) $U_* = 0.141\ U_y$

Where: U_* = friction velocity (m s^{-1})

U_y = current velocity (m s^{-1}) (Amos *et al.*, in press).

(6) $\tau_o = 1.99 \times 10^{-2}\ \rho\ U_y^2$

Where: τ_o = fluid induced bed shear stress (Pa)

ρ = fluid density (kg m^{-3})

U_y = current velocity (m s^{-1}) (Amos *et al.*, in press).

c. *Statistical Analysis*

All statistical analyses were analyzed using Minitab™ software unless otherwise noted.

Final suspended sediment concentrations (i.e. SSC at t= 140 min) of the various trials within treatments were ranked in order of lowest to highest within each treatment along with the corresponding settling rates of the algae used in the experiment. A Pearson correlation was performed on the ranked settling and ranked SSC data for each species to determine whether the settling rates of the algae influenced the SSC within treatments. Ranked data from both species were also grouped together, to increase the number of observations, and then analyzed using the same technique; thus, the statistical result was strengthened.

An autoregressive statistical model was developed to determine whether the algal treatments were statistically different from the control treatments and from one another. First a Durbin-Watson test was performed on a regression of SSC versus time to determine whether the SSC measurements, within a trial, were independent from one another. If the independence of this model was violated (i.e. SSC_{t+1} was not independent

from SSC_t), then an autoregressive model was fitted to the data using SAS software. The autoregressive slope of a trial was derived by fitting a line to a subset of the data within the slope segment of the SSC vs. time curve and the tails (0 slope) were ignored for the purposes of this test (see figure 2). Furthermore, slopes were derived using data points that covered the same time duration for all of the trials within a treatment. A test statistic (T) ratio was also calculated using the SAS software. If this T - ratio was greater than 2.42, then the slope of that trial was considered to be statistically different from a slope of 0 (control). The 0.05 alpha value (e.g. 2.42) was adjusted according to a Bonferroni Critical Values table for simultaneous comparisons (Cabilio and Masaro, 1999). This test was performed for all of the trials within all of the treatments. In addition, all of the slopes of trials within treatments were statistically compared to one another using equation 7:

(7) $$\text{Test Statistic } (t^*) = \text{ABS} \quad \frac{\text{Slope2} - \text{Slope1}}{((Se2)^2 + (Se1)^2)^{1/2}}$$

Where: ABS = Absolute Value

Slope2 = autoregressive slope estimate for algal trial 2

Slope1 = autoregressive slope estimate for algal trial 1

Se2 = autoregressive standard error for algal trial 2

Se1 = autoregressive standard error for algal trial 1

If this test statistic (t*) was greater than 2.42/adjusted value (p-value = 0.05), then the trials were statistically different from one another. If the test statistic was less than 2.42/adjusted value, then the trials were statistically the same. This test was performed on all trial combinations within treatments.

Significant parameters that affected the erosion rate of the bed (e.g. U_y, % contact with the bed, size, species) were deduced by performing a multiple regression analysis with erosion rate as the response. A backward elimination approach was used to generate the regression equation. First a regression model was produced by incorporating all measured parameters into the model. Then, predictors with the highest insignificant p-values (> 0.05) were removed one at a time. Individual r-squared values for each predictor variable were calculated by dividing the adjusted sum of squares value for that variable by the total sum of squares for all predictor variables. This method generates an individual r-squared value for a given predictor variable by treating it as the last variable to enter the multiple regression model. Furthermore, multicollinearity of predictor variables (i.e. correlations between predictor variables) was examined using variance inflation factors. Variance inflation factors are used to measure how much the variance of an estimated regression coefficient increases if predictors are correlated. Therefore, predictor variables with high variance inflation factors (i.e. greater than 10) were removed from the model and the remaining predictors were re-examined using the same technique to ensure that any correlations between predictors would not significantly alter the overall fit of the model.

This above procedure was only used on the size treatment data for both species. The medium and high abundance treatments were not used for this analysis as the higher number of pieces and high suspended sediment concentrations increased the difficulty measuring certain predictor variables (e.g. % time as aggregates, % contact, velocity of various aggregates). Thus, it was not possible to incorporate this information into the regression model.

Final suspended sediment concentrations, overall slopes (e.g. the slope calculated using the autoregressive technique), and the erosion thresholds were analyzed using a 1-way ANOVA to determine if these parameters were significantly affected by algal size and abundance. Average erosion rates (i.e. the average of all trials within a treatment) for size and abundance were analyzed with a 2-way ANOVA to determine if size and abundance had a significant effect on the erosion rates of the beds.

Ranked final SSC within a treatment were correlated with the rank of the average algal velocity (U_a) within the same treatment to determine if the algal velocity had an impact on the erosion of the beds. Furthermore, ranks of final SSC and U_a for both species were grouped together to increase the number of observations; thus, the statistical result was strengthened.

The ranking procedure mentioned above and the multiple regression model were not used to produce a numerical model to determine the effect of various predictors (e.g. settling rate, algal velocity, percent contact, etc.) on erosion of the artificial bed. Moreover, these analyses were used to identify variables that help explain variability within treatments (e.g. the use of ranking and correlation analysis) as well as identify variables that affect the rate of erosion of the bed (e.g. multiple regression analysis).

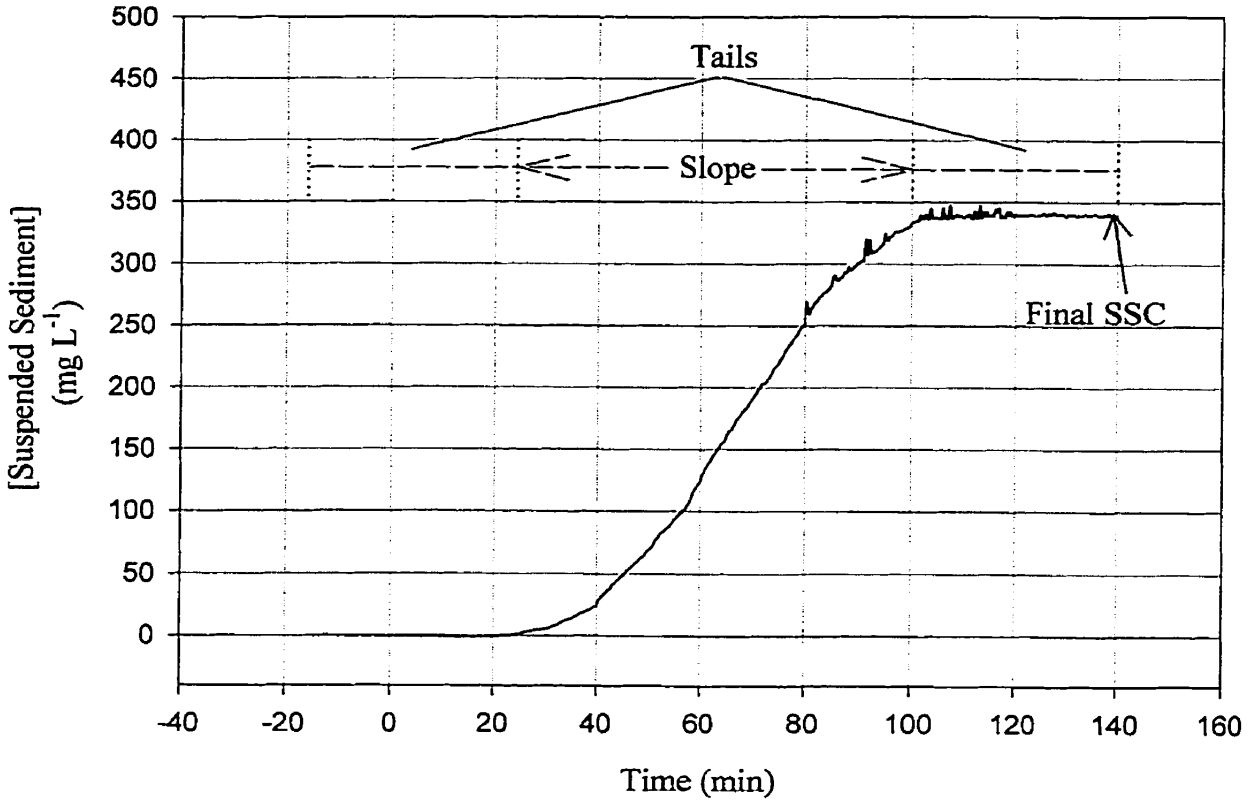

Figure 2. Typical sigmoid curve of OBS data showing overall slope, tails, and the final suspended sediment concentration.

RESULTS

3.0 PRELIMINARY SETTLING RESULTS

Complete preliminary results of settling experiments performed in Venice, Italy can be found in Appendix C. These experiments were used to help determine which species of macroalgae would be used in the flume erosion experiments. The results show that *Chondrus* and *Gracilaria* have much higher settling rates (on average) than those of *Ulva* and the seagrass *Cymedosia*.

3.1 SETTLING RATES

Both *C. crispus* and *F. lumbricalis* generally settled with their longest axis perpendicular to the settling direction. This consisted of the stipe being vertically aligned and generally facing downward for *C. crispus* and horizontally aligned for *F. lumbricalis*.

Graphs of still water settling rates versus algal mass for *C. crispus* and *F. lumbricalis* (Fig. 3) display the variability in settling rate with respect to the mass of the algae. Correlation analysis performed on these data revealed that the settling rates of the *C. crispus*, collected from P.E.I., were not statistically correlated with their mass (correlation coefficient = 0.111, p-value = 0.400); whereas, settling rates of *C. crispus* collected from the lagoon of Venice were (correlation coefficient = 0.537, p-value = 0.039). Furthermore, *F. lumbricalis*, collected from P.E.I., were statistically correlated with mass (correlation coefficient = 0.41, p-value = 0.002); whereas, *Gracilaria* sp. collected from the lagoon of Venice were not (correlation coefficient = -0.136, p-value=0.690).

Figure 3 shows that the Venetian *C. crispus* had similar settling rates with respect to mass to that of the *C. crispus* collected in P.E.I (i.e. the data overlapped). However, it

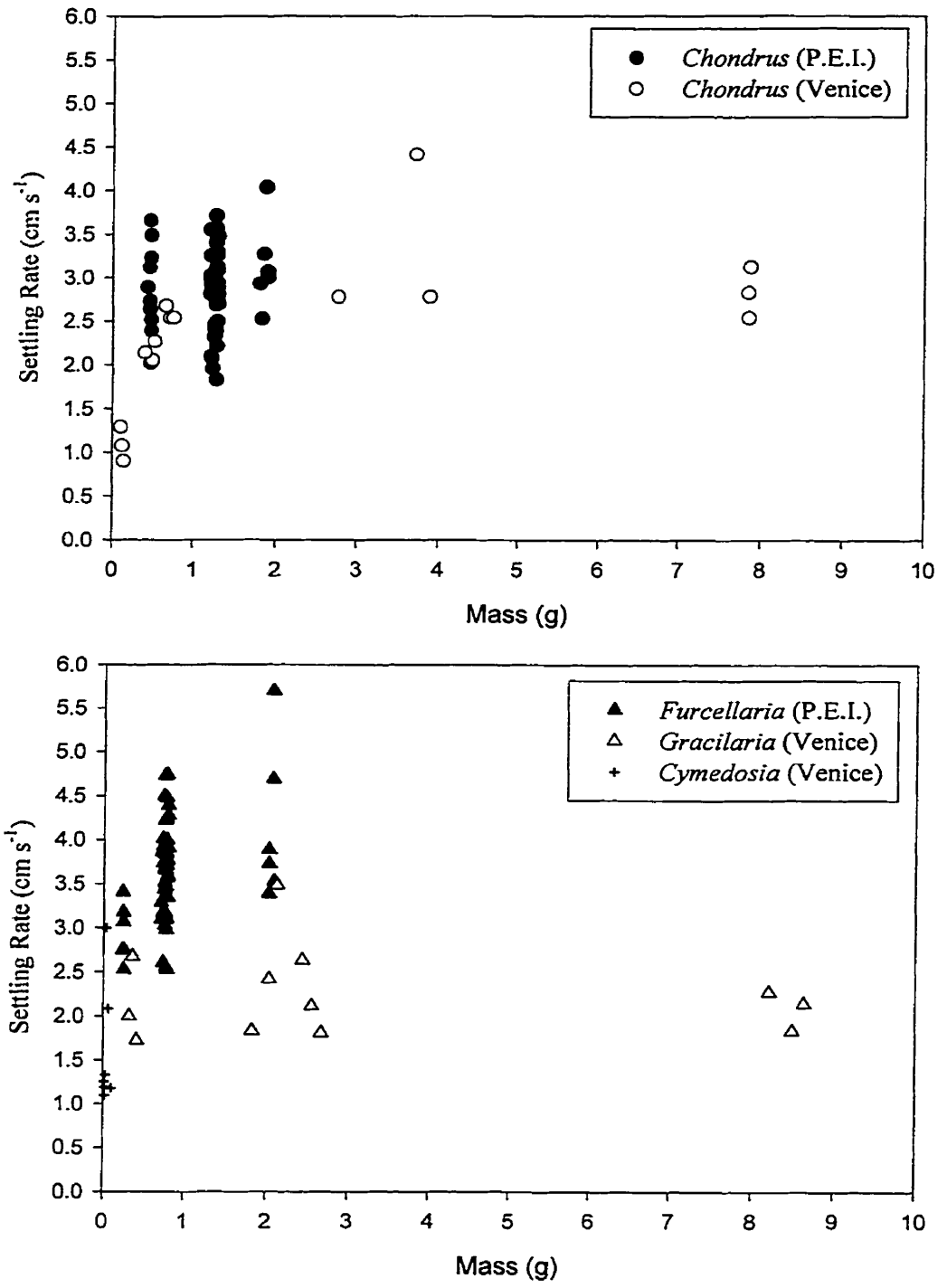

Figure 3. Scatter plot of macroalgal settling rates versus mass for specimens collected in P.E.I and Venice.

appears that the settling rates of the *F. lumbricalis* collected from P.E.I. are greater than the *Gracilaria* sp. collected from the lagoon of Venice. Correlation analysis within algal treatments showed that ranked settling rates of the algae were significantly correlated with the rank of the final SSC when grouped over all of the treatments and species (see table 2).

Species/Group	**Correlation Coefficient**	**P-value**
C. crispus	0.438	0.069
F. lumbricalis	0.432	0.080
***C. crispus* + *F. lumbricalis* (grouped together)**	0.433	0.008

Table 2. Correlation coefficients and respective p-values for the ranked settling rates versus ranked final suspended sediment concentrations.

Ranked correlation analysis of settling rate versus final SSC (table 2) showed that when the results for *C. crispus* and *F. lumbricalis* were combined (to increase the number of observations) 43.3 % of the ranked variability (p-value = 0.008) within a treatment could be explained by the ranked average settling rates of the algae used in that treatment. However, the average settling rate of the algae was found to be insignificant when it was incorporated into a multiple regression model, as a predictor variable, to determine its impact on the response (erosion rate) (Coefficient = 0.6210, p-value = 0.488).

3.2 VISUAL OBSERVATIONS

A summary of the results of video analysis can be found in Appendices D to G.

a. *Controls*

Video analysis of the control treatments revealed that, in the absence of algae, there was no visual evidence of erosion of the artificial clay bed.

b. *Chondrus Size*

Algae within all three size categories spent significant amounts of time moving both as aggregates and individual pieces. However, at higher current velocities the algae spent more time moving as individual pieces than as aggregates. Algae in the small size category began to slide along the bed soon after the motor began (step 1) and continued to move throughout all of the velocity steps. However, algae within some of the trials of the larger size categories spent a significant period of time not moving along the bed during step 1 (i.e. the current velocity was not great enough to move the individual piece/aggregates). For example, algae spent a significant period of time not moving in three of the trials of the medium size category (trials 2, 3 and 5) and all of the trials in the large size category. No motion, during step 1, usually resulted when two individual pieces came together to form an aggregate. After the onset of step 2, all previously static pieces began to move along the bed. The overall trend showed that the mode of algal transport varied with current velocity. Macroalgae initially began to move by sliding/rolling along the bed. This generally lasted for the first two velocity steps and was then followed by a phase in which the algal pieces spent significant periods of time in suspension as well as sliding/brushing the bed. This "mixed phase" generally occurred between steps 3 and 5. The final phase in algal transport occurred when the algae totally entered suspension and no longer contacted the bed.

c. *Chondrus Abundance*

Algae within all three abundance categories spent significant quantities of time moving as large (≥ 4 pieces) and small aggregates (≤ 3 pieces). However, algae spent more time moving as smaller aggregates at higher current velocities than as large

aggregates. Algae within trial 2 and 3 of the low abundance treatment, trial 3 of the medium abundance treatment and all three trials of the high abundance treatment spent large quantities of time not moving during the first velocity step. As mentioned above, this period of no motion usually resulted when the individual pieces combined to form aggregates. During velocity step 2, all previously static pieces resumed motion either as aggregates or individual pieces. The mode of algal transport followed the same trend as mentioned above in the size categories. When the algae initially began to move, they did so by rolling/sliding along the bed. This phase lasted for the first two to three velocity steps. The rolling/sliding phase was followed by a mixed phase between suspension and sliding along the bed, which occurred between steps 3 and 5 (depending upon the trial). Finally, the mixed phase was followed by complete suspension of the algae into the water column.

d. *Furcellaria Size*

Algae within all of the size categories spent significant amounts of time moving as aggregates and as individual pieces. Furthermore, pieces of *F. lumbricalis* followed a similar trend as *C. crispus* and spent more time moving as individual pieces during higher current velocities than as aggregates. Lack of motion of the *F. lumbricalis* pieces only occurred during step 1. During this first velocity step, all but one trial contained algae that spent significant periods of time (> 34 %) not moving. The only exception was trial 3 of the large size category. Algae within this trial began moving soon after the motor began and only spent approximately 4 % of step 1 not moving. Algae followed a consistent pattern for the mode of transport. Algae first began to move by sliding and brushing the bed. While sliding, some pieces of algae moved in a "corkscrew" rotation as

they slid along the bed. The sliding/brushing phase was followed by a mixture of suspension and sliding/brushing, which in turn was followed by complete suspension of the algae in some trials. During the sliding/brushing phase algae appeared to have no preferential orientation, except that they moved along the bed both horizontally (i.e. sliding) and vertically (i.e. brushing).

e. *Furcellaria Abundance*

Algae within all three abundance categories spent significant quantities of time travelling as large ($\geq$ 4 pieces) and small ($\leq$ 3 pieces) aggregates. However, as mentioned in the *C. crispus* trials, the algae spent more time travelling as smaller aggregates at higher current velocities than as the larger aggregates. Algae within all of the trials of all of the treatments spent the majority of time not moving during the first velocity increment. Motion generally ceased when the algae combined to form aggregates. Motion resumed for all of the static algae after the onset of velocity step 2. Algae followed the same general mode of transport pattern as they did in the size treatments. Algae initially moved by sliding and brushing the bed. This phase was followed by a mixed phase of suspension and sliding/brushing. Complete suspension of the algae only occurred in trial 1 of the low abundance category.

3.3 SUSPENDED SEDIMENT CONCENTRATIONS

Complete results of the suspended sediment concentrations for all of the trials are presented in figures 4-14. The scale range for figures 4-14, with the exception of figures 9 and 12, were kept the same to allow for easy relative comparisons between treatments.

a. *Controls*

The four control experiments (Fig. 4 and Appendix H) showed little variation with respect to suspended sediment concentration and the water velocity did not appear to reach the fluid induced erosion threshold of the artificial clay beds. Thus, the fluid induced erosion threshold was considered to be greater than 0.52 m s^{-1}. Erosion experiments involving algae support this observation: when the algae entered into continuous suspension, the suspended sediment concentration leveled off to a constant level and the erosion rates decreased to 0 mg m^{-2} s^{-1}. This suggests that the fluid induced erosion threshold had not yet been reached. If the fluid induced erosion threshold were reached before 0.52 m s^{-1}, then the suspended sediment concentration would significantly increase after the algae entered into continuous suspension.

The graph displaying the four control replicates (Fig. 4 and Appendix H) showed that the suspended sediment concentrations never reached values with a difference greater than 5 mg L^{-1} (i.e. that is when the final SSC are compared to the SSC at time 0 (when the motor started) and before). Visual observations revealed no erosion of the bed during any of the control experiments. Erosion threshold analysis on all of the data within trials (Appendix I) showed that the critical erosion threshold occurred at approximately 0 m s^{-1} for trials 1 through 3 and before 0 m s^{-1} for trial 4. These values resulted because the rate of increase of the SSC was small; thus, the slope of the regression line was also small causing it to be fitted to a value near the U_y - origin or before (e.g. trial 4). Furthermore, the SSC of filter samples oscillate across the seven velocity increments. None of the filter samples show a clear increasing suspended sediment concentration trend across the velocity steps. Oscillation of the SSC across the velocity steps is attributed to problems

associated with filtering water samples with very low suspended sediment concentrations (e.g. tears in filter during handling, small amounts of filter adhering to petri dish during drying procedure, etc.)

Variation displayed in figure 4 and Appendix H is assumed to result from noise of the OBS sensors during the course of the experiment, not due to erosion of the clay bed. Furthermore, this noise along with oscillating filtered sediment masses caused problems with the regression calibrations (low r-squared values) (e.g. average ($\pm$ 1sd) r^2 of 0.328 $\pm$ 0.078 and an average ($\pm$ 1sd) p-value of 0.146 $\pm$ 0.064, which may have led to SSC values that appear to be different from 0 mg L^{-1} in some instances. All that should be noted from figure 4 is that the SSC values of the control trials were essentially 0 mg L^{-1} for all of the velocity steps.

b. *Chondrus Size*

1-way ANOVA analysis showed that the size of *C. crispus* had an effect on final suspended sediment concentrations (p-value = 0.037) and overall slopes (p-value = 0.012) of the SSC versus time graphs. Furthermore, this analysis showed that the erosion threshold (τ_{crit}) was not significantly affected by the size of *C. crispus* (p-value = 0.071) (data displayed in figure 15). Results of a correlation analysis (data displayed in figure 19) revealed that the critical erosion threshold of the bed was correlated with the velocity in which the *C. crispus* fronds began to move (correlation coefficient = 0.708, p-value = 0.010).

There were four primary modes of algal transport, which varied with current velocity: (1) intermittent motion in which pieces intermittently rolled and slid along the bed; (2) continuous rolling/sliding; (3) a mixture of suspension and sliding (when in

contact) along the bed and (4) continuous suspension. The algae tended to roll more during the earlier velocity steps, then predominately slid during the latter part of this transport phase. During the first 40 minutes of a trial ($0 < U_y \leq 0.15$ m s^{-1}), movement was primarily by rolling and/or sliding. From 40 to 100 minutes ($0.22 \leq U_y \leq 0.37$ m s^{-1}), for the small and medium categories (Fig. 5 and 6 respectively), and between 40 and 80 minutes ($0.22 \leq U_y \leq 0.30$ m s^{-1}), for the large size category (Fig. 7), the predominant movement was a mixture of suspension and sliding. After 100 minutes from the start of a trial ($U_y \geq 0.45$ m s^{-1}), for small and medium pieces, and after 80 minutes ($U_y \geq 0.37$ m s^{-1}), for the large pieces, complete suspension of the algae was the primary mode of transport. During the rolling/sliding phase, pieces of *C. crispus* slid on their sides with no preferential orientation with respect to current velocity. For example, when sliding, the stipe could be oriented up, down, into or away from the current direction. During the suspension and sliding phase the algal pieces would slide along the bed in both a vertical and horizontal position (i.e. no preferential stipe orientation). Algae would stay in contact with the bed for a given number of revolutions and then enter suspension for a given period of time. Furthermore, no standard saltation period, height or length was evident; these parameters appeared to be random and varied greatly within a velocity step.

Complete results of the T-ratios for the autoregressive model can be found in Appendix J. Statistical analysis showed that suspended sediment concentrations in all of the trials within the three size categories were statistically greater than those of the controls (p-value < 0.001). Furthermore, replicates within treatments showed visual and statistical variation between the trials. The small size category (Fig. 5) showed the least amount of variability. All three trials appeared very similar in shape, SSC and slope, but

the statistical analysis showed that all of the trials were statistically different from one another.

The medium size/low abundance category (Fig. 6) appeared to display a significant amount of variation. The overall trend was the same sigmoid profile among the trials (e.g. fig 2); however, the slopes for all of the trials except for four pairs (trials 3 and 4, trials 3 and 5, trials 3 and 6 and trials 4 and 6 within the medium size/low abundance treatment) were statistically different from one another (see Appendix J). Statistical analysis showed that trials 3 and 4, trials 3 and 5, trials 3 and 6 and trials 4 and 6 had equal slopes to one another. Final SSC values in the medium size/low abundance category ranged from approximately 40 mg L^{-1} (trial 1) to 150 mg L^{-1} (trial 5).

SSC curves for the large size category (Fig. 7) also showed a significant level of variation. Trial 1 and 2 were similar in shape, in SSC values and in slopes. However, trial 3 had a much greater slope from 40 to 100 minutes, giving it a much higher final SSC (approximately 350 mg L^{-1}) compared to the final SSC of trials 1 and 2 (approximately 125 mg L^{-1}). Furthermore, trial 3 did not level off to a constant SSC value until t = 100 minutes (U_y = 0.37 m s^{-1}); whereas, trials 1 and 2 leveled off one step earlier at t = 80 minutes (U_y = 0.30 m s^{-1}). The statistical analysis on this treatment showed that none of the trials were equal to one another.

c. *Chondrus Abundance*

1-way ANOVA analysis showed that the abundance of *C. crispus* had an effect on final SSC (p-value = 0.005), and the overall slopes of the SSC versus time graphs (p-value = 0.003). However, this analysis showed that critical erosion thresholds were not

significantly affected by the number of pieces in the Mini Flume (p-value = 0.151) (data displayed in figure 16).

The small and medium abundance categories appear to be similar in terms of SSC and slopes. However, the suspension phase was reached one step earlier (step 5) in the medium abundance category than in the low abundance category (step 6). There were the same three primary modes of transport (outlined above). During the first 40 minutes ($U_y \leq 0.15$ m s^{-1}) the algae generally moved by sliding/rolling along the bed. From 40 to 100 minutes ($0.22 \leq U_y \leq 0.37$ m s^{-1}), for the low abundance treatment, and from 40 to 80 ($0.22 \leq U_y \leq 0.30$ m s^{-1}) minutes for the medium and high abundance treatments, the algae typically moved as a mixture of suspension and sliding on the bed. This mixed phase was followed by complete suspension of the algae, which occurred after 100 minutes for the low abundance category and after 80 minutes for the medium and high abundance treatments.

Replicates within each category visually showed variation. For the low abundance category description see medium size explanation above (as they were the same experiments). Trials 1 and 2 in the medium abundance category (Fig. 8) were similar in SSC and in slopes. However, trial 3 had a larger slope between step 2 and step 5 yielding higher SSC values for this trial. All three trials in this category appeared to achieve a 0 slope at the same time (step 5, $U_y = 0.37$ m s^{-1}); however, the slope in trial 3 leveled off much more abruptly than trial 1 and 2. SSC values within the high abundance category (Fig. 9) also visually displayed a degree of variation among the replicates. Trials 1 and 2 appeared to be similar to one another in terms of SSC and slope; whereas, trial 3 had much smaller slopes and achieved a much lower final SSC value (at t = 140 min, SSC =

200 mg L^{-1}) than trial 1 (SSC = 525 mg L^{-1}) and trial 2 (SSC = 675 mg L^{-1}). The slope of trial 2 reached 0 one step later (step 6) than the slopes of trials 1 and 3 (step 5).

Results of the autoregressive model (Appendix J) showed that all trials within this (i.e. *Chondrus* Abundance) category were statistically greater than the controls (p-value < 0.001). Even though some of the SSC profiles appear to be similar in terms of SSC and slope, statistical comparisons of the slopes within treatments revealed that all replicates, except trials 3 and 4, trials 3 and 5, trials 3 and 6 and trials 4 and 6 of the low abundance category, were statistically different from one another (see Appendix J).

d. *Furcellaria Size*

1-way ANOVA analysis showed that the size of *F. lumbricalis* specimens did not have an effect on the final suspended sediment concentrations (p-value = 0.082), overall slope (p-value = 0.058) or critical erosion thresholds (p-value = 0.430) (data displayed in figure 17). Furthermore, the results of a correlation analysis (data displayed in figure 19) showed that the critical erosion threshold of the bed was not correlated with the velocity in which the *F. lumbricalis* fronds began to move (correlation coefficient = 0.361, p-value = 0.275).

As with *C. crispus*, four primary modes of transport were observed during the experiments: (1) intermittent motion consisting predominately of sliding; (2) continuous sliding; (3) mixture of suspension and sliding/brushing the bed; and (4) continuous suspension. The suspension phase was primarily only achieved for the small pieces of *F. lumbricalis* and it occurred during step 7. The exceptions were trial 1 and 3 of the small size category (Fig. 10) and trial 1 of the medium size category (Fig. 11). Algal pieces in trial 1 of the small and medium size category entered into suspension during velocity step

6. Algae in trial 3 of the small size category did not enter fully into suspension during the final velocity step (e.g. percent contact = 10 %). Sliding occurred during the first 60 minutes ($0 < U_y \leq 0.22$ m s^{-1}) of the small size trials, followed by the mixture of suspension and sliding/brushing between 60 and 120 minutes ($0.30 \leq U_y \leq 0.45$ m s^{-1}); which in turn, was followed by the suspension phase (for the trials mentioned above) during the last 20 minutes of the experiment ($U_y = 0.52$ m s^{-1}). The sliding phase lasted one step longer for the medium (Fig.11) and large size (Fig. 12) categories ($0 < U_y \leq 0.30$ m s^{-1}) and full suspension of the algae was never achieved, as the algae were still contacting the bed during the final velocity step ($U_y = 0.52$ m s^{-1}).

Replicates within these categories visually showed variation among trials. The small size category (Fig. 10) appeared to have the least amount of variability, as the curves had similar SSC values and slopes. The medium size category (Fig. 11) visually showed a higher degree of variation among trials. Even though the overall trend was similar, the curves varied in SSC and in slope (erosion rate) with final SSC ranging from 30 to 170 mg L^{-1}. Trials 2 and 3 of the large size category (Fig. 12) were similar in slope and SSC (final SSC = approximately 150 mg L^{-1}); however, they varied greatly from trial 1 (final SSC = 500 mg L^{-1}). Trial 1 had a much greater slope and higher SSC values than the other two trials.

Results of the autoregressive statistical analysis (Appendix K) showed that all trials within this treatment were statistically greater than the control trials (p-value < 0.001). Statistical comparisons of the slopes within treatments showed that there were only three instances in which the slopes of trials were statistically equal to one another. These were trials 1 and 2 of the small size category, trials 3 and 5 of the medium size

category and trials 2 and 3 of the large size category. The rest of the replicates within treatments were statistically different from one another.

e. *Furcellaria Abundance*

1-way ANOVA results showed that the abundance of *F. lumbricalis* had an effect on final suspended sediment concentrations (p-value = 0.018) and overall slopes of SSC versus time graphs (p-value = 0.017). However, this analysis showed that the critical erosion thresholds were not affected by the number of algal pieces in the Mini Flume (p-value = 0.573) (data displayed in figure 18).

There were three predominant modes of transport for the algae within the abundance categories. The first was the intermittent sliding phase, which generally occurred during the first 20 minutes. This was followed by the continuous sliding phase for the next 60 minutes of the experiment ($0.075 < U_y \leq 0.30$ m s^{-1}). This phase was followed by the mixed phase of suspension and sliding along the bed which persisted through the remainder of the velocity steps ($0.37 \leq U_y \leq 0.52$ m s^{-1}). Complete suspension of the algae was only achieved during trial 1 of the low abundance treatment (Fig. 11). It did not occur during any of the other trials.

The autoregressive statistical analysis (Appendix K) revealed that all of the trials within these treatments were statistically greater than the controls (p-value < 0.001). Furthermore, comparison of slopes within treatments revealed that trials 2 and 3 of the high abundance category, trials 1 and 3 of the medium abundance category and trials 3 and 5 of the low abundance category had statistically equivalent slopes. All other replicates had slopes that were considered to be statistically different from one another.

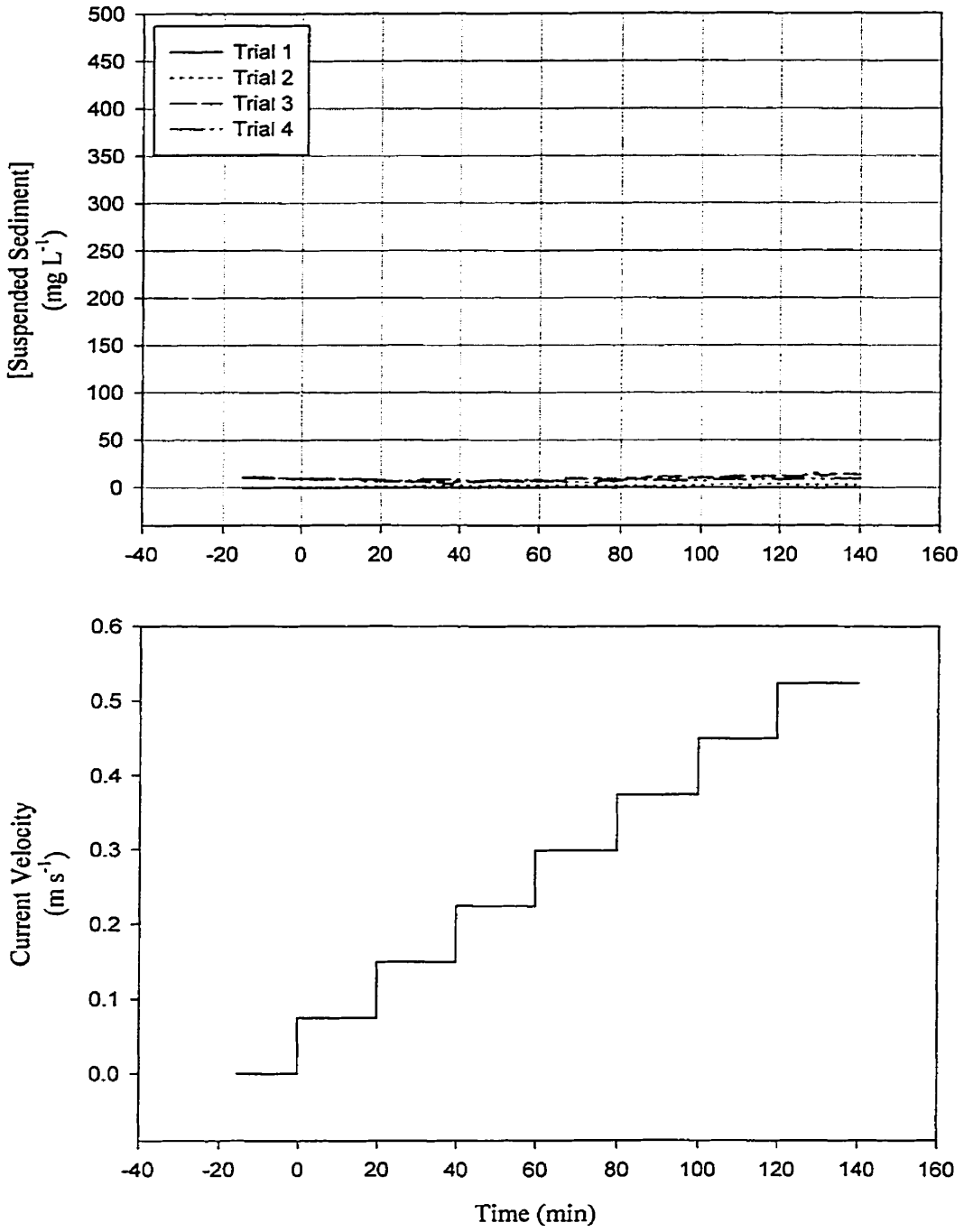

Figure 4. Graphs of SSC and respective current velocities for four trials within the control treatment.

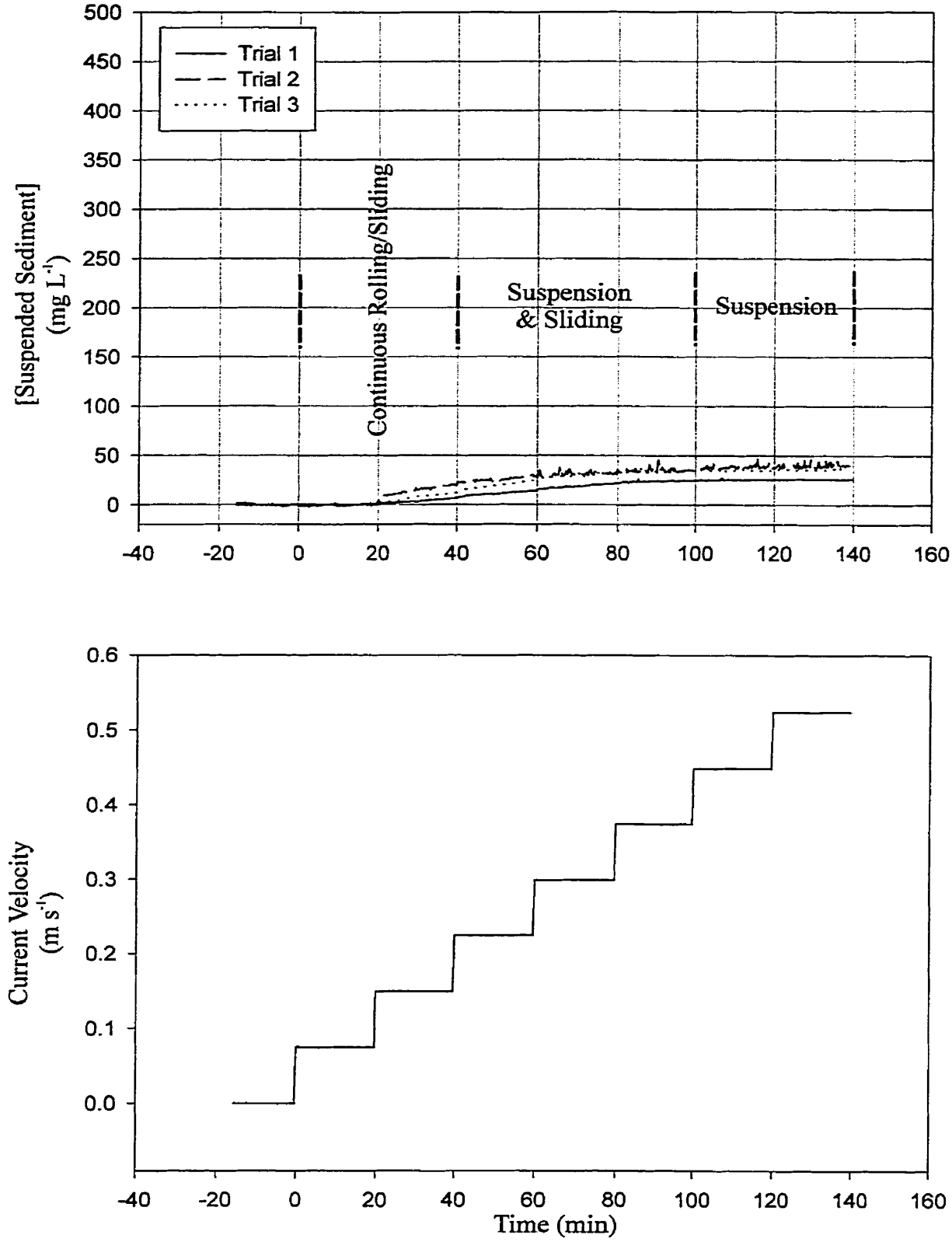

Figure 5. Graphs of SSC and respective current velocities for the three trials within the *Chondrus* small size treatment.

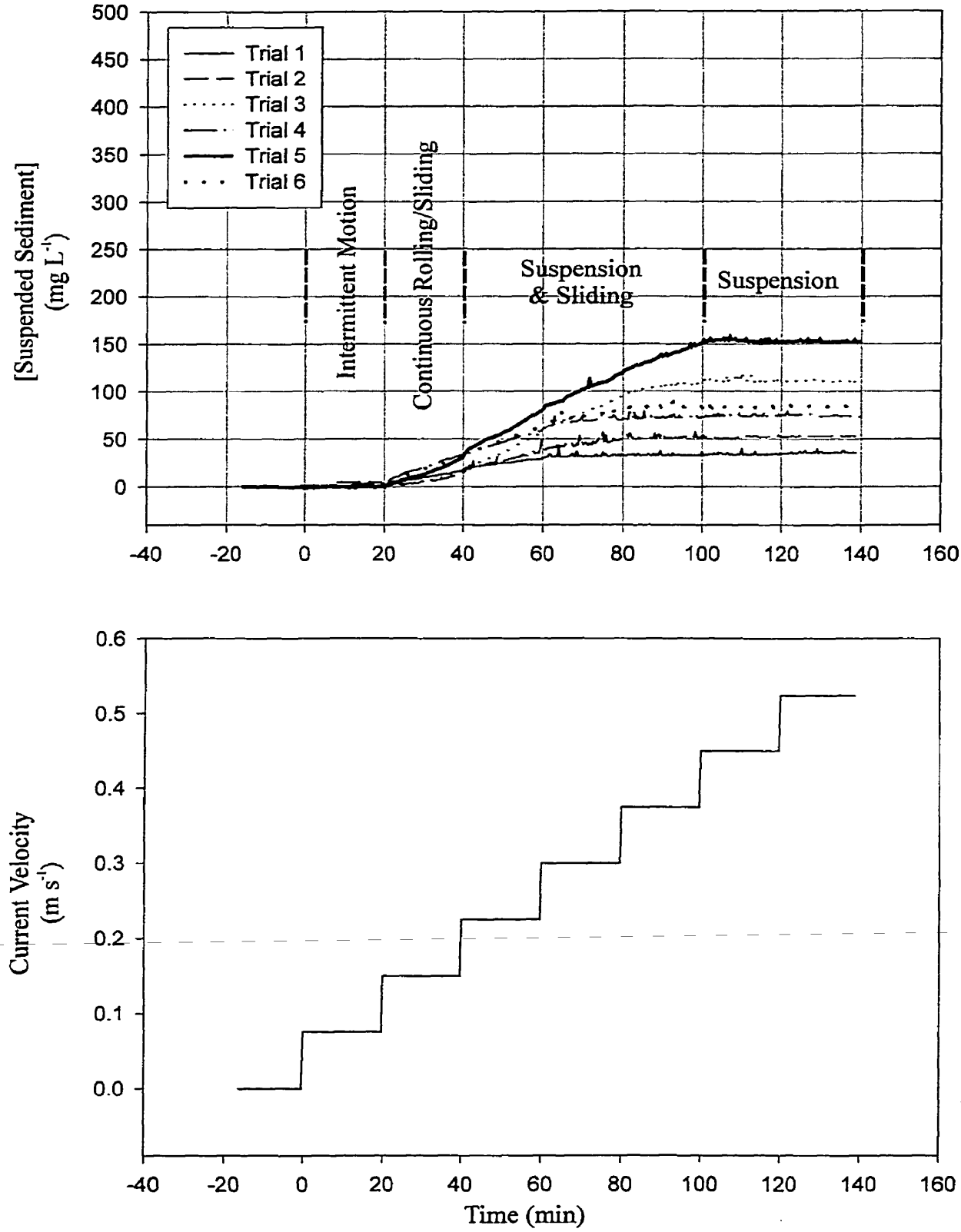

Figure 6. Graphs of SSC and respective current velocities for the six trials within the *Chondrus* medium size/low abundance treatment.

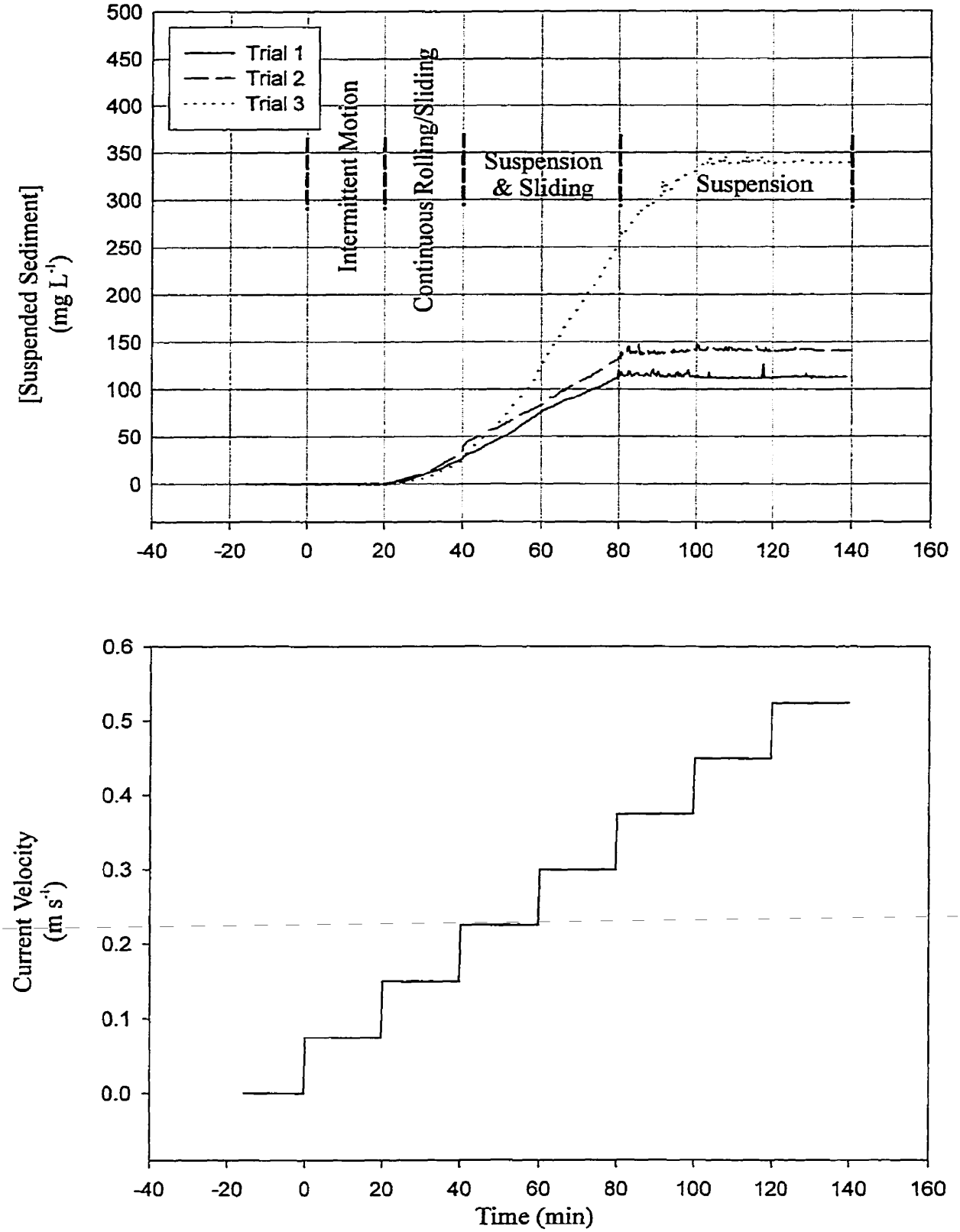

Figure 7. Graphs of SSC and respective current velocities for the three trials within the *Chondrus* large size treatment.

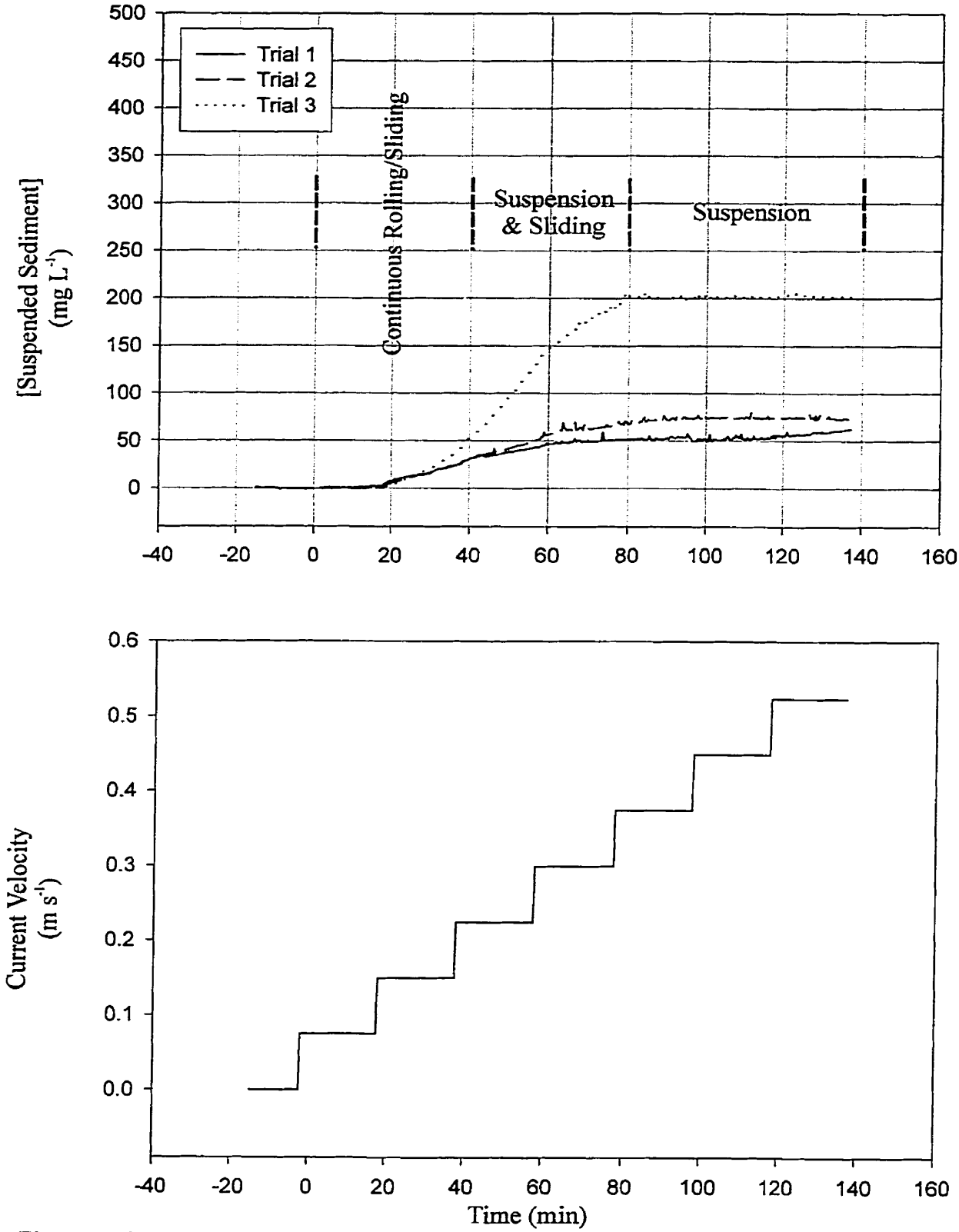

Figure 8. Graphs of SSC and respective current velocities for the three trials within the *Chondrus* medium abundance treatment.

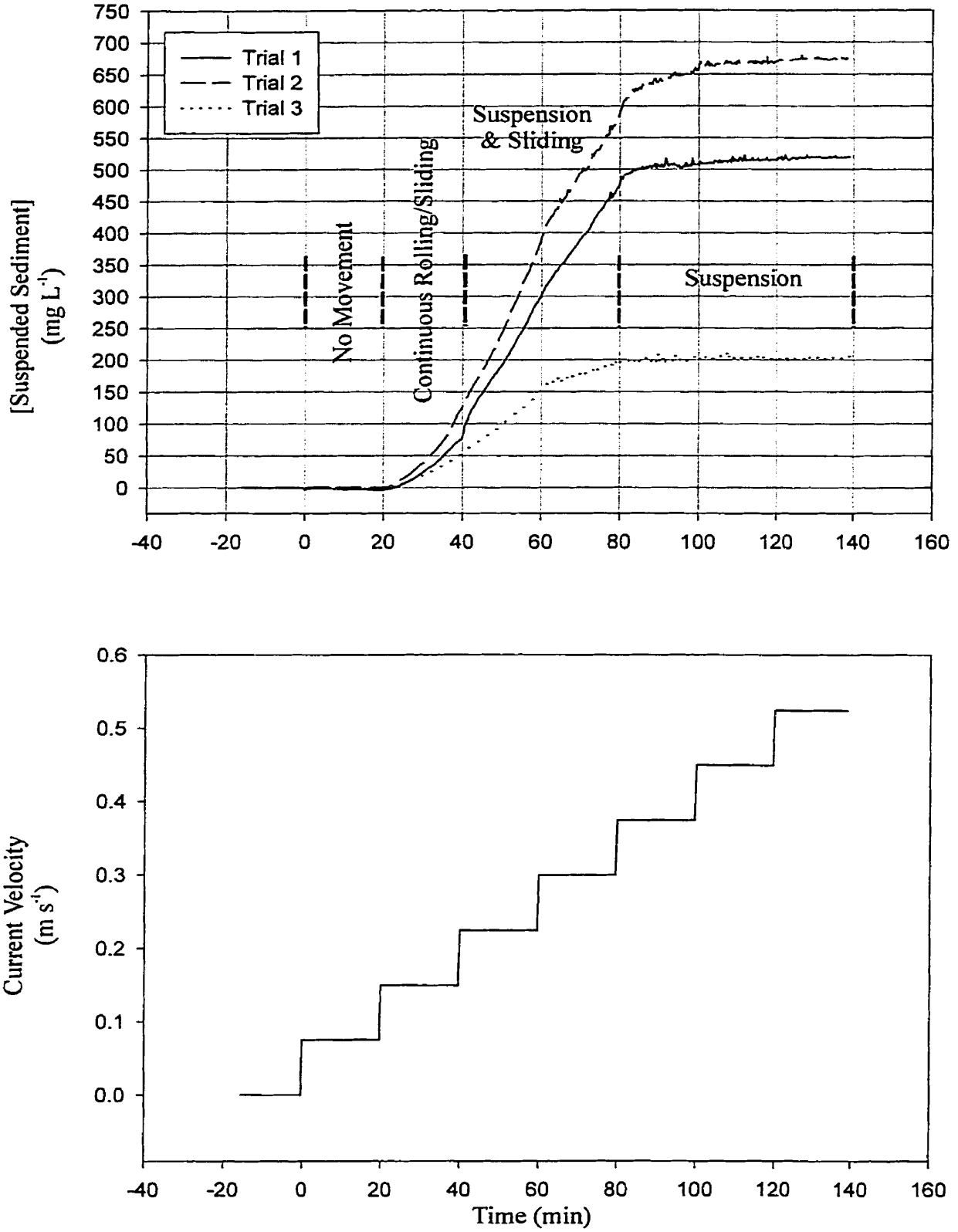

Figure 9. Graphs of SSC and respective current velocities for the three trials within the *Chondrus* high abundance treatment. Note: Scale was increased to accommodate data.

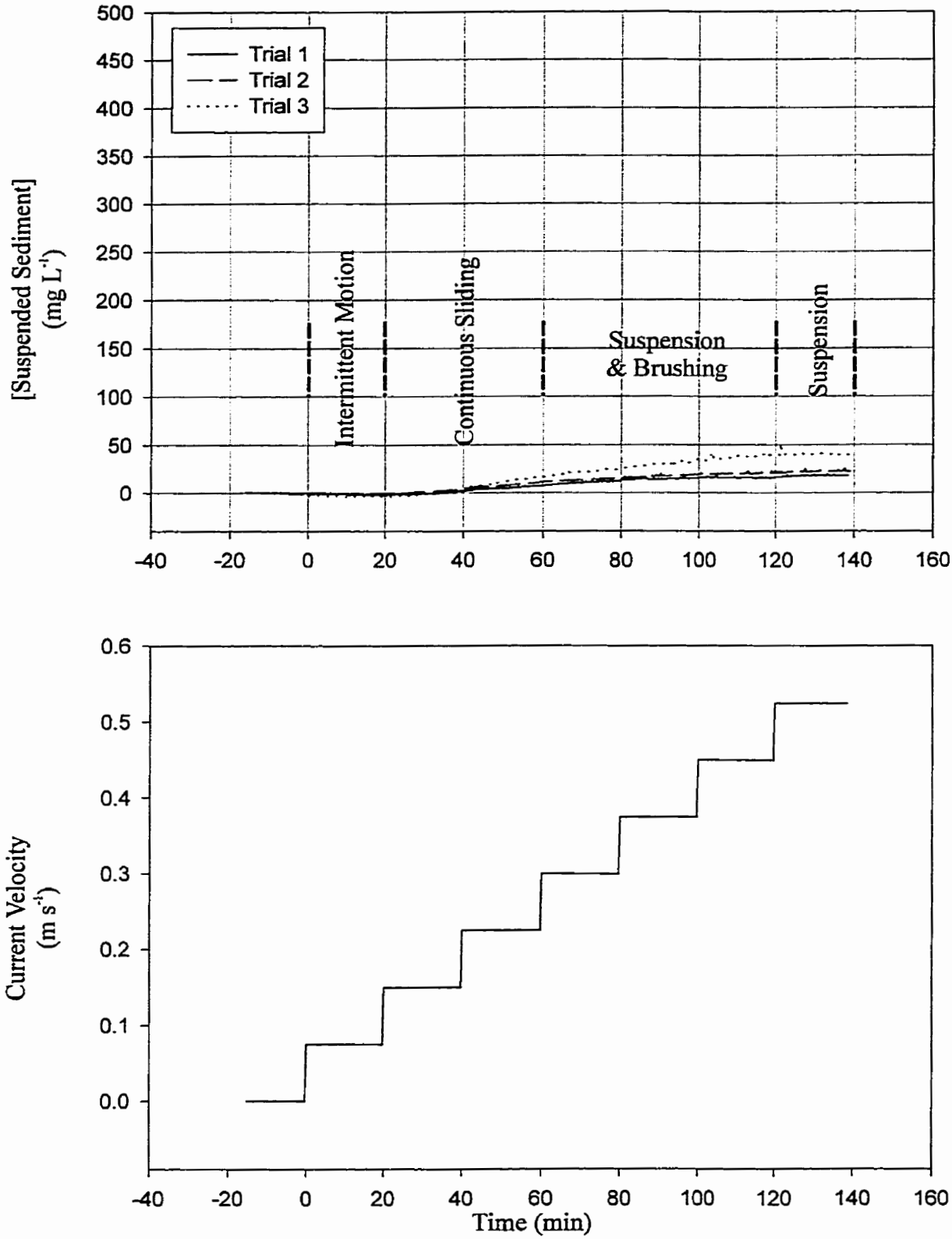

Figure 10. Graphs of SSC and respective current velocities for the three trials within the *Furcellaria* small size treatment.

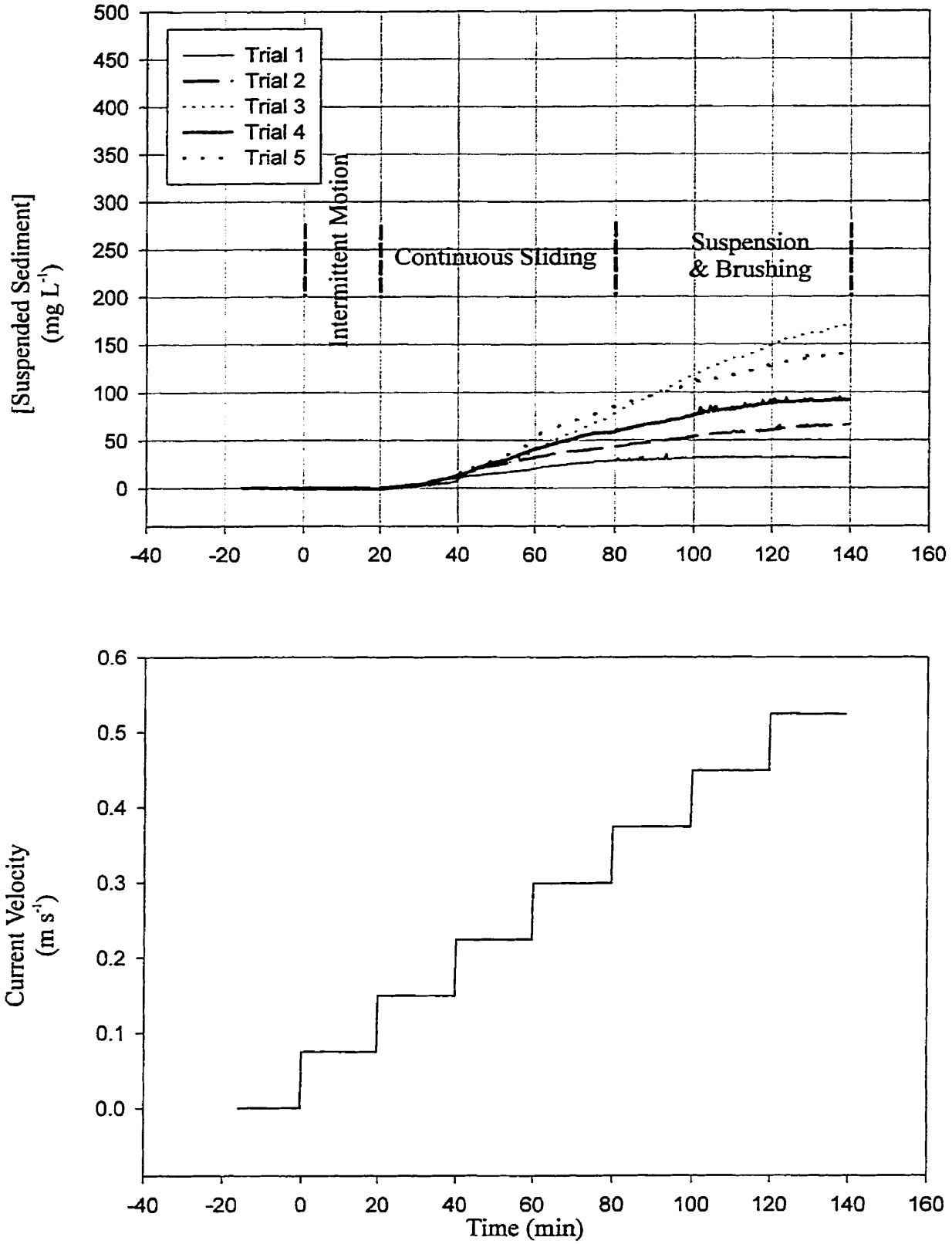

Figure 11. Graphs of SSC and respective current velocities for the five trials within the *Furcellaria* medium size/low abundance treatment.

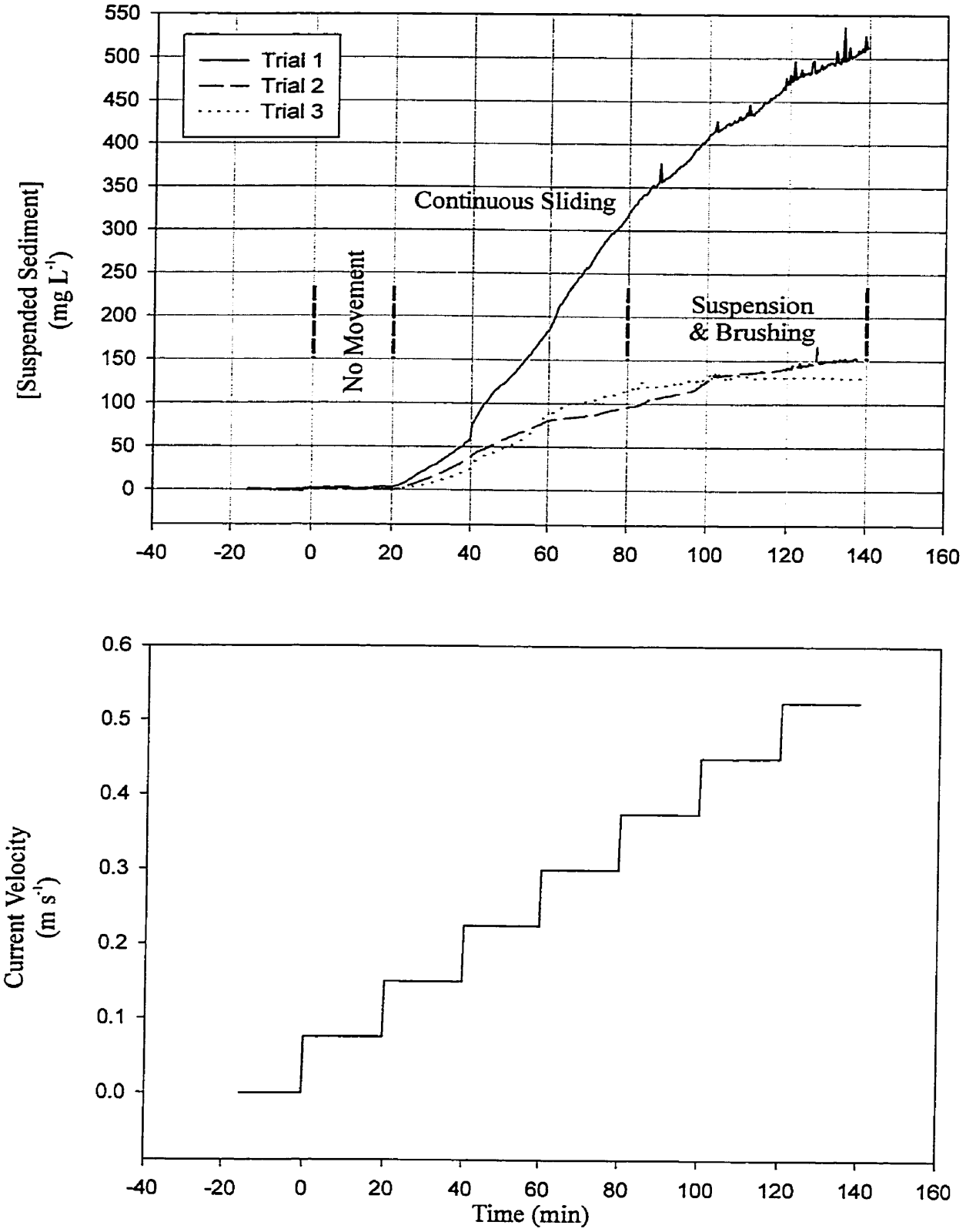

Figure 12. Graphs of SSC and respective current velocities for the three trials within the *Furcellaria* large size treatment. Note: Scale was increased to accommodate data.

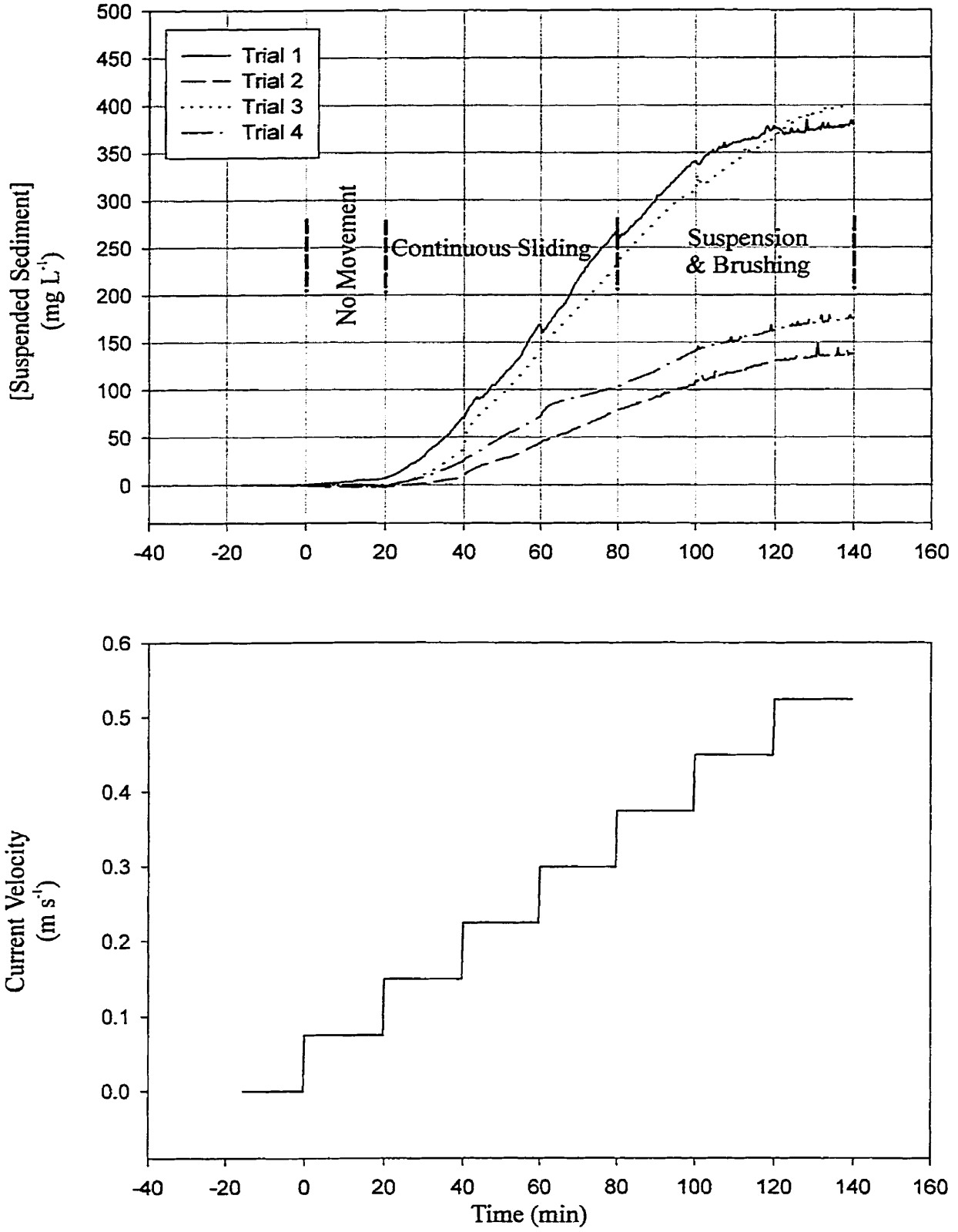

Figure 13. Graphs of SSC and respective current velocities for the four trials within the *Furcellaria* medium abundance treatment.

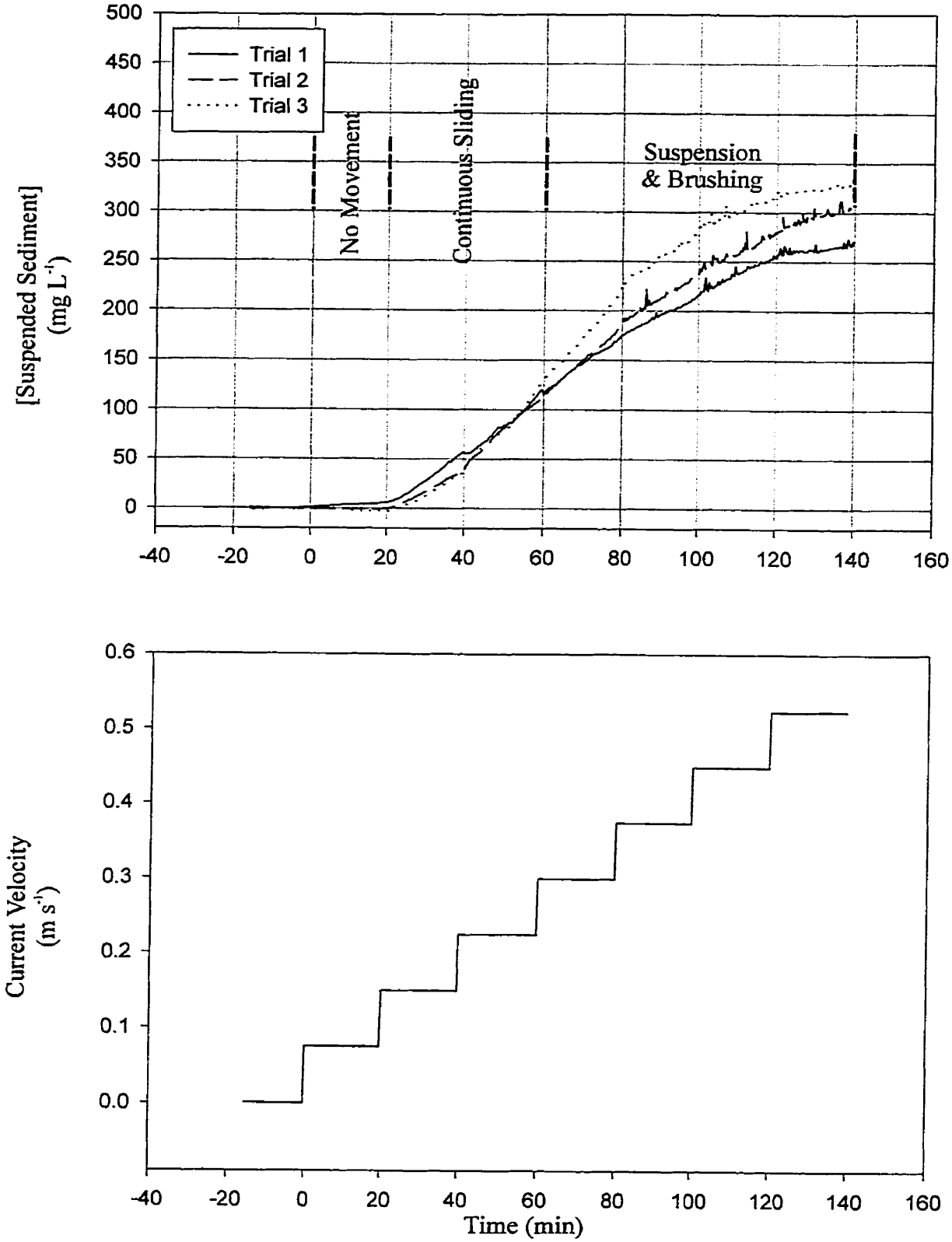

Figure 14. Graphs of SSC and respective current velocities for the three trials within the *Furcellaria* high abundance treatment.

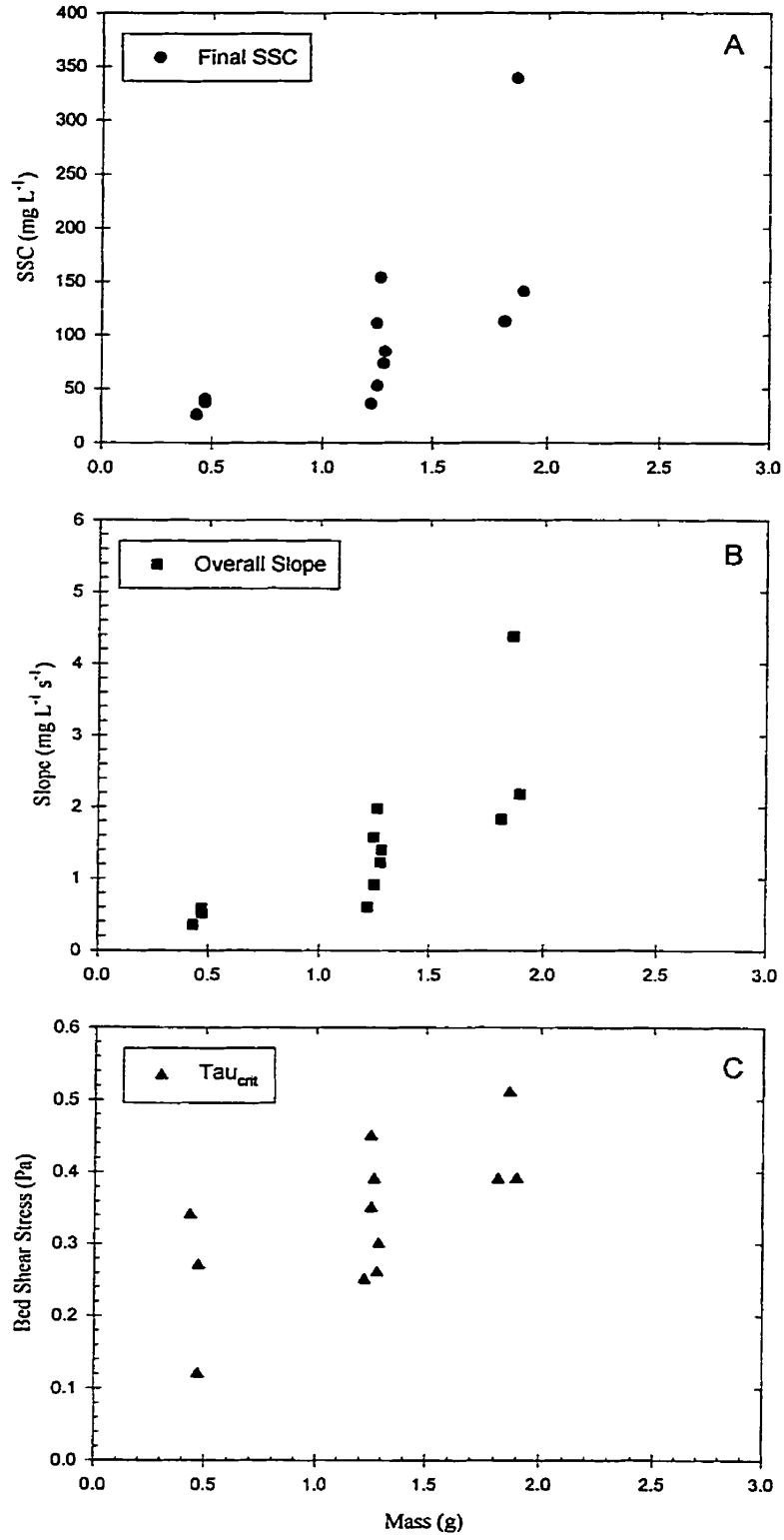

Figure 15. Graphs of final SSC (A), overall slope (B), and critical erosion threshold (C) versus algal mass for the three *Chondrus* size treatments.

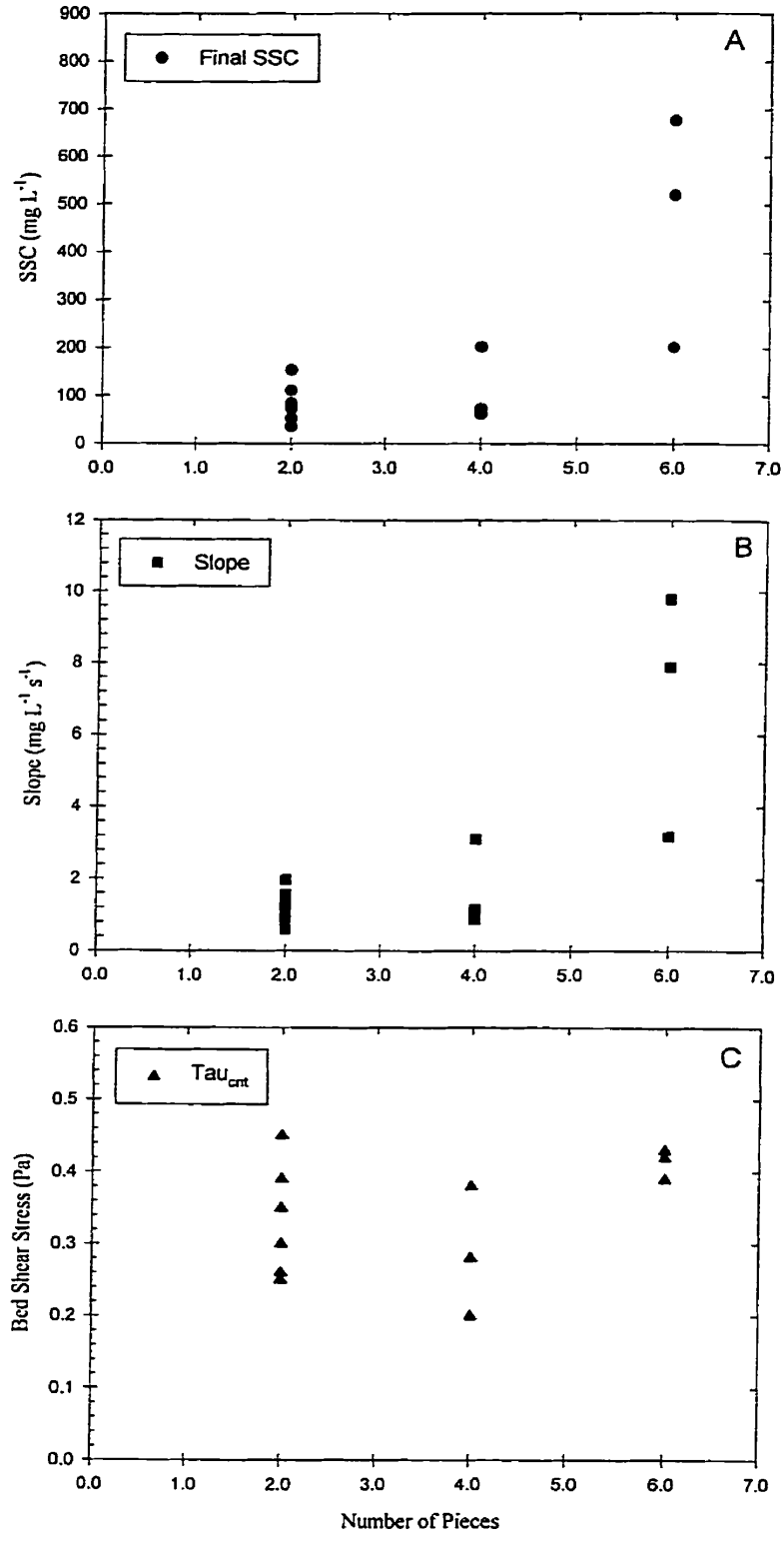

Figure 16. Graphs of final SSC (A), overall slope (B), and critical erosion threshold (C) versus algal abundance for the three *Chondrus* abundance treatments.

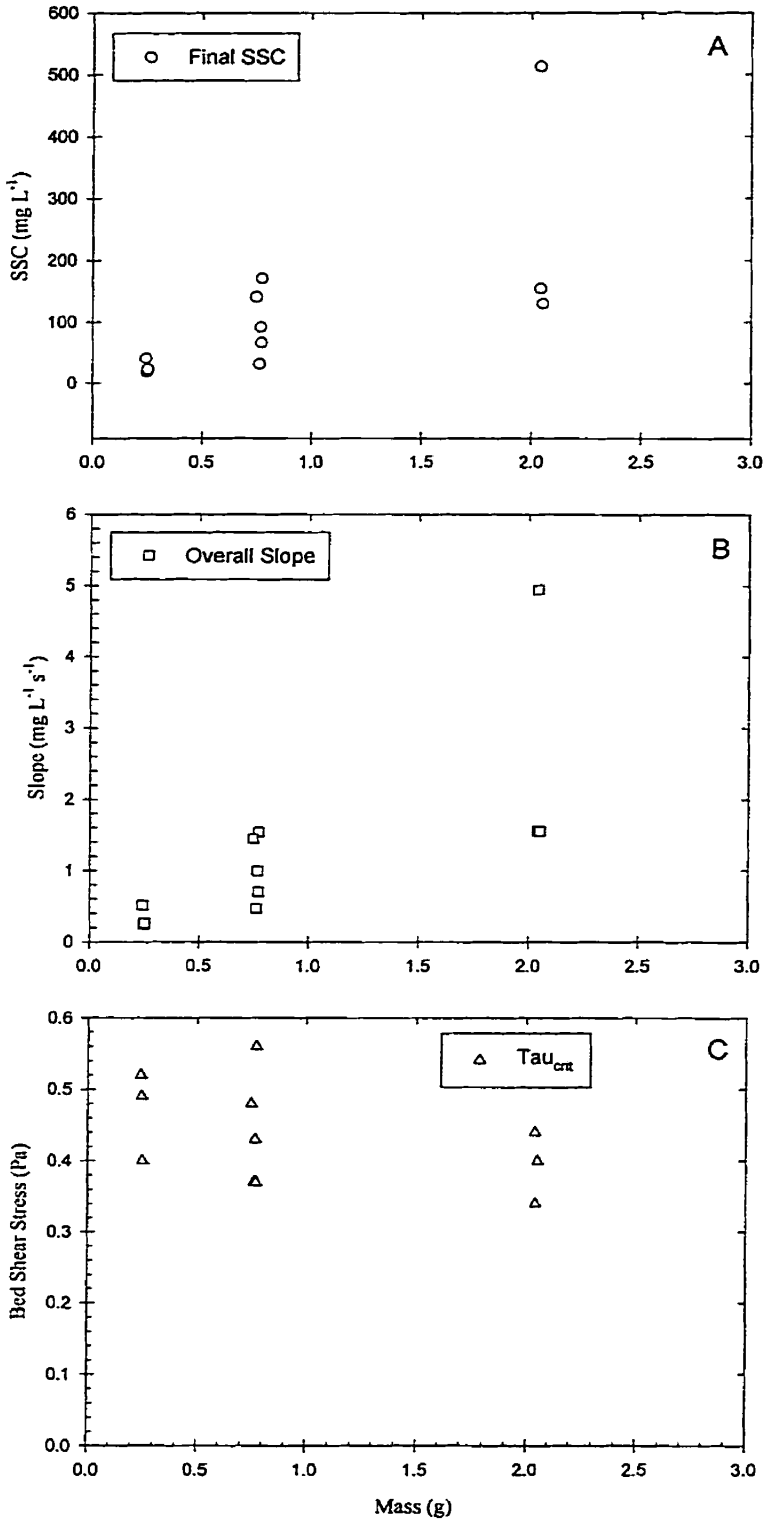

Figure 17. Graphs of final SSC (A), overall slope (B), and critical erosion threshold (C) versus algal mass for the three *Furcellaria* size treatments.

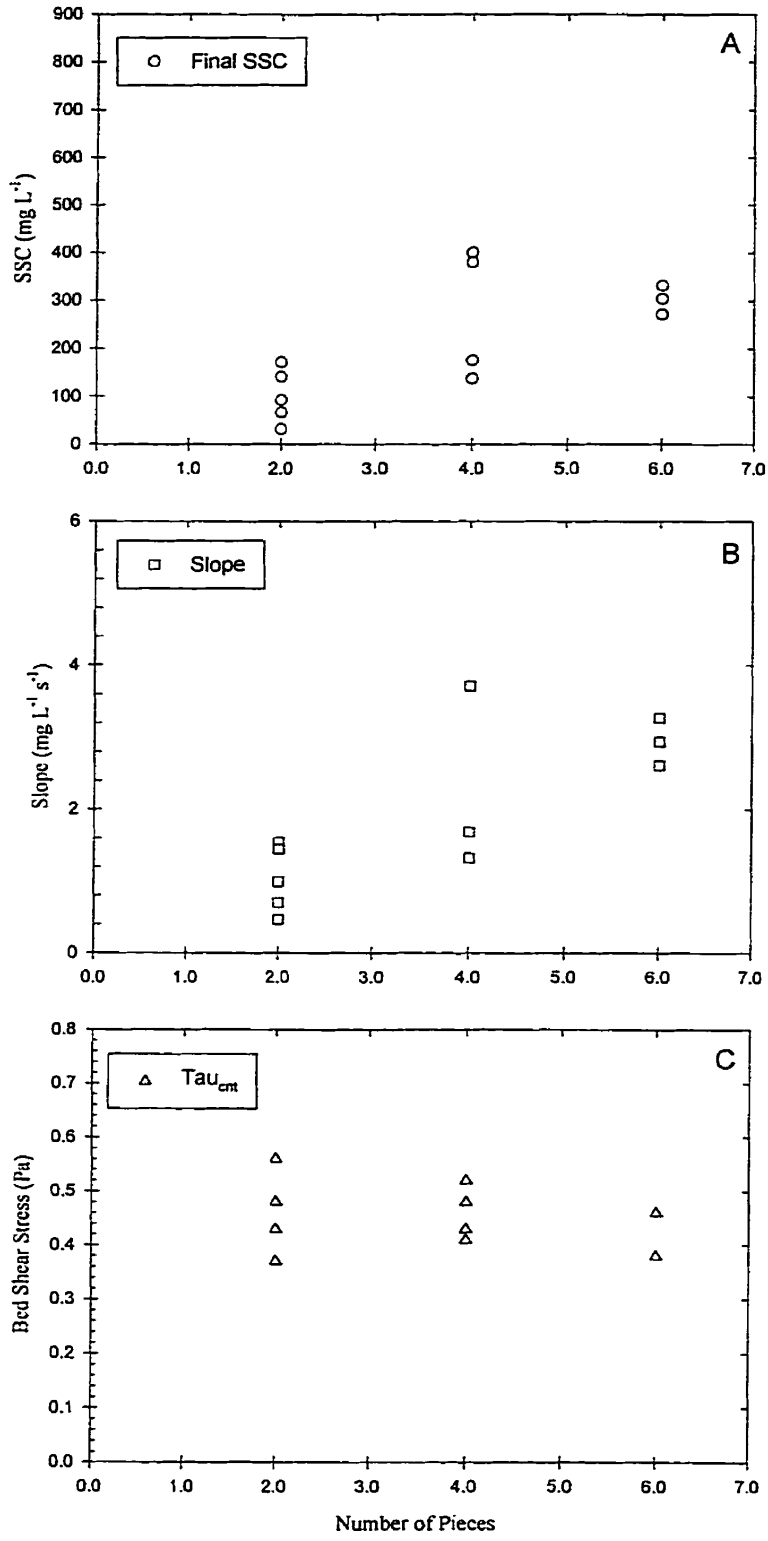

Figure 18. Graphs of final SSC (A), overall slope (B), and critical erosion threshold (C) versus algal abundance for the three *Furcellaria* abundance treatments.

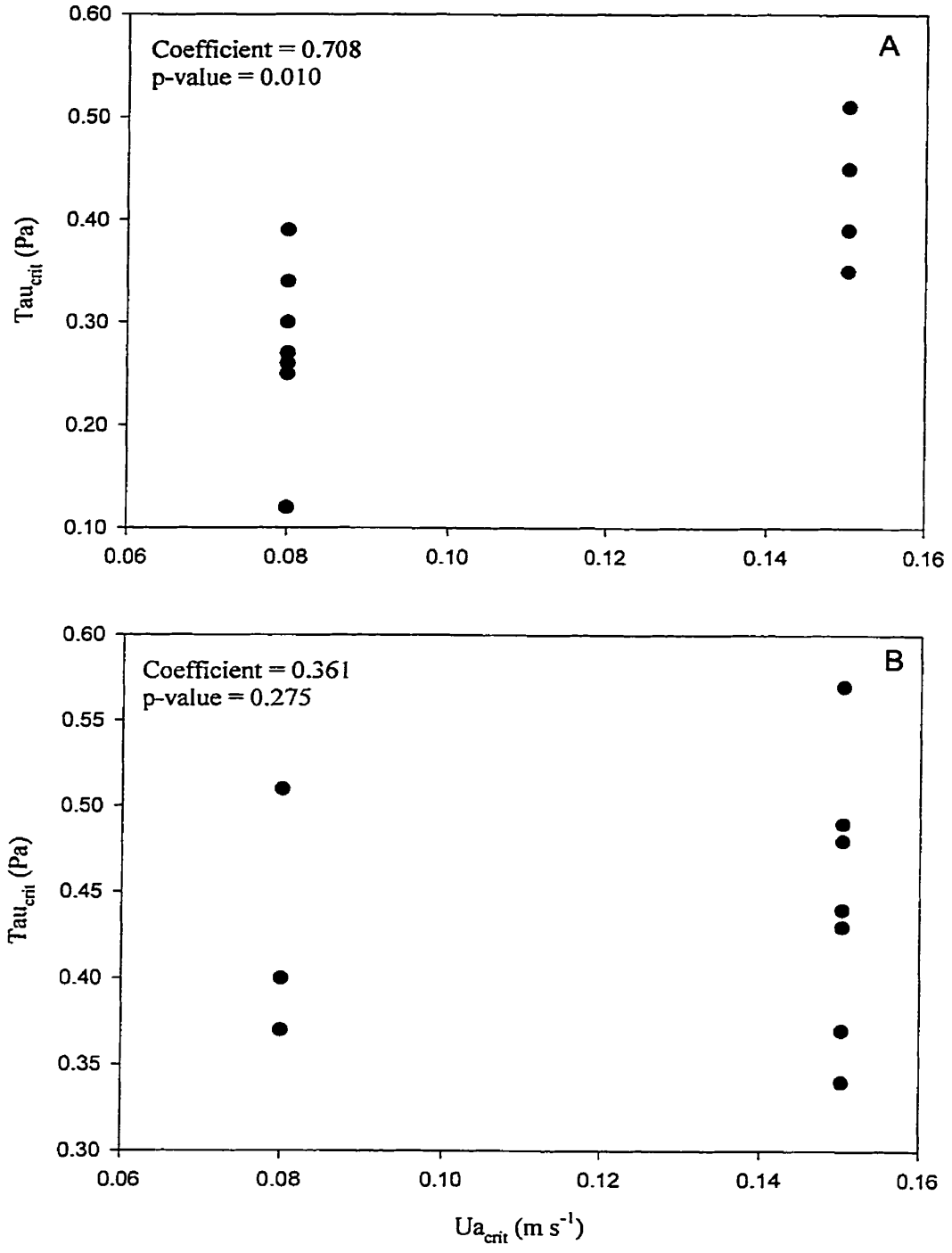

Figure 19. Scatter plots of critical erosion threshold (Tau_{crit}) vs. the current velocity that initiated algal motion (Ua_{crit}) for *C. crispus* (A) and *F. lumbricalis* (B).

3.4 ALGAL VELOCITIES AND PERCENT ENERGY TRANSFER

Average individual, and aggregates consisting of two and three pieces had similar velocities with respect to current velocity for both *C. crispus* and *F. lumbricalis* (see Fig. 20). Figure 20 shows that the velocities of individual pieces of alga versus aggregates consisting of two and three pieces were less variable with respect to one another for *C. crispus* than those of *F. lumbricalis*. Results showed that aggregates consisting of three pieces move slightly slower than those consisting of two pieces; which in turn, moved slightly slower than an individual piece.

Graphs of algal velocity (U_a), the difference between current velocity and algal velocity (U_y-U_a), and the approximate percent energy transfer versus current velocity are presented in figures 21-26.

Results of the Pearson correlation performed on the size treatment data (table 3) show that correlations between the rank of the final SSC and the rank of U_a within a treatment were not significant for *C. crispus* (correlation coefficient = -0.540, p-value = 0.070) or for *F. lumbricalis* (correlation coefficient = -0.582, p-value = 0.061). Yet, when ranks for both species were combined (to increase the number of observations) 56.0 % of the variability (p-value = 0.005) of ranked final SSC within a treatment could be explained by the ranked U_a. However, U_a was found to be an insignificant predictor variable (p-value = 0.136) for erosion rate when it was incorporated into the multiple regression model.

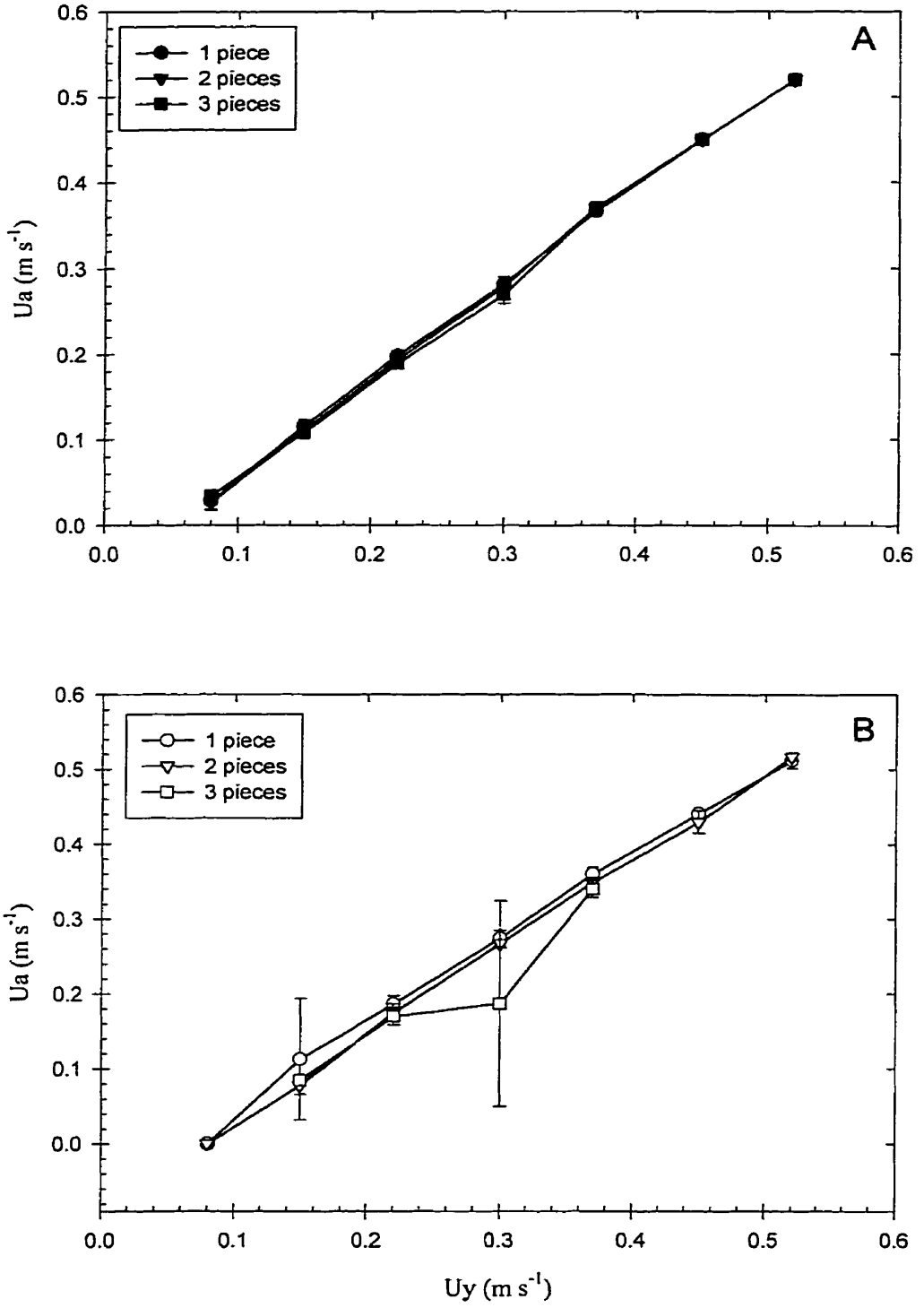

Figure 20. Average algal velocities for individuals and aggregates consisting of 2 and 3 pieces of *C. crispus* (A) and *F. lumbricalis* (B). Note: error bars display 1 sd.

Species/Group	Correlation Coefficient	P-value
C. crispus	-0.540	0.070
F. lumbricalis	-0.582	0.061
C. crispus + *F. lumbricalis* (grouped together)	-0.560	0.005

Table 3. Correlation coefficients and respective p-values for the ranked algal velocities (U_a) versus ranked final suspended sediment concentrations.

a. *Chondrus Size*

Results within *Chondrus* size treatments showed that the small size treatment (Fig. 21) appeared to display less variability with respect to algal velocities and percent energy transfer than the medium (Fig. 22) and large (Fig. 23) size treatments. However, all three size treatments displayed a similar trend with respect to U_y: both U_y-U_a, and the estimated percent energy transfer decreased with respect to current velocity until they reached values of 0 m s^{-1} and 0 % respectively. Velocity differences between current and algal velocity and percent energy transfer reached a value of 0 when the algae entered into continuous suspension. During this phase the algae were completely suspended in the water column and were travelling at the same velocity as the current; therefore, the algae could not transmit energy to the bed. In addition, trials 1 and 3 of the small size treatment and trials 1, 2, 4 and 6 of the medium size treatment maintained constant U_y-U_a values during velocity steps 3 and 4 (i.e. the first 2 two steps of the suspension and sliding phase). After velocity step 4 the algal velocities continued to approach those of the current velocity. Nonetheless, the estimated percent energy transfer, which is a relative comparison with respect to U_y, did not level off to a constant value during these

trials. Percent energy transfer continued to decrease with respect to U_y for all of the trials within size treatments.

b. *Furcellaria Size*

Results within the *Furcellaria* size treatments are similar to those of *Chondrus*. The *Furcellaria* small size treatment (Fig. 24) displayed the least amount of variability with respect to algal velocities and percent energy transfer than the medium (Fig. 25) and large (Fig. 26) size treatments. Furthermore, all three treatments displayed a similar trend with respect to current velocity: both U_y-U_a and the percent energy transfer decreased with respect to U_y. However, only pieces in trial 1 of the small size treatment entered into continuous suspension and ceased to contact the bed. Moreover, even though trial 1 of the small size treatment was the only trial that contained algae that entered continuous suspension, trials 2 and 3 of the small size treatment, trials 1, 3 and 4 of the medium size treatment and trial 2 of the large size treatment contained pieces that reached the same velocity as U_y during step 7. The remaining trials within the three size treatments traveled at a velocity slower than that of the current velocity; therefore, they may have transmitted this "lost" momentum/energy to the bed.

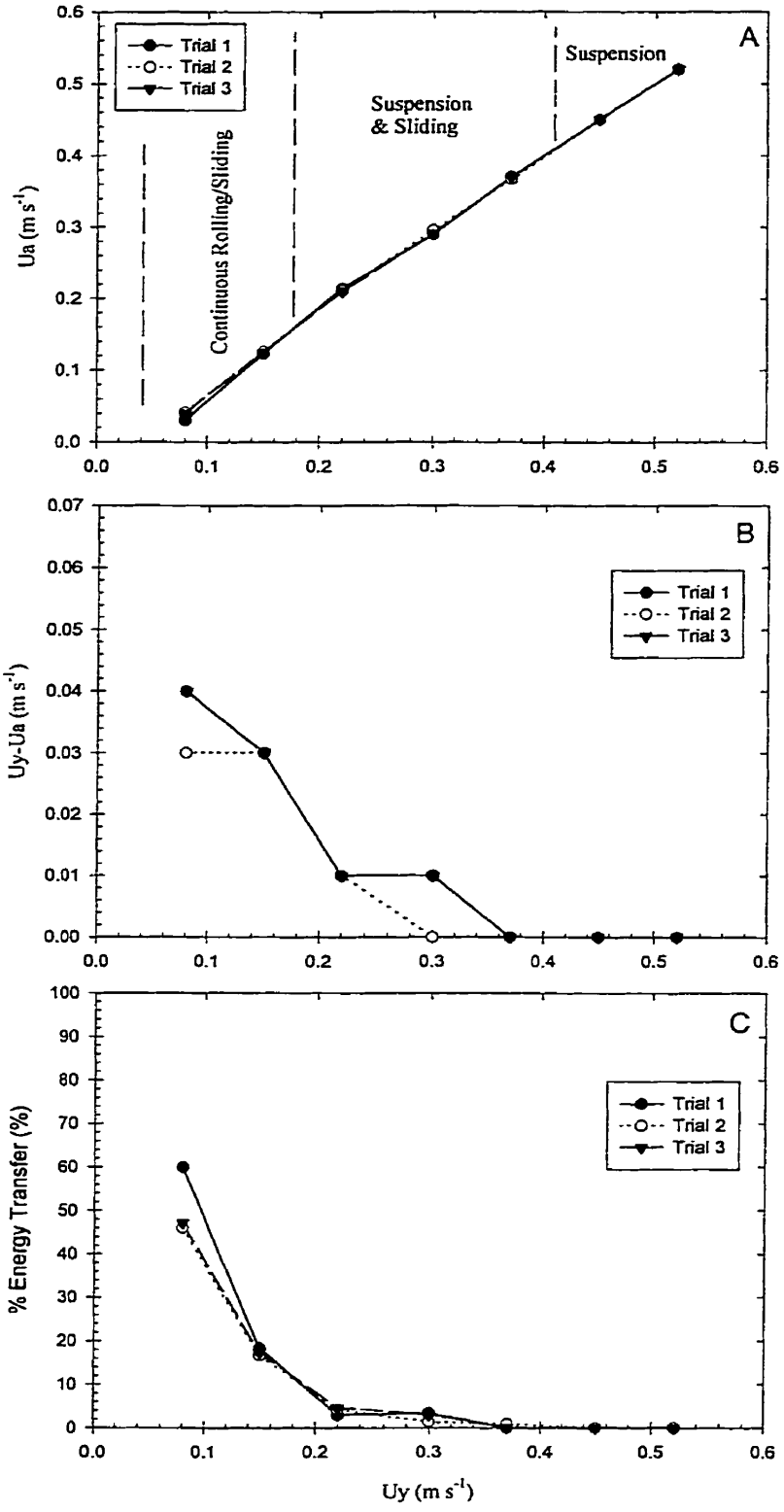

Figure 21. Graphs of algal velocity (A), current velocity minus algal velocity (B), and % energy transfer (C) for respective current velocities of the *Chondrus* small size treatment.

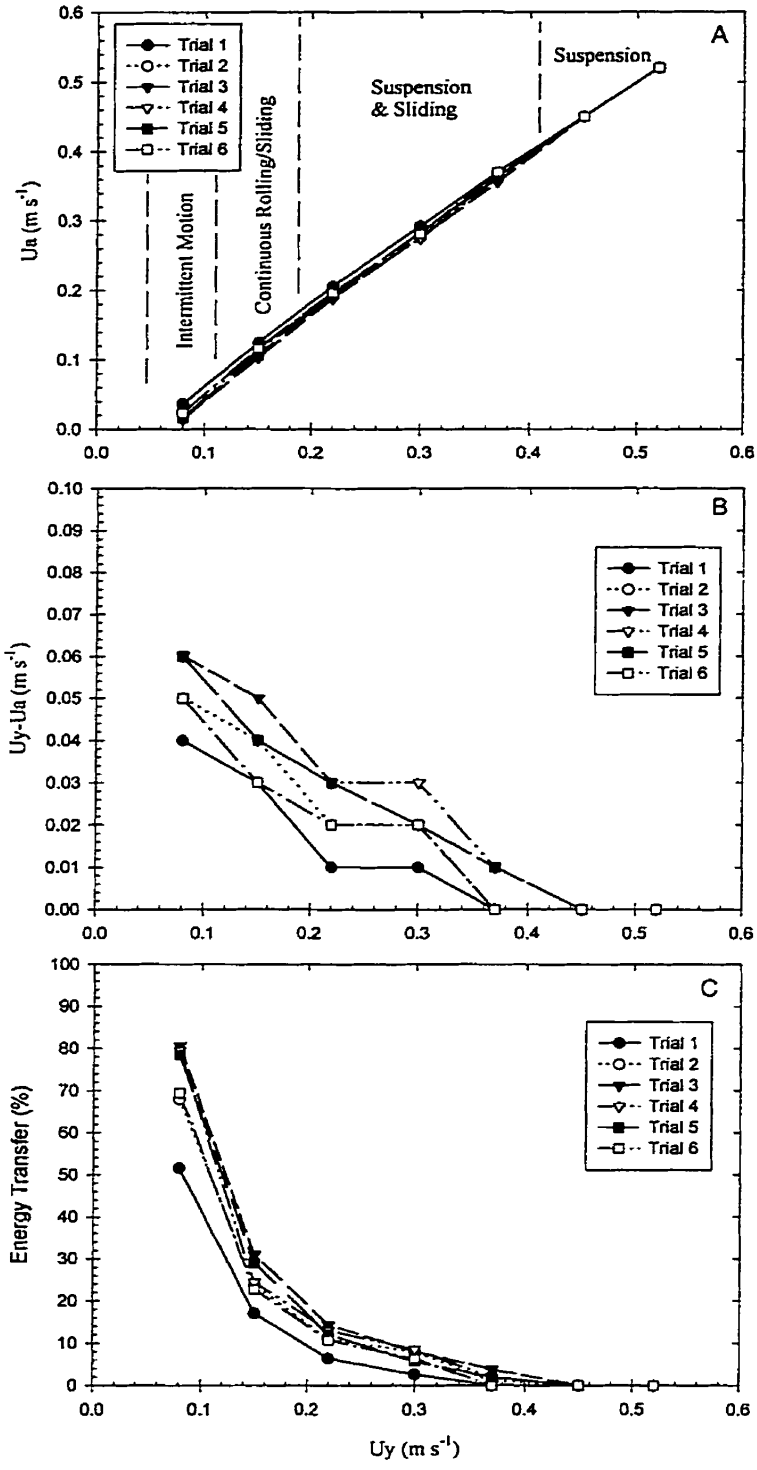

Figure 22. Graphs of algal velocity (A), current velocity minus algal velocity (B), and % energy transfer (C) for respective current velocities of the *Chondrus* medium size treatment.

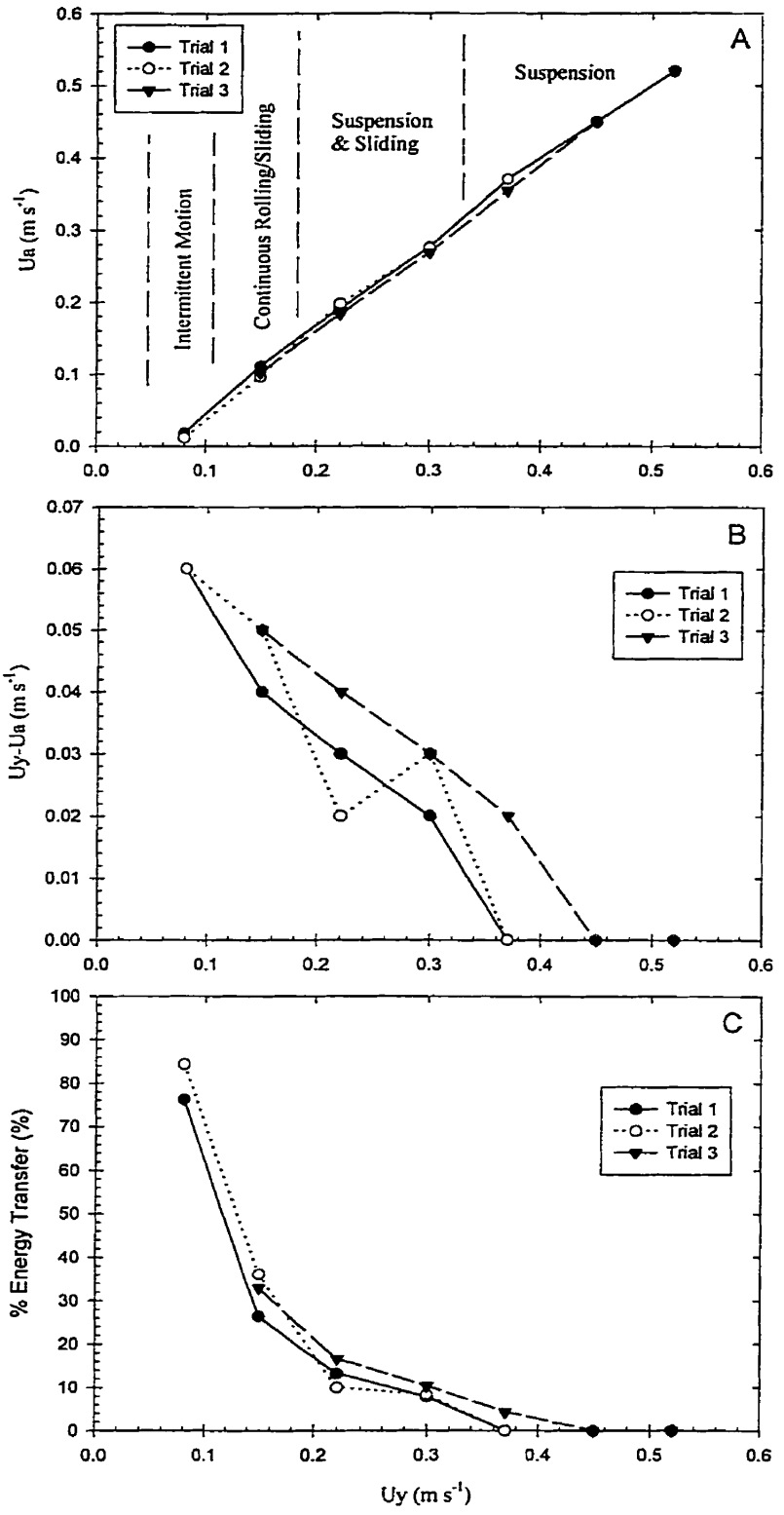

Figure 23. Graphs of algal velocity (A), current velocity minus algal velocity (B), and % energy transfer (C) for respective current velocities of the *Chondrus* large size treatment.

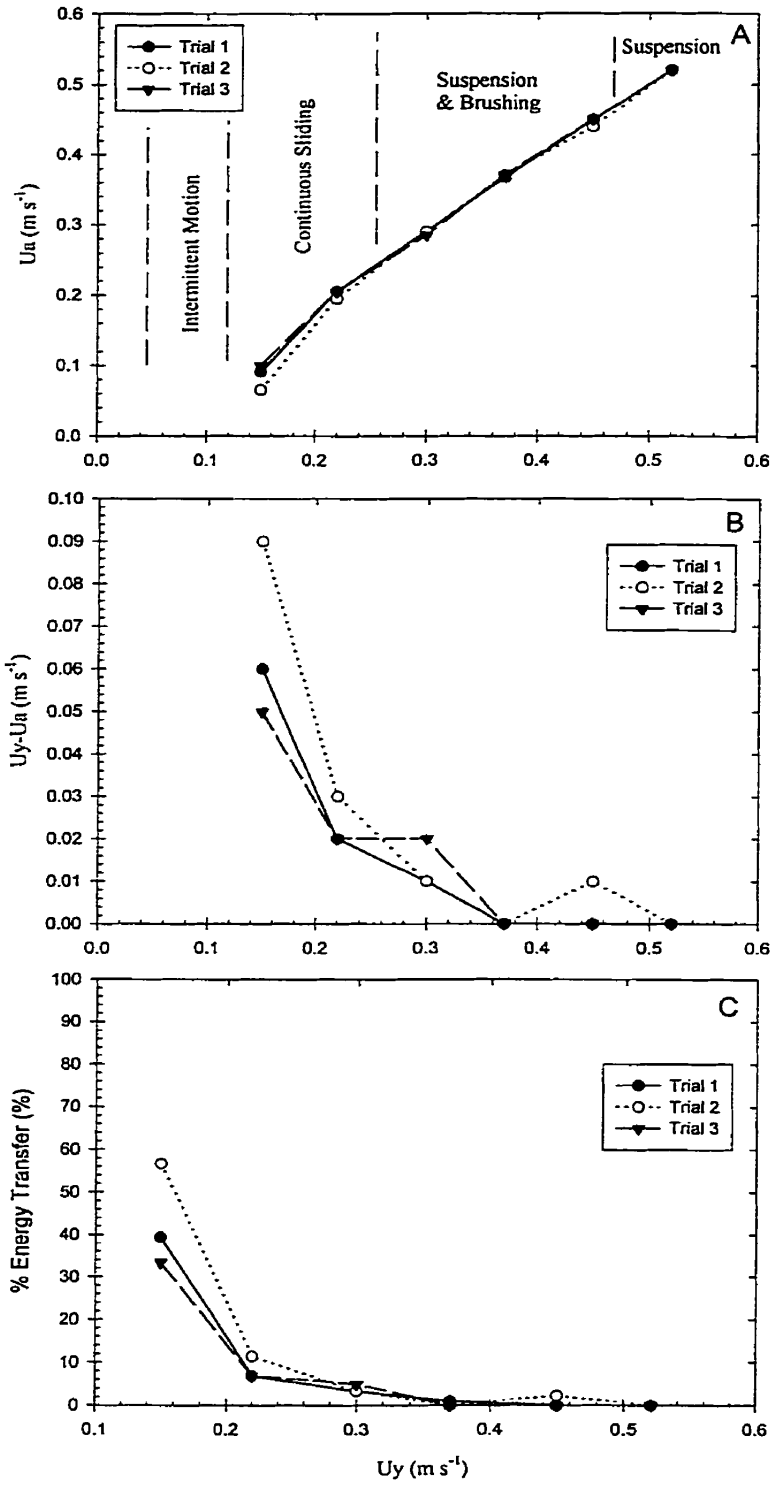

Figure 24. Graphs of algal velocity (A), current velocity minus algal velocity (B), and % energy transfer (C) for respective current velocities of the *Furcellaria* small size treatment.

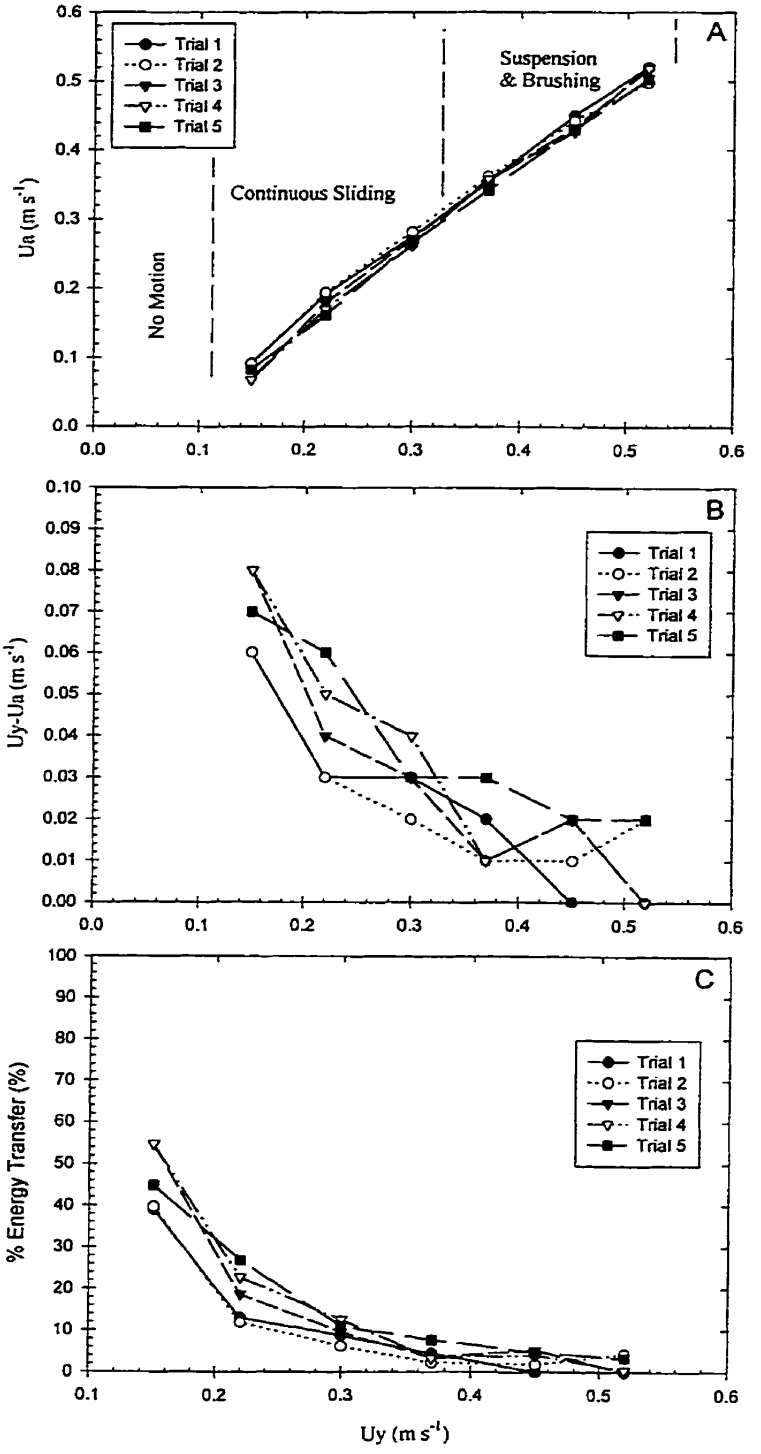

Figure 25. Graphs of algal velocity (A), current velocity minus algal velocity (B), and % energy transfer (C) for respective current velocities of the *Furcellaria* medium size treatment.

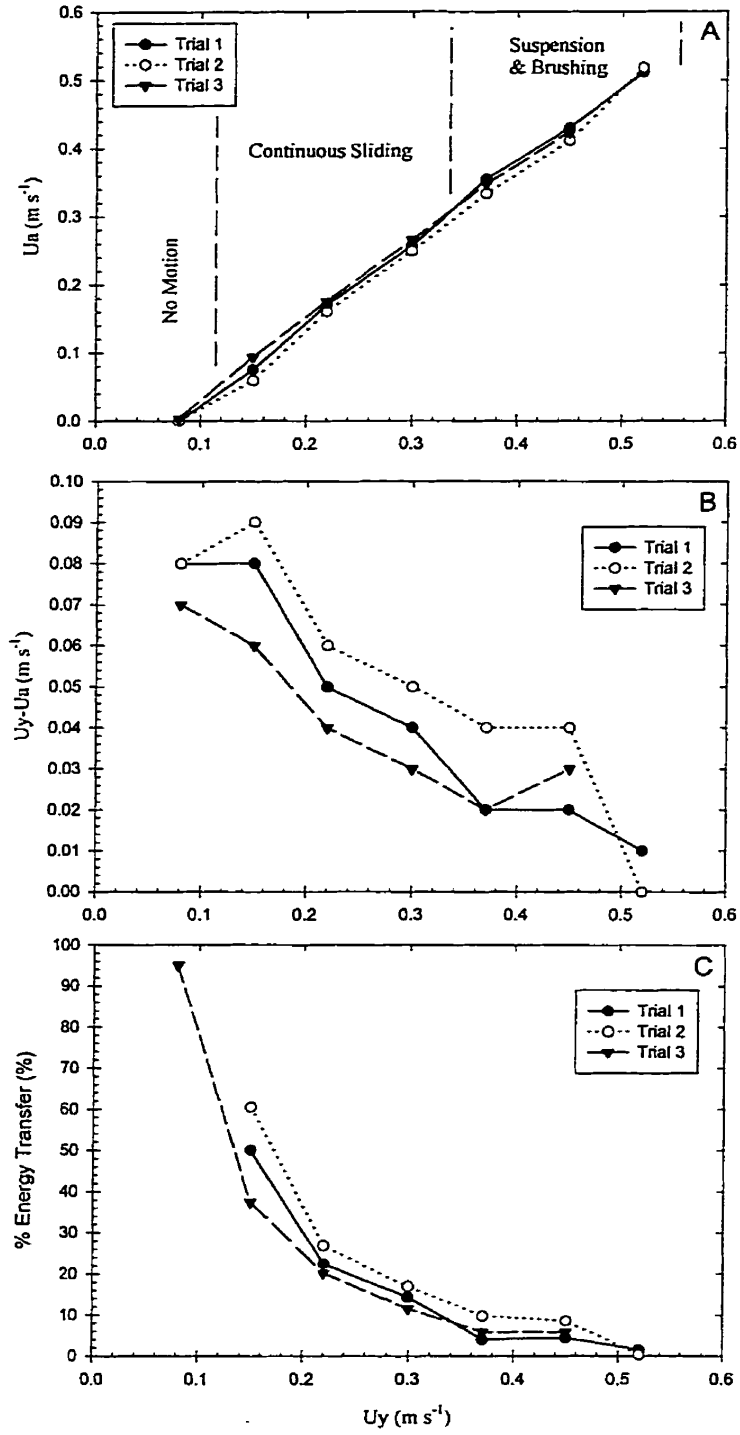

Figure 26. Graphs of algal velocity (A), current velocity minus algal velocity (B), and % energy transfer (C) for respective current velocities of the *Furcellaria* large size treatment.

3.5 EROSION RATES

a. *Overall Analysis*

Results of a multiple regression analysis performed on all of the size treatment erosion rate data showed that 40.3 % of the variability could be explained by the measured parameters, which are displayed in table 4.

Results of the multiple regression analysis showed that: 1) Current velocity (p-value < 0.001); 2) algal contact time with the bed (p-value < 0.001); and 3) the species of macroalgae used (p-value = 0.010), statistically altered the erosion rates of the artificial bed. Furthermore, the multiple regression analysis showed that the erosion rates of the small and medium size categories for both species (i.e. *Chondrus* and *Furcellaria* combined) were statistically lower than those of the large size category (p-value < 0.001). However, this analysis showed that the erosion rates of the medium and small size categories were not statistically different from one another (p-value = 0.918). Furthermore, individual r-squared values revealed that the percent contact of the algae and the current velocity within the flume were the most significant predictor variables in the model (r-squared = 0.195 and 0.125 respectively).

Variance inflation factors (VIF) showed that the correlations between percent contact and current velocity, algal velocity and mode of transport were great enough to significantly affect the overall fit of the model (i.e. VIF > 10); therefore, these variables were removed from the model as part of the backward elimination process. All other predictors within the remaining multiple regression model were re-checked using variance inflation factors to ensure that any remaining correlations between predictors (see Table 5) would not significantly influence the fit of the model.

Predictor	Coefficient	Standard Deviation	P-Value	r^2	VIF
U_y	28.474	5.121	< 0.001	0.125	6.2
% Contact	0.13142	0.01889	< 0.001	0.195	6.7
Species	1.8619	0.7108	0.010	0.028	1.4
Medium vs. Small Size	0.0793	0.7662	0.918	4.23×10^{-5}	1.6
Large vs. Small Size	3.612	0.8768	< 0.001	0.068	1.5

Table 4. Predictor variables and their respective coefficients, standard deviations, p-values, r-squared (r^2) values, and variance inflation factors (VIF) which were incorporated into the multiple regression model. Overall r-squared = 0.403 (p-value < 0.001).

	U_y	% Contact	Species	Medium vs. Small Size	Large vs. Small Size
U_y	1.000 < 0.001	-0.885 < 0.001	0.000 > 0.999	0.000 > 0.999	0.000 > 0.999
% Contact	-0.885 < 0.001	1.000 < 0.001	-0.219 0.006	0.019 0.813	0.093 0.253
Species	0.000 > 0.999	-0.219 0.006	1.000 < 0.001	0.045 0.567	-0.026 0.745
Medium vs. Small Size	0.000 > 0.999	0.019 0.813	0.045 0.567	1.000 < 0.001	-0.569 < 0.001
Large vs. Small Size	0.000 > 0.999	0.093 0.253	-0.026 0.745	-0.569 < 0.001	1.000 < 0.001

Table 5. Correlation matrix showing correlation coefficients (top number within a given cell) and respective p-values (bottom number in same cell) for comparisons between predictor variables within the multiple regression model.

Percent time as aggregates, algal velocities, estimated % energy transfer, and the interaction between species and the three size categories were found to be statistically insignificant predictor variables after completion of the backward elimination process.

b. *Controls*

Since erosion of the prepared bed was not achieved for the control trials, the erosion rates for all seven steps of all of the trials were essentially equal to 0 mg m^{-2} s^{-1}.

c. *Chondrus Size*

2-way ANOVA (the two factors being analyzed were size and U_y) results showed that algal size had an effect on the erosion rates of the beds (p-value = 0.034). Furthermore, visual examination of the graphs showed that the average erosion rates were greater for the larger pieces than the smaller pieces (Figs. 27 and 29). Erosion rates varied with current velocity. Erosion rates increased from the initial current velocity step to a maximum erosion rate, then declined to a rate of 0 mg m^{-2} s^{-1} over the course of the remaining velocity steps. Peak erosion rates were achieved at higher current velocities for the larger pieces than for the smaller pieces. Trials within the small size category reached their peak erosion rate at 0.15 m s^{-1}. Trials 1 and 4 in the medium size category reached their peak erosion rate at 0.15 m s^{-1}; whereas, trials 2, 3, 5 and 6 reached their peak erosion rate one step later at 0.22 m s^{-1}. Trials 2 and 3 of the large size category reached the peak erosion rates at 0.30 m s^{-1} and trial 1 reached its peak erosion rate one step earlier at 0.22 m s^{-1}.

d. *Chondrus Abundance*

2-way ANOVA (the two factors being analyzed were abundance and U_y) results showed that the number of *C. crispus* pieces had an effect on the erosion rates of the beds

(p-value = 0.028). Average erosion rates were greater for the higher abundance categories than the lower abundance categories (Figs. 28 and 29). Erosion rates varied with the current velocity. The graphs of the erosion rate versus current velocity show a similar pattern as the size category, with an increasing rate up to a maximum, followed by a decline to an erosion rate of 0 mg m^{-2} s^{-1} over the remaining velocity steps. The maximum rate of erosion was generally achieved at 0.22 m s^{-1} for all three abundance categories. Exceptions were trials 1 and 4 of the low abundance category and trial 1 of the medium abundance category: these trials achieved their maximum erosion rate one step earlier at a current velocity of 0.15 m s^{-1}.

e. *Furcellaria Size*

2-way ANOVA results showed that the size of *F. lumbricalis* had an effect on the erosion rates of the beds (p-value = 0.001). On average, trials with the larger pieces of *F. lumbricalis* had greater maximum erosion rates than the average trials of smaller pieces (Figs. 30 and 32). The overall shape of the erosion rate versus current velocity showed a similar trend to that of the *C. crispus* curves (i.e. increase to a maximum rate followed by a decline in erosion rate). However, the *F. lumbricalis* curves generally did not decline to an erosion rate of 0 mg m^{-2} s^{-1} at the final velocity step. Furthermore, trial 2 of the large size category had a second peak in erosion rate that occurred after the first peak. The second peak occurred at a current velocity of 0.37 m s^{-1}. This peak was not as large as the first and the erosion rate declined steadily afterward. The majority of trials in all of the size categories achieve their maximum erosion rate at a current velocity of 0.22 m s^{-1}. Exceptions were trial 3 in the medium size category and trial 1 in the large size category: they achieved their maximum rates of erosion at a current velocity of 0.30 m s^{-1}.

f. *Furcellaria Abundance*

2-way ANOVA results showed that the number of pieces had an effect on the erosion rates of the beds (p-value = 0.001). The average erosion rates for the medium and high abundance categories were similar in numerical value along with the shape of the erosion rate versus current velocity curve. However, both of these categories had greater erosion rates than the low abundance category. Shapes of these abundance curves (Figs. 31 and 32) were similar to those of the *C. crispus* curves; however, there was a less distinctive peak in erosion rate for the *F. lumbricalis* species. In many instances the erosion rates did not decline as quickly after the maximum values, as they did in the *C. crispus* graphs. In several instances the maximum erosion rate occurred over a range of current velocities, instead of having one clear maximum rate/peak. The shape of the curve in the low abundance category followed the typical profile in the majority of the trials (trials 1,2, 4 and 5). The typical profile showed an increase in erosion rate with changing current velocity to a maximum erosion rate, which occurred at 0.22 m s^{-1} followed by a decline in erosion rate. Trial 3 in the low abundance category reached its maximum rate of erosion at 0.30 m s^{-1}, which lasted into the next current step (U_y = 0.37 m s^{-1}) before declining in value. This trend was also evident in trial 1 and trial 2 (maximum rates of erosion at U_y = 0.22 to 0.30 m s^{-1}) of the medium abundance category and trial 1 and trial 2 (maximum rates of erosion at U_y = 0.22 to 0.30 m s^{-1}) of the high abundance category. Trial 3 of the medium abundance category and trial 3 of the high abundance category displayed the more typical trend of increasing to a maximum rate of erosion and then declining. Maximum rates of erosion were reached at current velocities of 0.22 m s^{-1} and 0.30 m s^{-1} respectively. Trial 4 of the medium abundance category

achieved two peaks in erosion rate: the first one occurred at a current velocity of 0.22 m s^{-1}; that was followed by a subsequent decline in erosion rate, which in turn was followed by a less significant second peak at a current velocity of 0.37 m s^{-1}.

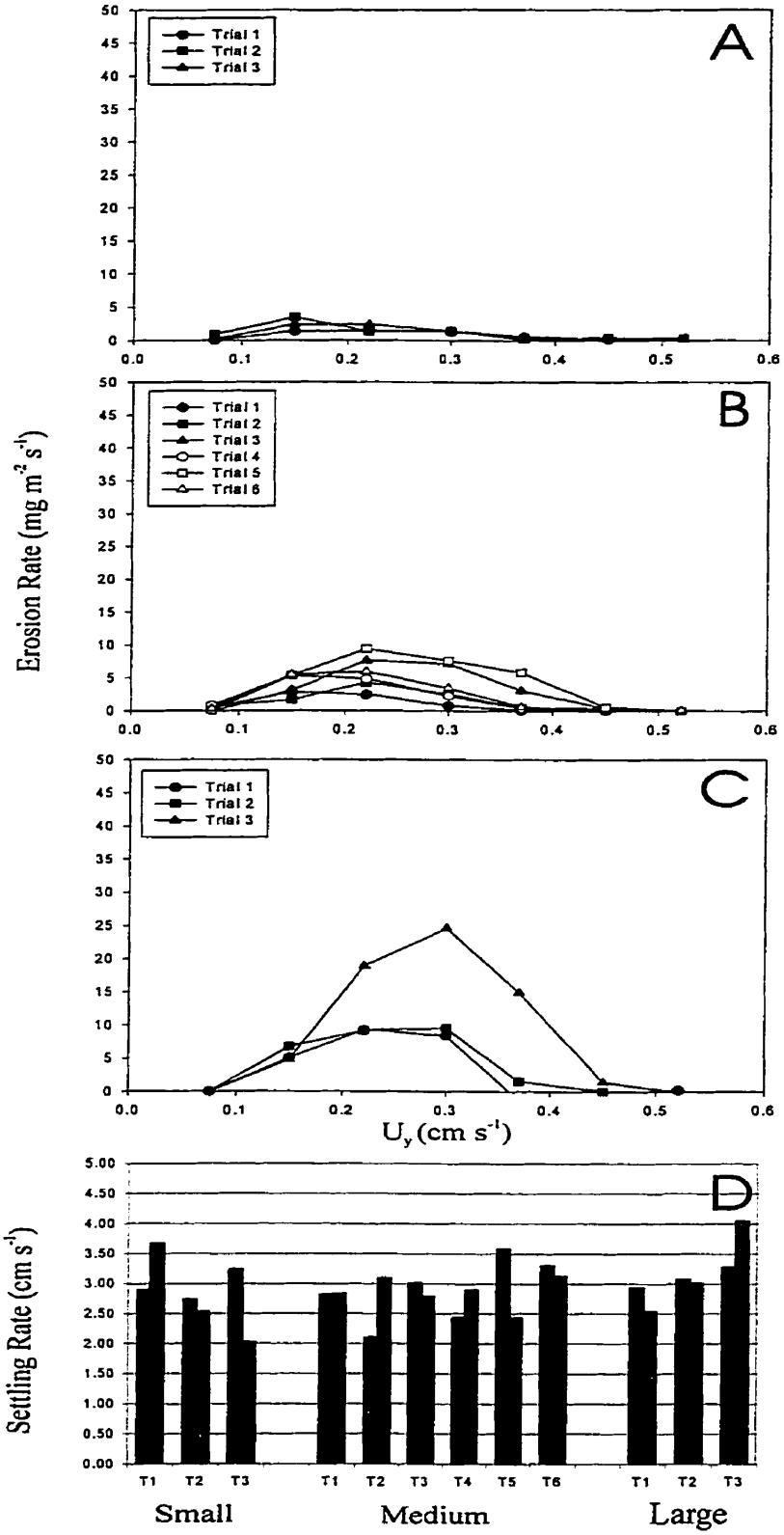

Figure 27. Erosion rates for the small (A), medium (B), and large (C) *Chondrus* size treatments and settling rates (D) of the algae used in these treatments.

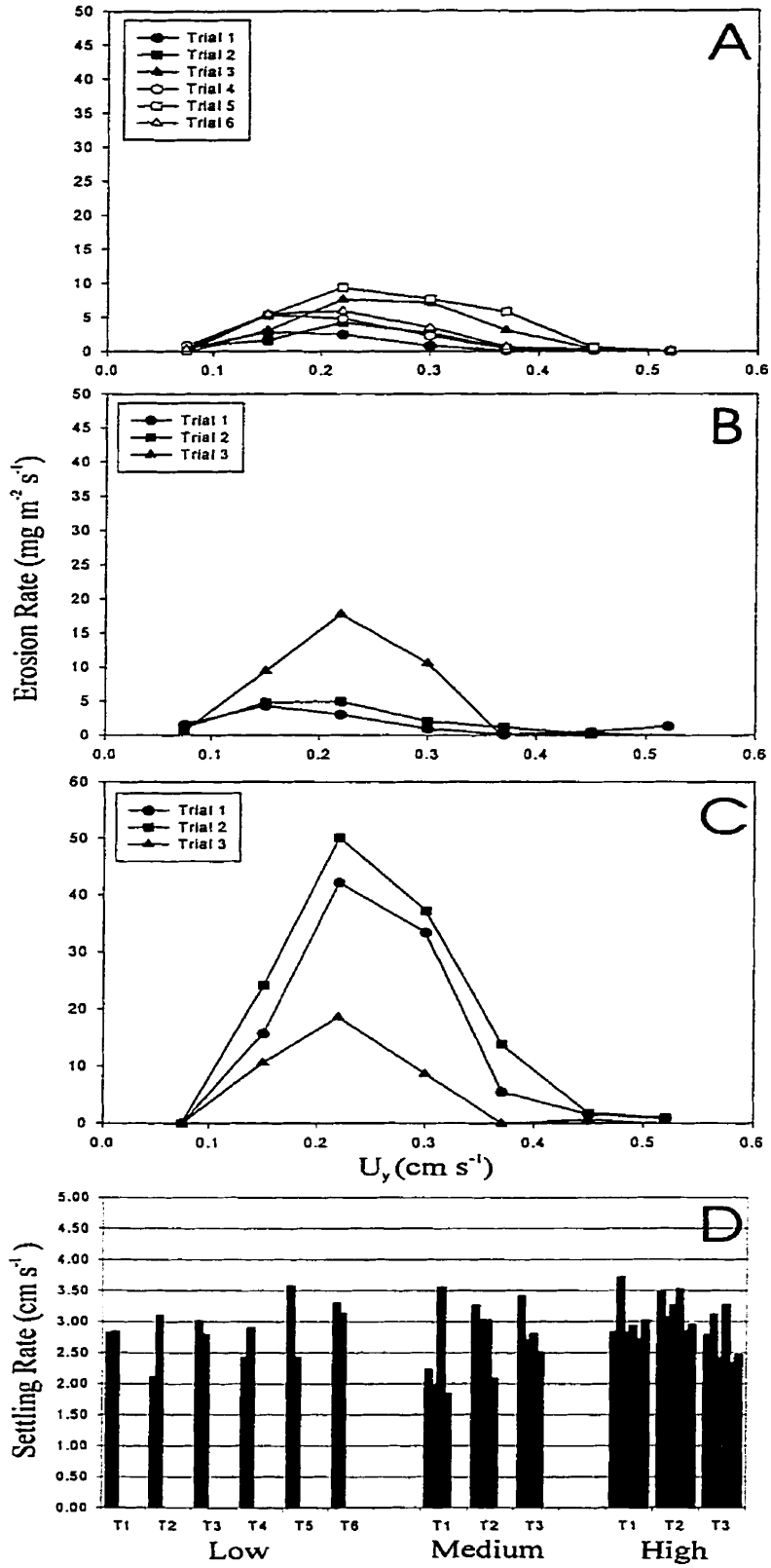

Figure 28. Erosion rates for the low (A), medium (B), and high (C) *Chondrus* abundance treatments and settling rates (D) of the algae used in these treatments.

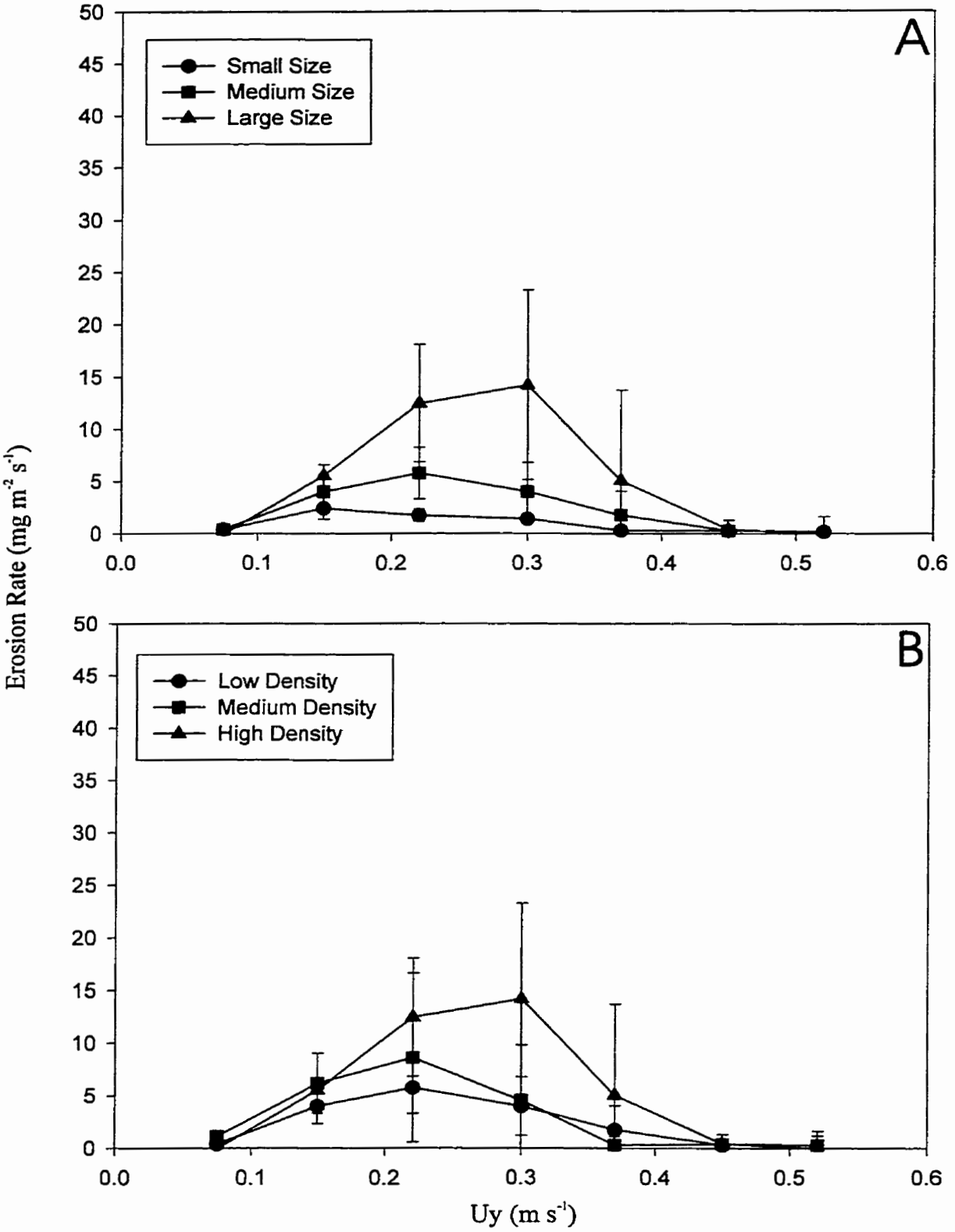

Figure 29. Average erosion rates (± 1 sd) of the trials within the *Chondrus* size (A) and abundance categories (B).

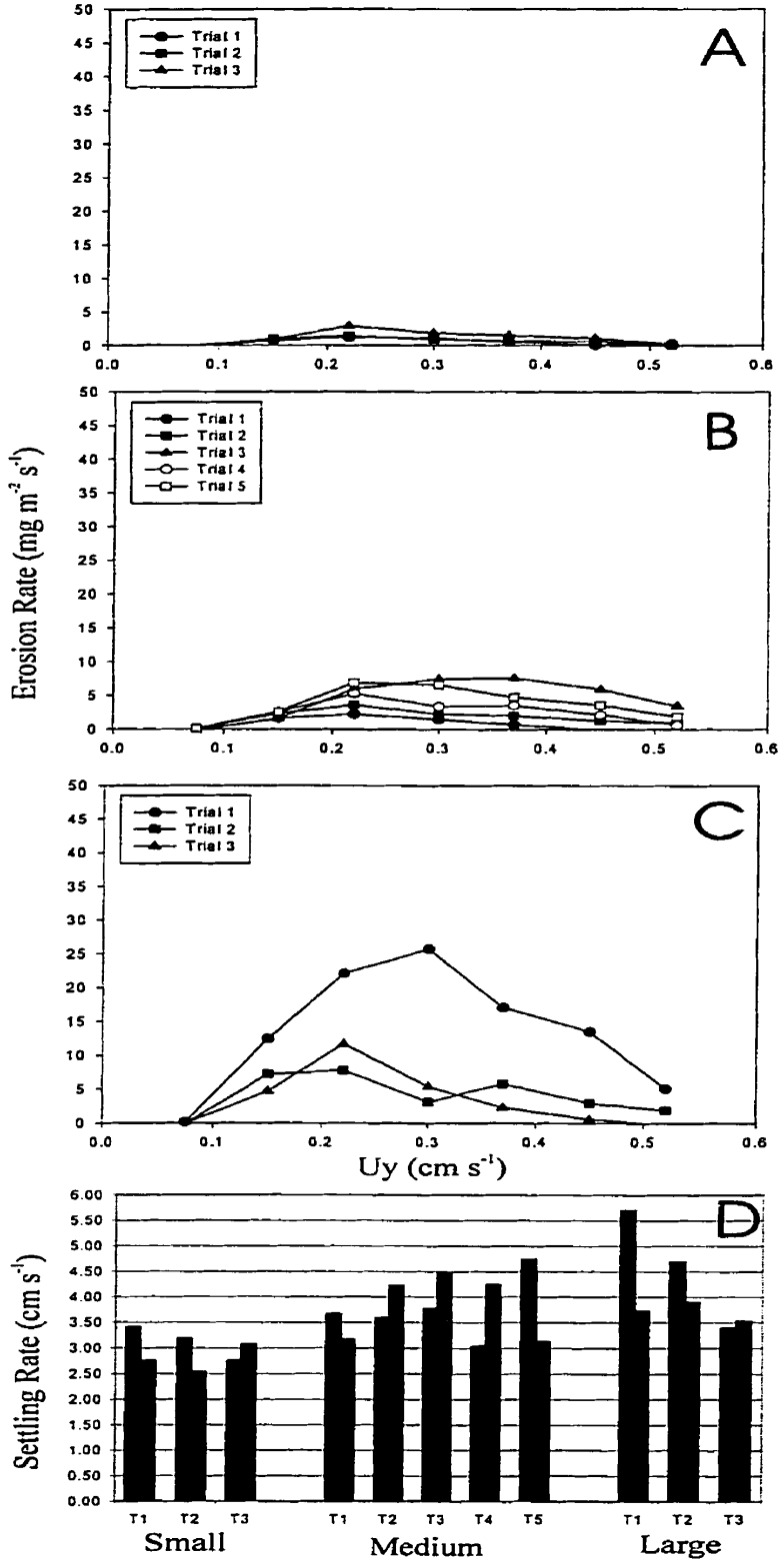

Figure 30. Erosion rates for the small (A), medium (B), and large (C) *Furcellaria* size treatments and settling rates (D) of the algae used in these treatments.

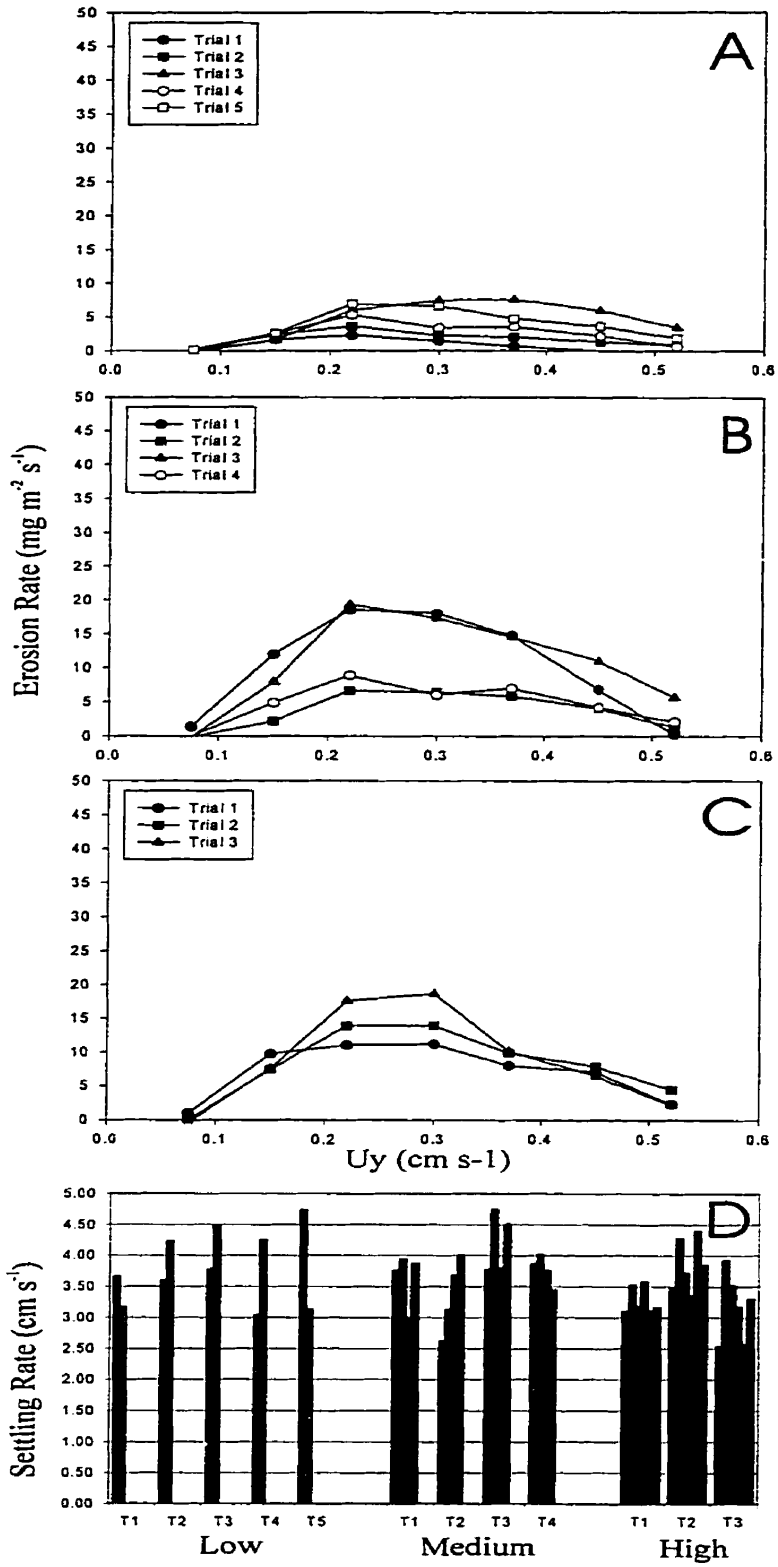

Figure 31. Erosion rates for the low (A), medium (B), and high (C) *Furcellaria* abundance treatments and settling rates (D) of the algae used in these treatments.

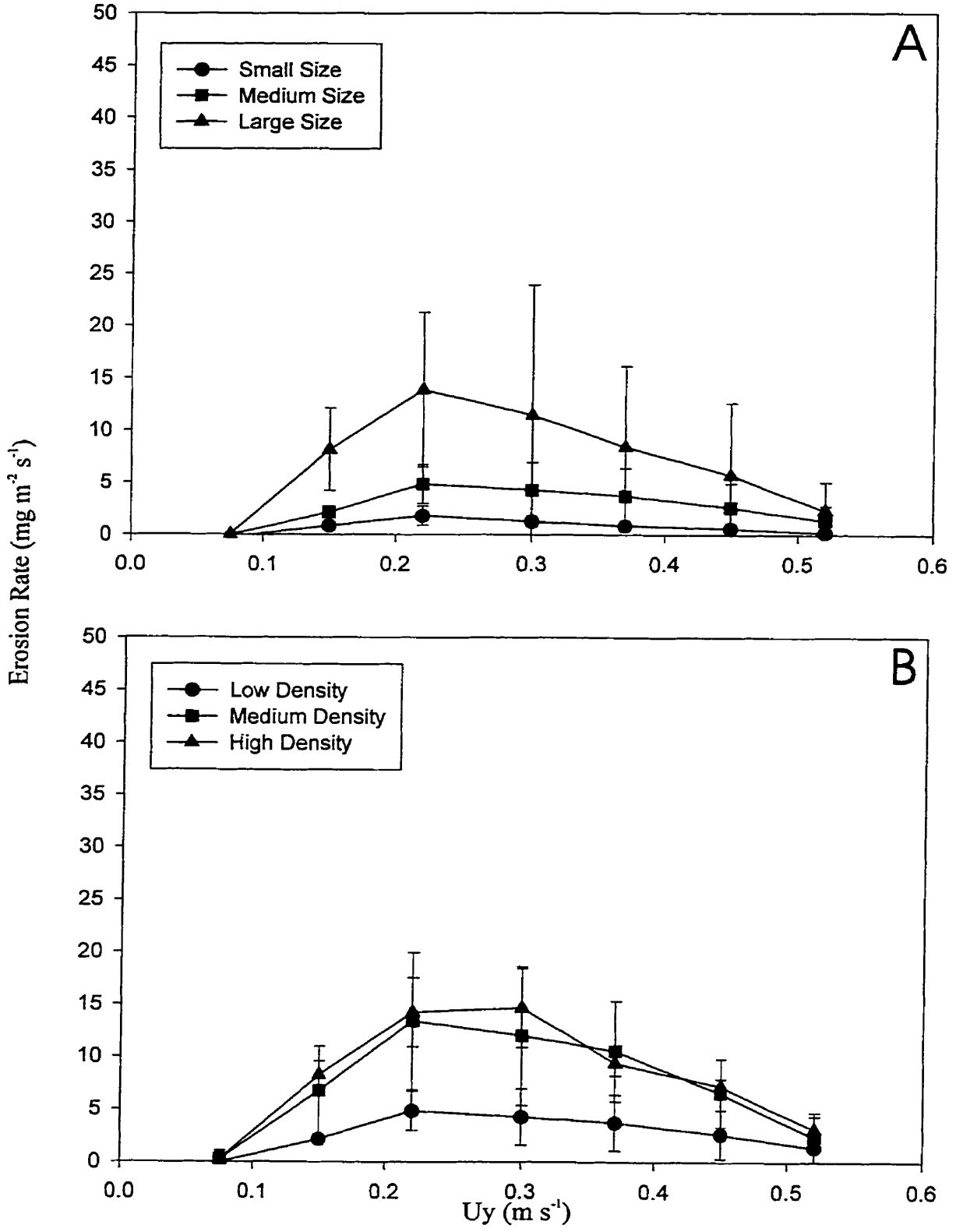

Figure 32. Average erosion rates (± 1 sd) of the trials within the *Furcellaria* size (A) and abundance (B) categories.

DISCUSSION

4.0 SETTLING RATES

Particulate settling rates are a function of the density of the fluid, and the size, shape and the density of the settling particle. Furthermore, the rate at which a particle settles is influenced by the upward forces of the fluid (i.e. the buoyancy of the fluid and the viscous resistance (drag)) and the downward force of gravity (Alldredge & Gotschalk, 1988, Boggs, 1995). Alldredge & Gotschalk (1988) mention that measuring drag coefficients for non-spherical particles is complex and is a function of shape and Reynolds number. Carrington (1990) showed that drag coefficients of macroalgae decrease with respect to current velocity and that macroalgae with vastly different morphologies (i.e. the pattern of branching and shape of thalli) had similar drag coefficients at high current velocities. Furthermore, Carrington (1990) concluded that drag coefficients (at high current velocities) could be approximated by measuring the area of a thallus and the water velocity to which it is exposed. Wet weight, length, branching morphology, papillar density (i.e. little round projections on thalli), and reconfiguration of the thalli at high water velocities were found to be of little predictive use by their study.

As mentioned above, defining the characteristics that govern the settling rates and drag coefficients of non-spherical particles (e.g. macroalgal fronds), is complex and was not explored in this study. However, a rudimentary explanation of the settling rates and behavior of *C. crispus* and *F. lumbricalis* is outlined below.

Settling rates of *Gracilaria* sp., collected from the lagoon of Venice appeared to be slower than those of *F. lumbricalis* collected from P.E.I. Correlation analysis revealed

that the settling rates of *F. lumbricalis* were correlated with the mass of the settling alga (correlation coefficient = 0.41, p-value = 0.002); whereas, those of *Gracilaria* sp., were not (correlation coefficient = -0.136, p-value = 0.690). Furthermore, settling rates of *C. crispus*, collected in P.E.I, overlapped those of *C. crispus* that were collected from the lagoon of Venice. An overall analysis of settling rate versus mass for *C. crispus* specimens collected from both areas showed that settling rates were not correlated with mass (correlation coefficient = 0.205, p-value = 0.082). Moreover, it was found that settling rates of *C. crispus* collected from P.E.I. were not correlated with algal mass (correlation coefficient = 0.111, p-value = 0.400); whereas, specimens collected from the lagoon of Venice were (correlation coefficient = 0.537, p-value = 0.039). Specimens collected from the lagoon of Venice covered a broader mass range than those collected from P.E.I. (see figure 3). Further analysis revealed that if the data from the smallest mass range (e.g. approximately 0.12 g) of the Venetian *C. crispus* were ignored, then the settling rates were no longer correlated with mass (correlation coefficient = 0.384, p-value = 0.218). This suggests that settling rates of *C. crispus* may increase with respect to mass to a point and then no longer increase in the same manner because of a surface area to mass relationship as outlined below.

Although both *C. crispus* and *F. lumbricalis* generally settled in a similar manner (i.e. both species settled with their longest axis perpendicular to the settling direction), the morphological differences between the two species had a significant impact on their settling rates. *F. lumbricalis* had a more elongate and less bushy morphology than *C. crispus*. In addition, the branches and stipes of *F. lumbricalis* were more cylindrical than those of *C. crispus*, which had much flatter morphologies. Dudgeon and Johnson (1992)

showed that macroalga morphologies that expose less surface area per unit biomass to flowing water had reduced hydrodynamic drag forces. If this theory is applied to settling velocities, then algae with less surface area per unit mass would experience less drag and therefore would settle at a faster rate than algae with a greater surface area per unit mass. Therefore, the sleeker morphology of *F. lumbricalis* may have enabled it to have settling rates that were more correlated with mass, as there was less surface area (drag) with respect to mass to slow the settling alga. On the contrary, settling rates of *C. crispus* were not significantly correlated with the mass of the alga. This lack of correlation resulted from the excess drag produced by the broad "bushy" thallus, which slowed *C. crispus'* settling rates more than the mass increased them. For example, pieces of *C. crispus* generally settled with their stipe facing downward, followed by the branches, which were spread out above the stipe. Spreading of the branches greatly increased the surface area of the alga and slowed the settling rate (i.e. the spread out branches behaved like a parachute for the settling alga). Furthermore, as the mass of the alga increased, so did the surface area and number of the trailing branches, which in turn, counteracted the increased mass of the larger pieces.

As mentioned earlier, the scatter plot of mass versus settling velocity (Fig. 3) showed that *F. lumbricalis* specimens collected from the shores of P.E.I had faster settling velocities than *Gracilaria* sp. specimens collected from the lagoon of Venice. The difference in settling velocities and the differences in branching patterns between *F. lumbricalis* and *Gracilaria* sp. would suggest that the erosion experiments involving *F. lumbricalis* would not directly represent the impact of *Gracilaria* sp. specimens from the lagoon of Venice. However, it is believed that both *Gracilaria* sp. and *F. lumbricalis*

would follow the same general mode of transport pattern with respect to current velocity (e.g. intermittent motion, continuous sliding/brushing, mixture between sliding/brushing and suspension, and continuous suspension). Furthermore, the choice of *F. lumbricalis* was still of use as it demonstrated the impact of a species of different morphology than that of *C. crispus*.

4.1 FLUME EROSION EXPERIMENTS

Overall, laboratory flumes are great assets for measuring physical processes in benthic environments. They allow one to make detailed observations and measurements while controlling the speed in which water flows through the system and the turbulent stress exerted by the fluid on the substrate (Muschenheim *et al.*, 1986). Moreover, Muschenheim *et al.* (1986) stated that large scale detritus transport and small scale food availability are best addressed with the use of a laboratory flume, as these experiments are more replicable and well characterized than they would be if carried out in the field.

The fluid induced erosion threshold did not appear to be attained during the control experiments. Appendix I shows that the majority of estimates of the fluid induced erosion threshold was near 0 Pa. However, this is not an accurate estimate of the erosion threshold. On the contrary, it is an artifact of having a small increase in SSC with respect to U_y; therefore, the determination of the erosion threshold by the extrapolation method was not valid for the control trials. Moreover, it was concluded that this threshold would occur at a current velocity greater than 0.52 m s^{-1} as the SSC increase was negligible up to this point. This lack of erosion during the control experiments did not allow for direct comparisons with erosion thresholds of the algal experiments. However, it can be concluded that the addition of algae to the flume caused the beds to erode at lower current

velocities than they would have from the fluid shear stress alone (see Appendix I). Furthermore, results of the erosion experiments showed that both species of macroalgae significantly increased the suspended sediment concentrations (SSC) and the erosion rates of the clay beds over those of the control experiments (Appendices J and K). Despite the large degree of variation within treatments, 2-way ANOVA results showed that both size and abundance of *C. crispus* (p-values = 0.034 and 0.028 respectively) and *F. lumbricalis* (p-values = 0.001 and 0.001 respectively) influenced the erosion rates of the artificial beds. However, 1-way ANOVA results showed that erosion thresholds did not appear to be significantly affected by size or abundance for *C. crispus* (p-values = 0.071 and 0.151) and *F. lumbricalis* (p-values = 0.430 and 0.573 respectively).

a. *Variability within treatments*

The high degree of suspended sediment variation within the majority of treatments can be attributed to a variety of factors. Correlation analysis revealed that the ranks of the average algal settling rates used in each trial were correlated with the ranks of the final suspended sediment concentrations within respective treatments (correlation coefficient = 0.433, p-value = 0.008). Thus, a significant amount of the ranked SSC variability within treatments was explained by the average settling rate of the algae used in the trial (i.e. the faster the average algal settling rate, the greater the final SSC). Furthermore, the same type of analysis revealed that ranked final SSC were correlated with the ranked algal velocities within treatments (correlation coefficient = - 0.560, p-value = 0.005). Thus, trials containing slower moving algae with respect to U_y had higher final SSC than those with faster moving pieces. In theory, the slower moving pieces would be transmitting more energy to the bed; therefore, their impact on the erosion rate

of the sediment would be greater than those that transmit less energy (Amos *et al.*, in press).

Other factors that could explain the SSC variation within treatments include variability in the shear strength of the artificial clay bed, the morphology and flexibility of the algae used in the experiments, per cent contact of the algae with the bed, and interactions between algae (e.g. % time as aggregates). Even though care was taken to ensure that the clay bed was prepared in a consistent manner before each experiment, there was no record of the cohesive strength of the bed before the experiment began. Control experiments showed that all of the prepared beds had fluid induced erosion thresholds greater than 0.52 m s^{-1}. However, since fluid induced erosion thresholds of the beds were never reached, it was not determined whether all of the beds had uniform shear strengths. There are some trials that appear to show evidence for variability of the bed's shear strength. In these treatments (e.g. *Chondrus* high abundance (Fig. 9), *Furcellaria* large size (Fig. 12), *Furcellaria* medium abundance (Fig. 13)) the SSC of the trials with the greater final SSC appear to always have greater SSC from the beginning and throughout the duration of the experiment. For example, the curve for trial 2 of the *Chondrus* high abundance treatment (Fig. 9) begins to increase earlier than trial 1 and trial 3 and continues to maintain a greater SSC throughout all of the velocity steps. The bed used for trial 2 may have had a lower shear strength than the other two beds within this treatment, causing it to fail more easily than the beds in trial 1 and trial 3. However, analysis of ranked erosion thresholds and final SSC within a treatment did not support this hypothesis. On the contrary, the highest SSC ranks within a treatment were correlated with the highest ranked critical erosion thresholds (correlation coefficient =

0.643, 0.004). This suggests that beds that failed at higher shear stresses yielded higher suspended sediment concentrations. This trend was also evident for *C. crispus* when examined across treatments. Correlations between shear strength and final SSC over all treatments showed that they were positively correlated for *C. crispus* (correlation coefficient = 0.562, p-value = 0.004) and not significantly correlated for *F. lumbricalis* (correlation coefficient = 0.072, p-value = 0.744). For *C. crispus*, shear stress is correlated with final SSC because of variability in the onset of algal motion. Larger pieces did not move as much during the first velocity step ($U_y = 0.075$ m s^{-1}) as the smaller pieces (see Appendix D). Therefore, the larger pieces had less impact on the erosion of the bed during the first velocity step; thus, the beds failed at higher shear stresses for larger pieces. Moreover, the larger pieces had more of an effect on the erosion rates of the beds after the onset of their motion; therefore, they caused higher final SSC. This trend was not as significant for *F. lumbricalis'* treatments because all three size treatments spent significant quantities of time not moving during the first velocity step. Algae in the smaller size treatments moved slightly more during the first velocity step; however, this slight increase in movement may not have been enough to significantly change the erosion thresholds from the other treatments.

Algal morphology and rigidity may have also caused variation in the SSC and erosion rates within treatments. There were a few instances in which algal stipes and thalli were observed digging into the bed and causing a plume of sediment to be dispersed around the stipe/thallus (e.g. trial 1 and 2 of the *Furcellaria* large size treatment (Fig. 12), trial 2 of the *Furcellaria* medium abundance treatment (Fig. 13) and trial 1 of the *Chondrus* small size treatment (Fig. 5)). Macroalgae are flexible and change shape

with respect to current velocity (Carrington, 1990). Carrington (1990) hypothesized that species of macroalgae that are less flexible may have higher drag coefficients as they are less likely to bend under stress than those with more flexibility. Therefore, variations in the structural rigidity and morphology of the algae may have influenced how energy was transferred to the bed (i.e. less flexible branches would be more likely to disturb the bed than flexible branches) and therefore influenced the erosion rates of the beds.

Due to having only three replicates within a treatment in most instances, it was not statistically feasible to test whether some factors (e.g. % contact time, % time as aggregates and mode of transport) significantly influenced the SSC variability within a treatment. However, overall it is most likely that a combination of all the mentioned factors had some role in influencing the variability of suspended sediment concentrations within treatments.

b. *Effects of Algal Size*

ANOVA results showed that suspended sediment concentrations (with the exception of the *F. lumbricalis* size treatment) and erosion rates were effected by algal size for both *C. crispus* and *F. lumbricalis*. However, statistically it was difficult to determine accurately whether the erosion rates, suspended sediment concentrations, overall slopes and critical erosion thresholds of the small, medium and large size categories were different from one another, as the p-values were close to the alpha 0.05 significance level in some instances (p-values displayed in Appendix L and M). This may have been due to the high degree of variability within the various treatments and due to the small number of replications (e.g. three in most instances) within a treatment.

A multiple regression model (table 4) for the combined *C. crispus* and *F. lumbricalis* size data was developed to determine the impact of various predictor variables on the erosion rates for both species. Results of the model showed that 40.3 % of the erosion rate variability could be explained by the various predictor variables outlined in table 4. Percent contact time and current velocity explained the majority of the variation in erosion rate within the multiple regression model (see table 4); however, the size and species of alga were also revealed to have a significant impact on the erosion rates of the beds. Furthermore, a backward elimination procedure revealed that: (1) percent time as aggregates; (2) the interaction between species and medium vs. small size; and (3) the interaction between species and medium vs. large size did not significantly alter the erosion rates of the treatments. The data for the two species were grouped together to increase the number of observations and thus make the model more statistically significant. As a result, the model helped identify significant predictor variables that influenced erosion rates for both species of macroalgae.

(i) *Chondrus Size*

Mode of transport of the algae followed a consistent trend for all of the size treatments. *C. crispus* initially began to move by sliding/rolling along the bed, followed by a mixed phase of suspension and sliding, which in turn was followed by complete suspension of the algae into the water column. Boggs (1995) outlined a similar trend when describing sediment loads and transport paths of siliciclastic sediment particles in aquatic environments. Boggs (1995) referred to the rolling/sliding phase as traction, the mixed phase as intermittent suspension and complete suspension of a particle as continuous suspension. Boggs (1995) explained that the incorporation of a particle into

the flow results when the upward components of fluid motion (resulting from the increased turbulence associated with the increased current velocity) increase to the point where they balance the downward settling rate. Furthermore, intermittent suspension results when the lift forces arising from turbulence are erratic and do not continuously maintain this balance of upward lift with downward settling (mentioned above). This appears to be the same general trend for the algae used in these experiments. Moreover, the constantly changing form of the macroalgae would add to the turbulent effect outlined above and would increase the chances of intermittent suspension over that of saltation. Intermittent suspension is different from saltation because the suspended particles tend to be carried higher above the bed and in the flow for longer periods of time than they would be for a saltating particle (Boggs, 1995).

Maximum erosion rates of *C. crispus* were achieved during the sliding/rolling phase for the small pieces and during the mixed phase of suspension and sliding for the medium and large pieces (Fig. 27 and 29). During the mixed phase pieces of *C. crispus* impacted the bed in a similar, yet more subtle, manner as outlined by Amos *et al.* (1998a). For example, pieces of *C. crispus* gradually settled out of suspension and slid along the bed for a period of time before being reincorporated into the flow as an intermittent suspended particle. However, no standard saltation height or length as explained by Amos *et al.* (1998a, in press) was observed while watching the experiments and videos. As mentioned earlier, this lack of consistent saltation height and length is most likely attributed to the turbulent flow within the flume and to the changing shape of the algae with respect to turbulence. Therefore, the algal motion was much more chaotic than that of a particle of constant shape (e.g. clast, littorinid shell, etc.).

Suspended sediment concentrations ceased to increase and erosion rates declined to 0 mg m^{-2} s^{-1} when the algae entered fully into suspension (Figs. 5-7, 27 and 29). Erosion ceased because algae no longer made contact with the bed to erode the sediment and the fluid induced erosion threshold had not yet been reached. The general trend for the mode of transport did not vary greatly with algal size; however, the large pieces of *C. crispus* entered into suspension one step earlier than the medium and small pieces. Large pieces most likely entered into suspension earlier (despite their increased mass) than the small and medium pieces because the larger pieces had a greater surface area per unit of mass exposed to the flow. Increased surface area with respect to mass would provide more resistance to flow (i.e. more drag); thus, larger particles would be more likely to become entrained into the flow (Dudgeon and Johnson, 1992).

(ii) *Furcellaria Size*

Mode of transport followed a similar trend as the *C. crispus*. Algae initially began to move by sliding/brushing the bed, followed by a mixed phase of brushing and suspension, which in turn was followed by complete suspension of the algae in a few trials. Complete suspension was only observed in trial 1 and trial 2 of the small size treatment (Fig. 10) and trial 1 of the medium size treatment (Fig. 11). As mentioned earlier, complete suspension of the algae was achieved when upward forces increased to a point where they balanced the downward force of gravity (Boggs, 1995). After complete suspension, the SSC no longer increased and the erosion rate declined to 0 mg m^{-2} s^{-1} (Figs. 10, 11, 30 and 32). Throughout the majority of the trials, the algae did not become fully suspended into the flow; therefore, the SSC did not level off to a constant value because the algae were still contacting and eroding the bed. During higher current

velocities *F. lumbricalis* assumed a more vertical orientation than that of *C. crispus*. While being transported in this vertical orientation, algae generally contacted the bed by brushing with the stipe and/or tips of the branches. Maximum rates of erosion for *F. lumbricalis* were achieved during the sliding/brushing phase for all three size categories. As mentioned earlier, the medium and large sizes of *C. crispus* achieved their maximum erosion rate during the mixed phase of sliding and suspension. *F. lumbricalis* did not appear to impact the bed as abruptly as *C. crispus* during the mixed phase. After the pieces of *F. lumbricalis* came out of suspension, they resumed brushing the bed in a vertical orientation with the stipe oriented up or down.

c. *Effects of Algal Abundance*

ANOVA analysis showed that algal abundance had an effect on the erosion rates, final suspended sediment concentrations and the overall slopes for both species of macroalgae. Erosion rates increased with respect to the number of pieces in the flume due to an increased number of algae contacting and eroding the bed per unit of time.

Statistically it was not feasible to accurately determine whether the erosion rates of the low, medium and high abundance treatments were different from one another (p-values are displayed in Appendix L). This shortcoming was attributed to the high SSC variability within treatments and to the low number of replications.

The size of aggregates (i.e. the number of individual pieces that compose the aggregate) varied with current velocity in a similar manner as it did in the size treatments. It was also observed that larger aggregates generally traveled at slower velocities than smaller aggregates and individual pieces. The relationship between aggregate size and mode of transport was complex. There are numerous occasions throughout the course of

the experiments where aggregates were observed to remain in contact with the bed longer than smaller aggregates and/or individual pieces. However, it was also observed that the medium and high abundance treatment of *C. crispus* reached the suspension phase one step earlier than that of the small abundance category. This "premature" entry into suspension observed by the high abundance treatments can be explained by an increased surface area with respect to mass relationship associated with the increased number of pieces in the flume. The greater the number of pieces of algae in the flume, the more likely they are to interact with one another and form aggregates. Larger aggregates (e.g. 4 to 6 pieces) may have a larger surface area with respect to mass than the smaller aggregates (e.g. 2 pieces), enabling them to be incorporated into the flow more easily as they have a greater resistance to flow (Dudgeon and Johnson, 1992). Furthermore, packing of aggregates was also observed to influence their mode of transport. Loosely packed aggregates (i.e. individuals that were not tightly joined together) were generally incorporated into the intermittent suspension phase more easily than tightly packed aggregates, which generally remained in contact with the bed longer. Longer contact times for more tightly packed aggregates, may be explained by the surface area to mass relation explained earlier: more tightly packed aggregates would offer less surface area with respect to mass, decreasing their chances of being entrained into the flow.

(i) *Chondrus Abundance*

Mode of transport varied with current velocity and the algae followed the same general trend as the size treatment data. Algae initially began to move by sliding along the bed; this was followed by a mixed phase of suspension and sliding, which in turn was followed by continuous suspension of the algae. Maximum rates of erosion were

generally achieved during the mixed phase of suspension and sliding along the bed (U_y = 0.22 m s^{-1}) for all of the abundance treatments. Although, the algae were travelling in an intermittent suspension phase, they still made contact with the bed frequently. Furthermore, the impacts of the algae may have enabled them to transmit momentum to the bed via the ballistic impacts as outlined by Amos *et al.* (1998a). As mentioned earlier, *C. crispus* did not appear to abruptly impact the bed after leaving "suspension". However, a significant quantity of momentum could have been transmitted to the bed via this transition.

(ii) *Furcellaria Abundance*

The mode of transport did not appear to change with respect to alga abundance. However, as mentioned earlier, the greater surface area with respect to algal mass relationship allowed algae within the high abundance category to become incorporated into the flow one step earlier than the algae in the lower abundance categories.

The greatest erosion rates occurred during the sliding phase for the low and medium abundance treatments and during both the sliding phase and the mixed phase for the high abundance treatment. The high abundance treatment appeared to be slightly more misleading because the maximum erosion rates occurred during the sliding phase and the intermittent suspension phase. However, further analysis revealed that during velocity step 4 the algae were only in suspension for less than 20 % of the time (Appendix G). Therefore, the algae were still predominately sliding along the bed in the same manner as the previous step. Furthermore, the increased number of pieces inhibited the individual pieces from brushing the bed with their stipes and the tips of the fronds, as observed in the low and medium abundance categories. Instead *F. lumbricalis* generally

slid along the bed as aggregates during the intermittent suspension phase of the high abundance treatment, which may have enabled them to transfer more energy to the bed than if they were "lightly" brushing the bed as observed in the lower abundance treatments.

Many researchers have mentioned that the intense eutrophication of the lagoon of Venice has caused an increase in biomass of many macroalga species. Furthermore, Flindt *et al.* (1997b) determined that different species of macroalgae (e.g. *Chaetomorpha aerea*, *Zostera* sp. and *Ulva* sp.) are transported at different water depths within the lagoon and that some macroalgae species move as bedload.

This study supports the statement by Amos *et al.* (1998a) that suggests that mobile detritus increases the erosion rates of cohesive sediments over that of the fluid induced erosion. More specifically, this study showed that mobile fragments of macroalgae have the potential to significantly increase the erosion rates of cohesive sediments when algal fronds are in contact with an erodable bed (i.e. via sliding or intermittent suspension). Furthermore, it was revealed that current velocity, percent contact time, size, species, abundance, and mode of transport affected the erosion rates of the beds.

The implications of macroalgal drift on the erosion of cohesive sediments in a natural environment, such as the lagoon of Venice, is more complex than in a laboratory setting. This study revealed that the erosion rates of cohesive sediments were significantly increased by two different species of macroalgae (e.g. *Chondrus crispus* and *Furcellaria lumbricalis*) contacting the bed. Thus, it is believed that the large quantities of macroalgae moving as bedload in the lagoon of Venice would add to the impact of the

fluid stress, causing the beds to erode at lower current velocities and at greater rates than if they were solely acted upon by the fluid. However, quantification of macroalgal impacts would be much more difficult to assess in the lagoon of Venice due to spatial variability of the sediments and the difficulty of characterizing macroalgal fragments in the field. It appears that the impact of macroalgae on the erosion process in a natural environment would be governed by a variety of factors. Erosion of sediment induced by algae would vary with respect to the species of algae (e.g. a study performed by Sfriso and Marcomini (1997) showed that sediment resuspension at the sediment water interface was inhibited by coverage of *Ulva* fronds), the mode that the algae are transported in the water column, interactions with other species, and the size and abundance of the drifting fragments. Therefore, it would be difficult to quantify the impact of macroalgae drift on the erosion of sediments based solely on measured parameters, such as the species, size, abundance and diversity.

CONCLUSIONS

(1) Macroalgae (or any organic/inorganic detritus) moving as bedload has the potential to significantly increase the erosion rates of cohesive sediments.

(2) Erosion rates increased with increasing size and abundance for both *Furcellaria lumbricalis* and *Chondrus crispus*.

(3) Erosion rates varied with current velocity, percent contact, species, algal size, abundance, and the mode of transport of the algal fronds.

(4) The changing form of the macroalgae (i.e. the variability of shape with respect to current velocity and turbulence due to the flexibility of the thalli) along with the turbulent flow of the flume increased the probability of intermittent suspension as opposed to saltation.

(5) The Mini Flume and artificial clay bed proved to be useful in determining whether macroalgae increased the erosion of a cohesive bed over that of fluid induced erosion. However, it did not prove to be as effective when trying to quantify the impacts of size and abundance on the erosion process (experimental design was also at fault for this as well). Perhaps a larger flume would be more appropriate as it would allow one to track individual pieces of alga and more accurately measure their impacts.

(6) Influence of drifting macroalgae on the erosion of cohesive sediments in a natural environment is complex and depends upon a variety of factors. Species of alga, mode of transport, interactions with other species and sediment, and the size and abundance of the drifting fragments would all influence the impact that drifting fronds have on cohesive sediments.

REFERENCES

ALLDREDGE, A.L. and GOTSCHALK, C. 1988. In situ settling behavior of marine snow. Limnology and Oceanography, 33, No.3, 339-351.

AMOS, C.L., GRANT, J., DABORN, G.R., and BLACK, K. 1992. Sea Carousel – a benthic, annular flume. Estuarine, Coastal and Shelf Science, 34, 557-577.

AMOS, C.L., FEENEY, T., SUTHERLAND, T.F., and LUTERNAUER, J.L. 1997. The stability of fine-grained sediments from the Fraser River Delta. Estuarine, Coastal and Shelf Science, 45, pp. 507-524.-

AMOS, C.L., BRYLINSKY, M., SUTHERLAND, T.F., and O'BRIEN, D. 1998b. The stability of a mudflat in the Humber estuary, South Yorkshire, UK. *In* Sedimentary processes in the intertidal zone. *Edited by* K.S. Black, D.M. Paterson, and A. Cramp. Geological Society Special Publications 139, London, pp. 25-43.

AMOS, C.L., LI, M.Z., and SUTHERLAND, T.F. 1998a. The contribution of ballistic momentum flux to the erosion of cohesive beds by flowing water. Journal of Coastal Research, 14, No.2, 564-569.

AMOS, C.L., SUTHERLAND, T.F., CLOUTIER, D., and PATTERSON, S. *In press.* Corrasion of a remolded cohesive bed by saltating littorinid shells. *In* Intertidal Mudflats: Properties and Processes. *Edited by* K.R. Dyer. Continental Shelf Research.

BACH, H., JENSEN, O.K., and WARREN, R. 1993. Venice lagoon eutrophication modelling. *In* First international conference on the Mediterranean coastal environment, MEDCOAST 93. *Edited by* E. Ozhan. Middle East Technical University, Ankara, pp. 405-437.

BIRD, C.J. and McLACHLAN, J.L. 1992. Seaweed flora of the maritimes. 1. Rhodophyta – the red algae. Biopress Ltd., Bristol, 177 p.

BOGGS, S. JR. 1995. Principles of sedimentology and stratigraphy: second edition. Prentice-Hall, Inc., Englewood Cliffs, 774p.

CABILIO, P., and MASARO, J. 1999. Basic statistical procedures and tables: eighth edition. Acadia University, 93p.

CARRINGTON, E. 1990. Drag and dislodgment of an intertidal macroalga: consequences of morphological variation in *Mastocarpus papillatus* Kützing. Journal of Experimental Marine Biology and Ecology, 139, 185-200.

CALVO, C., GRASSO, M., and GARDENGHI, G. 1991. Organic carbon and nitrogen in sediments and in resuspended sediments of Venice Lagoon: relationship with PCB contamination. Marine Pollution Bulletin, 22, No.11, pp. 543-547.

DAY, J.W. JR, FRANCESCO, S., RISMONDO, A., and ARE, D. 1998. Rapid deterioration of a salt marsh in Venice Lagoon. Journal of Coastal Research, 14, No.2, pp. 583-590.

DEN HARTOG, C., VERGEER, L.H.T., and RISMONDO. 1996. Occurrence of *Labyrinthula zosterae* in *Zostera marina* from Venice Lagoon. Botanica Marina, 39, pp. 23-26.

DUDGEON, S.R. and JOHNSON, A.S. 1992. Thick vs. thin: thallus morphology and tissue mechanics influence differential drag and dislodgment of two co-dominant seaweeds. Journal of Experimental Marine Biology and Ecology, 165, 23-43.

FLINDT, M., KAMP-NIELSEN, L., MARQUES, J.C., PARDAL, M.A., BOCCI, M., BENDORICCHIO, G., SALOMONSEN, J., NIELSEN, S.N., and JØRGENSEN,

S.E. 1997a. Description of the three shallow estuaries: Mondego River (Portugal), Roskilde Fjord (Denmark) and the Lagoon of Venice (Italy). Ecological Modelling, 102, pp. 17-31.

FLINDT, M., SALOMONSEN, J., CARRER, M., BOCCI, M., and KAMP-NIELSEN, L. 1997b. Loss, growth and transport dynamics of *Chaetomorpha aerea* and *Ulva rigida* in the Lagoon of Venice during an early summer field campaign. Ecological Modelling, 102, pp. 133-141.

FUNG, A. 1997. Calibration of flow field in mini-flume. Unpublished contract report submitted to Geological Survey of Canada, Atlantic, Dartmouth, Nova Scotia. 109 p.

GATTO, P. and CARBOGNIN, L. 1981. The Lagoon of Venice: natural environmental trend and man-induced modification. Hydrological Sciences Bulletin, 26, No.4, pp. 379-391.

GRANT, J., BATHMANN, U.V., and MILLS, E.L. 1986. The interaction between benthic diatom films and sediment transport. Estuarine, Coastal and Shelf Sciences, 23, pp. 225-238.

HOLLAND, A.F., ZINGMARK, R.G., and DEAN, J.M. 1974. Quantitative evidence concerning the stabilization of sediments by marine benthic diatoms. Marine Biology, 27, pp. 191-196.

MCCOMB, A.J. and DAVIS, J.A. 1993. Eutrophic waters of southwestern Australia. Fertilizer Research, 36, pp. 105-114.

MEHTA, A.J. and PARTHENIADES, E. 1982. Resuspension of deposited cohesive sediment beds. Eighteenth Conference on Coastal Engineering, pp. 1569-1588.

MORAND, P. and BRIAND, X. 1996. Excessive growth of macroalgae: a symptom of environmental disturbance. Botanica Marina, 39, pp. 491-516.

MUSCHENHEIM, D.K., GRANT, J. and MILLS, E.L. 1986. Flumes for benthic ecologists: theory, construction and practice. Marine Ecology Progress Series, 28, pp. 185-196.

NEUMANN, A.C., GEBELEIN, C.D., and SCOFFIN, T.P. 1970. The composition, structure and erodability of subtidal mats, Abaco, Bahamas. Journal of Sedimentary Petrology, 40, No.1, pp. 274-297.

NOWELL, A.R.M. and JUMARS, P.A. 1987. Flumes: Theoretical and experimental considerations for simulation of benthic environments. Oceanography Marine Biology Annual Review, 25, 91-112.

PATERSON, D.M., and UNDERWOOD, G.J.C. 1990. The mudflat ecosystem and epipelic diatoms. Proceedings of the Bristol Naturalists' Society, 50, pp.74–82.

PIGNATTI, S. 1962. Associazioni di alghe marine sulla costa veneziana. Memorie Istituto Veneto Lettere Science Arti, 32, No.3, pp. 1-134.

RUNCA, E., BERNSTEIN, A., POSTMA, L., and DI SILVIO, G. 1993. Control of Macroalgae blooms in the Lagoon of Venice. *In* First International Conference on the Mediterranean Coastal Environment, MEDCOAST 93. *Edited by* E. Ozhan. Middle East Technical University, Ankara, pp. 421-435.

SCHIFFNER, V. and VATOVA, A. 1938. Le alghe della laguna: Chlorophyceae, Phaeophyceae, Rhodophyceae, Myxophyceae. *In* La Laguna di Venezia, 3. *Edited by* M. Minio. Venezia, 250 p.

SFRISO, A. 1987. Flora and vertical distribution of macroalgae in the lagoon of Venice: a comparison with previous studies. Giornale Botanico Italiano, 121, pp. 69-85.

SFRISO, A. and MARCOMINI, A. 1996. Decline of *Ulva* growth in the lagoon of Venice. Bioresource Technology, 58, pp. 299-307.

SFRISO, A. and MARCOMINI, A. 1997. Macrophyte production in a shallow coastal lagoon. Part I: coupling with chemico-physical parameters and nutrient concentrations in waters. Marine Environmental Research, 44, No.4, pp. 351-375.

SFRISO, A. and PAVONI, B. 1994. Macroalgae and phytoplankton competition in the central Venice Lagoon. Environmental Technology, 15, pp. 1-14.

SFRISO, A., MARCOMINI, A., and PAVONI, B. 1987. Relationships between macroalgal biomass and nutrient concentrations in a hypertrophic area of the Venice Lagoon. Marine Environmental Research, 22, pp. 297-312.

SFRISO, A., PAVONI, B., and MARCOMINI, A. 1989. Macroalgae and phytoplankton standing crops in the central Venice lagoon: primary production and nutrient balance. The Science of the total environment, 80, pp. 139-159.

SFRISO, A., MARCOMINI, A., PAVONI, B., and ORIO, A.A. 1993. Species composition, biomass, and net primary production in shallow coastal waters: the Venice lagoon. Bioresource Technology, 44, pp. 235-250.

SFRISO, A., MARCOMINI, A., and PAVONI, B. 1994. Gracilaria distribution, production and composition in the Lagoon of Venice. Bioresource Technology, 50, pp. 165-173.

SUTHERLAND, T.F., AMOS, C.L., and GRANT, J. 1998. The erosion threshold of biotic sediments: a comparison of methods. *In* Sedimentary processes in the

intertidal zone. *Edited by* K.S. Black, D.M. Paterson, and A. Cramp. Geological Society Special Publications 139, London, pp. 295-307.

TAGLIAPIETRA, D., PAVAN, M., and WAGNER, C. 1998. Macrobenthic community changes related to eutrophication in Palude della Rosa (Venetian Lagoon, Italy). Estuarine, Coastal and Shelf Science, 47, pp. 217-226.

TERZAGHI, K. and PECK, R.B. 1967. Soil Mechanics in engineering practice. John Wiley & Sons, New York, 729 p.

THETIS, 1997. Feed-backs of estuarine circulation and transport of sediments on phytobenthos (F-ECTS). Unpublished proposal submitted to the EC MAST III Programme. 57 p.

VOS, P.C., DE BOER, P.L., and MISDORP, R. 1988. Sediment stabilization by benthic diatoms in intertidal sandy shoals; qualitative and quantitative observations. *In* Tide-influenced sedimentary environments and facies. *Edited by* P.L. De Boer, A. Van Gelder and S.D. Nio. D. Reidel Publishing Company, Dordrecht, Holland, pp.511-526.

WIDDOWS, J., BRINSLEY, M.D. BOWLEY, N., and BARRETT, C. 1998. A benthic annular flume for *in situ* measurement of suspension feeding/biodeposition rates and erosion potential of intertidal cohesive sediments. Estuarine, Coastal and Shelf Science, 46, pp. 27-38.

APPENDIX A
OVERALL OBS2 CALIBRATION FOR EROSION EXPERIMENTS

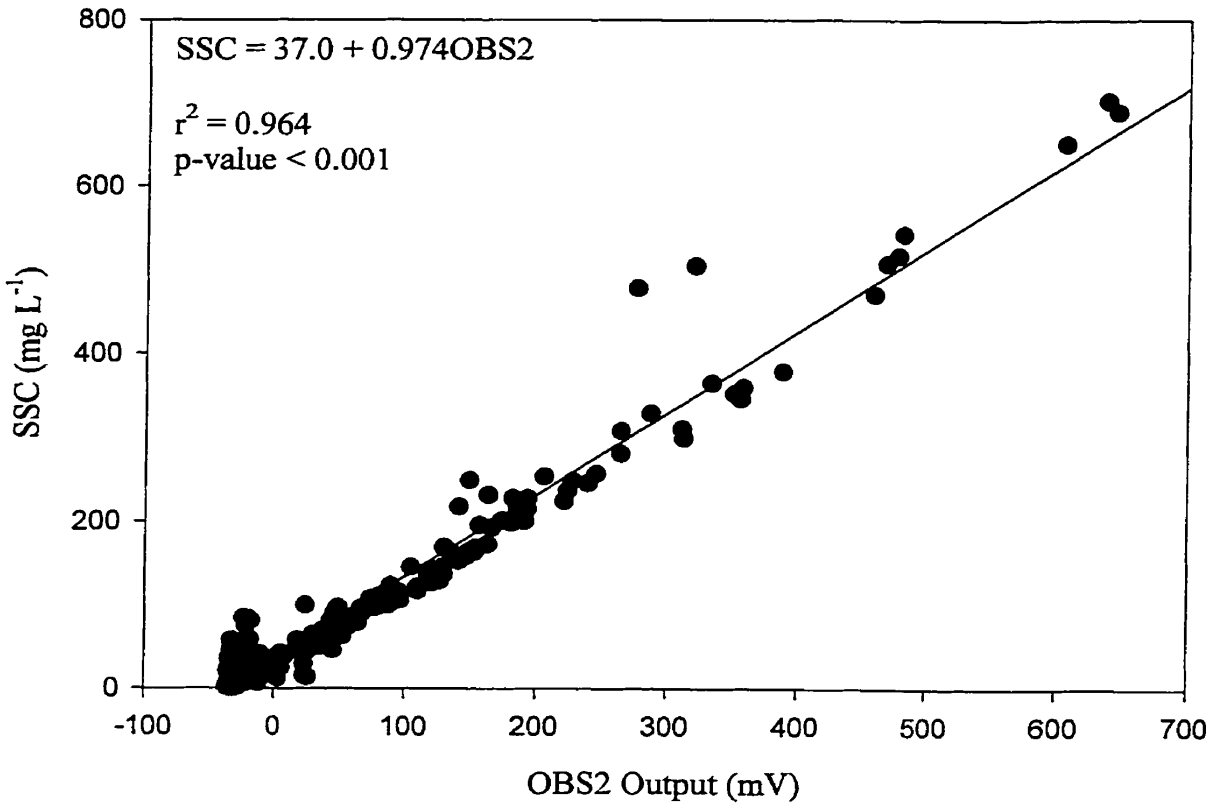

APPENDIX B
OVERALL OBS2 CALIBRATION FOR CONTROL EXPERIMENTS

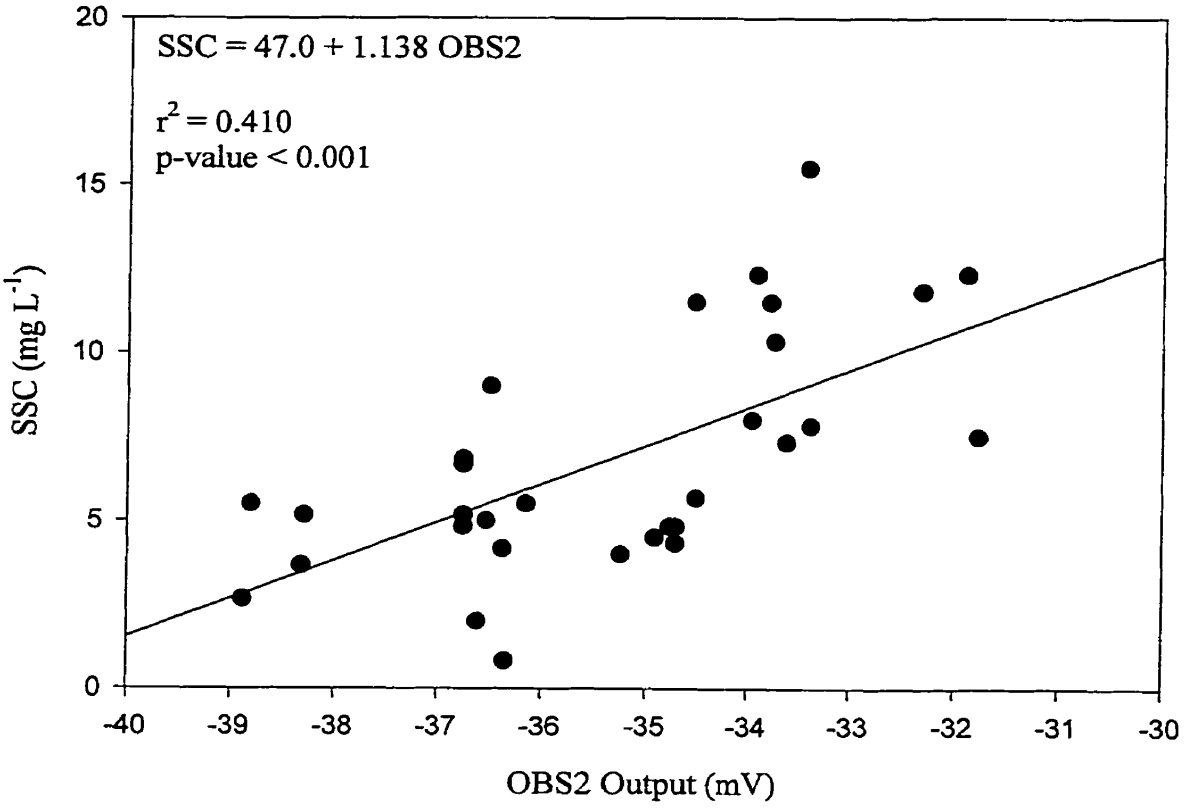

APPENDIX C
VENICE SETTLING EXPERIMENTS

Species	Condition	Shape	Mass (g)	Area (cm^2)	Settling Velocity ($cm\ s^{-1}$)	Average	$\pm$ 1 sd
Ulva	Uncleaned light green	Circle	n/a	9.4	0.91		
Ulva	Uncleaned light green	Circle	n/a	9.4	1.23		
Ulva	Uncleaned light green	Circle	n/a	9.4	1.43	1.19	0.26
Ulva	Uncleaned light green	1/2 Circle	n/a	4.7	1.05		
Ulva	Uncleaned light green	1/2 Circle	n/a	4.7	1.06		
Ulva	Uncleaned light green	1/2 Circle	n/a	4.7	1.22	1.11	0.09
Ulva	Uncleaned light green	Square	n/a	1.0	0.88		
Ulva	Uncleaned light green	Square	n/a	1.0	0.96		
Ulva	Uncleaned light green	Square	n/a	1.0	0.85	0.90	0.06
Ulva	Uncleaned light green	Square	n/a	4.0	1.09		
Ulva	Uncleaned light green	Square	n/a	4.0	0.89		
Ulva	Uncleaned light green	Square	n/a	4.0	1.12	1.03	0.13
Ulva	Uncleaned light green	Square	n/a	9.0	0.96		
Ulva	Uncleaned light green	Square	n/a	9.0	1.92		
Ulva	Uncleaned light green	Square	n/a	9.0	1.55	1.47	0.49
Ulva	Uncleaned dark green	Circle	n/a	9.4	1.06		
Ulva	Uncleaned dark green	Circle	n/a	9.4	0.86		
Ulva	Uncleaned dark green	Circle	n/a	9.4	0.86	0.93	0.11
Ulva	Uncleaned dark green	1/2 Circle	n/a	4.7	0.95		
Ulva	Uncleaned dark green	1/2 Circle	n/a	4.7	0.79		
Ulva	Uncleaned dark green	1/2 Circle	n/a	4.7	0.82	0.86	0.08
Ulva	Uncleaned dark green	Square	n/a	1.0	1.03		
Ulva	Uncleaned dark green	Square	n/a	1.0	1.02		

Ulva	Uncleaned dark green	Square	n/a	1.0	1.15	1.07	0.07
Ulva	Uncleaned dark green	Square	n/a	4.0	0.97		
Ulva	Uncleaned dark green	Square	n/a	4.0	1.01		
Ulva	Uncleaned dark green	Square	n/a	4.0	1.18	1.06	0.11
Ulva	Uncleaned dark green	Square	n/a	9.0	1.23		
Ulva	Uncleaned dark green	Square	n/a	9.0	1.81		
Ulva	Uncleaned dark green	Square	n/a	9.0	2.08	1.71	0.44
Ulva	Cleaned light green	Circle	n/a	9.4	0.92		
Ulva	Cleaned light green	Circle	n/a	9.4	1.42		
Ulva	Cleaned light green	Circle	n/a	9.4	1.20	1.18	0.25
Ulva	Cleaned light green	1/2 Circle	n/a	4.7	1.16		
Ulva	Cleaned light green	1/2 Circle	n/a	4.7	2.08		
Ulva	Cleaned light green	1/2 Circle	n/a	4.7	1.23	1.49	0.51
Ulva	Cleaned light green	Square	n/a	1.0	1.32		
Ulva	Cleaned light green	Square	n/a	1.0	0.93		
Ulva	Cleaned light green	Square	n/a	1.0	1.36	1.20	0.24
Ulva	Cleaned light green	Square	n/a	4.0	1.50		
Ulva	Cleaned light green	Square	n/a	4.0	1.52		
Ulva	Cleaned light green	Square	n/a	4.0	1.07	1.36	0.25
Ulva	Cleaned light green	Square	n/a	9.0	0.88		
Ulva	Cleaned light green	Square	n/a	9.0	0.93		
Ulva	Cleaned light green	Square	n/a	9.0	1.90	1.24	0.57
Ulva	Cleaned dark green	Circle	n/a	9.4	0.93		
Ulva	Cleaned dark green	Circle	n/a	9.4	0.94		
Ulva	Cleaned dark green	Circle	n/a	9.4	0.89	0.92	0.03
Ulva	Cleaned dark green	1/2 Circle	n/a	4.7	0.89		
Ulva	Cleaned dark green	1/2 Circle	n/a	4.7	0.82		
Ulva	Cleaned dark green	1/2 Circle	n/a	4.7	1.11	0.94	0.15

Ulva	Cleaned dark green	Square	n/a	1.0	1.11		
Ulva	Cleaned dark green	Square	n/a	1.0	1.11		
Ulva	Cleaned dark green	Square	n/a	1.0	1.26	1.16	0.09
Ulva	Cleaned dark green	Square	n/a	4.0	1.46		
Ulva	Cleaned dark green	Square	n/a	4.0	0.93		
Ulva	Cleaned dark green	Square	n/a	4.0	1.47	1.29	0.31
Ulva	Cleaned dark green	Square	n/a	9.0	0.98		
Ulva	Cleaned dark green	Square	n/a	9.0	0.93		
Ulva	Cleaned dark green	Square	n/a	9.0	1.16	1.02	0.12
Chondrus	Cleaned	Aggregate	0.123	n/a	1.08		
Chondrus	Cleaned	Aggregate	0.144	n/a	0.90		
Chondrus	Cleaned	Aggregate	0.104	n/a	1.29	1.09	0.20
Chondrus	Cleaned	Aggregate	0.495	n/a	2.05		
Chondrus	Cleaned	Aggregate	0.400	n/a	2.14		
Chondrus	Cleaned	Aggregate	0.520	n/a	2.27	2.16	0.11
Chondrus	Cleaned	Aggregate	0.658	n/a	2.68		
Chondrus	Cleaned	Aggregate	0.717	n/a	2.54		
Chondrus	Cleaned	Aggregate	0.757	n/a	2.54	2.59	0.08
Chondrus	Cleaned	Aggregate	3.713	n/a	4.41		
Chondrus	Cleaned	Aggregate	2.760	n/a	2.78		
Chondrus	Cleaned	Aggregate	3.893	n/a	2.78	3.46	0.94
Chondrus	Cleaned	Aggregate	7.851	n/a	2.54		
Chondrus	Cleaned	Aggregate	7.846	n/a	2.83		
Chondrus	Cleaned	Aggregate	7.871	n/a	3.13	2.83	0.29
Gracilaria	Cleaned	Aggregate	0.324	n/a	2.00		
Gracilaria	Cleaned	Aggregate	0.419	n/a	1.72		
Gracilaria	Cleaned	Aggregate	0.362	n/a	2.68	2.13	0.49
Gracilaria	Cleaned	Aggregate	2.119	n/a	3.49		

Gracilaria	Cleaned	Aggregate	1.824	n/a	1.83		
Gracilaria	Cleaned	Aggregate	2.028	n/a	2.42	2.58	0.84
Gracilaria	Cleaned	Aggregate	2.436	n/a	2.63		
Gracilaria	Cleaned	Aggregate	2.550	n/a	2.11		
Gracilaria	Cleaned	Aggregate	2.668	n/a	1.81	2.18	0.42
Gracilaria	Cleaned	Aggregate	8.213	n/a	2.27		
Gracilaria	Cleaned	Aggregate	8.498	n/a	1.83		
Gracilaria	Cleaned	Aggregate	8.638	n/a	2.14	2.08	0.23
Cymedosia	Cleaned brown	Rectangle	0.0301	2.1	1.33		
Cymedosia	Cleaned brown	Rectangle	0.0142	2.1	1.25		
Cymedosia	Cleaned brown	Rectangle	0.0335	3.3	3.00		
Cymedosia	Cleaned brown	Rectangle	0.0231	3.28	1.09		
Cymedosia	Cleaned brown	Rectangle	0.0202	4.83	1.09		
Cymedosia	Cleaned brown	Rectangle	0.0202	2.94	1.19		
Cymedosia	Cleaned brown	Rectangle	0.0659	9.4	2.08		
Cymedosia	Cleaned brown	Rectangle	0.1032	17.35	1.18		

APPENDIX D

CHONDRUS SIZE VIDEO RESULTS

Small Size

Uy ($m\ s^{-1}$)	**Contact (%)**						**Mode of Transport**					
	Trial 1		**Trial 2**		**Trial 3**		**Trial 1**		**Trial 2**		**Trial 3**	
	A	***I***	***A***	***I***	***A***	***I***	***A***	***I***	***A***	***I***	***A***	***I***
0.08	100	100	100	100	100	100	1	1	1	1	1	1
0.15	100	100	100	100	100	100	1	1	1	1	1	1
0.22	82	60	N/A	55	78	76	1	2	N/A	2	2	2
0.30		23		12	71	19		2	3	2	2	2
0.37	N/A	6	N/A	8	N/A	5	N/A	2	N/A	2	N/A	2
0.45	0	0	0	0	0	0	3	3	3	3	3	3
0.52	0	0	0	0	0	0	3	3	3	3	3	3

Uy ($m\ s^{-1}$)	**No Movement (% Time)**			**Individual (% Time)**			**Aggregate (% Time)**		
	T1	**T2**	**T3**	**T1**	**T2**	**T3**	**T1**	**T2**	**T3**
0.08	0	0	0	10	80	70	90	20	30
0.15	0	0	0	50	91	63	50	9	37
0.22	0	0	0	79	100	69	21	0	35
0.30	0	0	0	97	96	90	3	4	11
0.37	0	0	0	100	100	100	0	0	0
0.45	0	0	0	N/A	N/A	N/A	N/A	N/A	N/A
0.52	0	0	0	N/A	N/A	N/A	N/A	N/A	N/A

Medium Size - Note: the other 3 trials can be found under the Low Abundance Heading

Uy ($m\ s^{-1}$)	Contact (%)						Mode of Transport					
	Trial 1		Trial 2		Trial 3		Trial 1		Trial 2		Trial 3	
	A	*I*	*A*	*I*	*A*	*I*	*A*	*I*	*A*	*I*	*A*	*I*
0.08	100	100	100	100	100	100	1	1	Int.	Int.	Int.	Int.
0.15	100	100	100	100	100	100	1	1	1	1	1	1
0.22		71	100	64.9	100	91		2	1	2	1	1
0.30	N/A	13		39	76	60	N/A	2		2	2	2
0.37	0	0		11	N/A	18	3	3		2	N/A	2
0.45	0	0	0	0	0	0	3	3	3	3	3	3
0.52	0	0	0	0	0	0	3	3	3	3	3	3

Uy ($m\ s^{-1}$)	No Movement (% Time)			Individual (% Time)			Aggregate (% Time)		
	T1	T2	T3	T1	T2	T3	T1	T2	T3
0.08	0	62	93	20	16	6	80	21	2
0.15	0	0	0	54	41	67	46	59	33
0.22	0	0	0	98	64	91	2	36	9
0.30	0	0	0	100	87	83	0	13	18
0.37	0	0	0	N/A	96	100	N/A	4	0
0.45	0	0	0	N/A	N/A	N/A	n/a	N/A	N/A
0.52	0	0	0	N/A	N/A	N/A	N/A	N/A	N/A

Large Size

Uy ($m\ s^{-1}$)	Contact (%)						Mode of Transport					
	Trial 1		Trial 2		Trial 3		Trial 1		Trial 2		Trial 3	
	A	*I*	*A*	*I*	*A*	*I*	*A*	*I*	*A*	*I*	*A*	*I*
0.08	100	100	100	100	100	100	Int.	Int.	Int.	Int.	Int.	Int.
0.15	100	100	100	100	100	100	1	1	1	1	1	1
0.22	92	82	100	82	100	98	2	2	1	2	1	1
0.30	92	47	86	30	100	83	3	2	2	2	1	1
0.37	0	0	0	0	N/A	39	3	3	3	3	2	2
0.45	0	0	0	0	0	0	3	3	3	3	3	3
0.52	0	0	0	0	0	0	3	3	3	3	3	3

Uy ($m\ s^{-1}$)	No Movement (% Time)			Individual (% Time)			Aggregate (% Time)		
	T1	T2	T3	T1	T2	T3	T1	T2	T3
0.08	69	82	85	17	9	6	14	9	9
0.15	0	0	0	39	1	38	61	99	62
0.22	0	0	0	73	50	12	27	50	88
0.30	0	0	0	88	60	86	12	40	14
0.37	0	0	0	N/A	N/A	92	N/A	N/A	8
0.45	0	0	0	N/A	N/A	N/A	N/A	N/A	N/A
0.52	0	0	0	N/A	N/A	N/A	N/A	N/A	N/A

Note:
Mode of transport
Int. = Intermittent Motion
1 = Continuous Rolling/Sliding/Brushing
2 = Mixture of Sliding/Brushing & Suspension
3 = Suspension

N/A - Not Applicable
A = Aggregate
I = Individual piece of alga

APPENDIX E

CHONDRUS ABUNDANCE VIDEO RESULTS

Low Abundance

Uy ($m\ s^{-1}$)	**Contact (%)**						**Mode of Transport**					
	Trial 1		**Trial 2**		**Trial 3**		**Trial 1**		**Trial 2**		**Trial 3**	
	A	***I***	***A***	***I***	***A***	***I***	***A***	***I***	***A***	***I***	***A***	***I***
0.08	100	N/A	100	100	100	100	1	N/A	Int.	Int.	1	1
0.15	100	100	100	100	100	100	1	1	1	1	1	1
0.22	88	72	100	91	100	92	2	2	1	2	1	2
0.30	72	34	N/A	72	64	32	2	2	N/A	2	2	2
0.37		5	N/A	5	0	0		2	N/A	2	3	3
0.45	0	0	0	0	0	0	3	3	3	3	3	3
0.52	0	0	0	0	0	0	3	3	3	3	3	3

Uy ($m\ s^{-1}$)	**No Movement (% Time)**			**Individual (% Time)**			**Aggregate (% Time)**		
	T1	**T2**	**T3**	**T1**	**T2**	**T3**	**T1**	**T2**	**T3**
0.08	0	32	2	0	6	6	100	62	92
0.15	0	0	0	55	67	47	45	33	50
0.22	0	0	0	83	79	80	17	21	21
0.30	0	0	0	88	100	79	12	0	21
0.37	0	0	0	99	100	N/A	1	0	N/A
0.45	0	0	0	N/A	N/A	N/A	N/A	N/A	N/A
0.52	0	0	0	N/A	N/A	N/A	N/A	N/A	N/A

Medium Abundance

Uy ($m\ s^{-1}$)	Contact (%)											
	Trial 1				**Trial 2**				**Trial 3**			
	1 pc	*2 pc*	*3 pc*	*4 pc*	*1 pc*	*2 pc*	*3 pc*	*4 pc*	*1 pc*	*2 pc*	*3 pc*	*4 pc*
0.08	100	100	100	100	100	100	N/A	100	100	100	100	100
0.15	84		100	100	100	100	100	100	100	100	100	100
0.22	45	78		N/A	74	95	100	100	100	100	100	100
0.30	14		N/A	N/A	41		N/A	N/A	44	95	100	N/A
0.37	0	0	0	0	0	0	0	0	0	0	0	0
0.45	0	0	0	0	0	0	0	0	0	0	0	0
0.52	0	0	0	0	0	0	0	0	0	0	0	0

Uy ($m\ s^{-1}$)	Mode of Transport											
	Trial 1				**Trial 2**				**Trial 3**			
	1 pc	*2 pc*	*3 pc*	*4 pc*	*1 pc*	*2 pc*	*3 pc*	*4 pc*	*1 pc*	*2 pc*	*3 pc*	*4 pc*
0.08	1	1	1	1	1	N/A	N/A	1	Int.	N/A	Int.	Int.
0.15	2	1	1	1	1	1	1	1	1	1	1	1
0.22	2	2		N/A	2	2	1	1	1	1	1	1
0.30	2		N/A	N/A	2	2	N/A	N/A	2	1	1	N/A
0.37	3	3	3	3	3	3	3	3	3	3	3	3
0.45	3	3	3	3	3	3	3	3	3	3	3	3
0.52	3	3	3	3	3	3	3	3	3	3	3	3

Uy ($m\ s^{-1}$)	No Movement (% time)			Individual (% time)			1 Clump of 2 pc (% time)			2 Clumps of 2 pc (% time)			1 Clump of 3 pc (% time)			1 Clump of 4 pc (% time)		
	T1	**T2**	**T3**	**T1**	**T2**	**T3**	**T1**	**T2**	**T3**	**T1**	**T2**	**T3**	**T1**	**T2**	**T3**	**T1**	**T2**	**T3**
0.08	0	0	50	2	5	5	10	1	4	3	0	0	9	0	11	75	94	30
0.15	0	0	0	25	21	10	34	35	31	9	11	13	19	27	30	14	6	16
0.22	0	0	0	67	39	11	30	25	57	1	7	4	2	22	21	0	8	7
0.30	0	0	0	97	92	57	3	8	33	0	0	3	0	0	6	0	0	0
0.37	0	0	0	N/A	N/A	N/A	N/A	N/A	N/A	N/A	N/A	N/A	N/A	N/A	N/A	N/A	N/A	N/A
0.45	0	0	0	N/A	N/A	N/A	N/A	N/A	N/A	N/A	N/A	N/A	N/A	N/A	N/A	N/A	N/A	N/A
0.52	0	0	0	N/A	N/A	N/A	N/A	N/A	N/A	N/A	N/A	N/A	N/A	N/A	N/A	N/A	N/A	N/A

High Abundance

Uy ($m\ s^{-1}$)	Contact (%)						Mode of Transport					
	Trial 1		Trial 2		Trial 3		Trial 1		Trial 2		Trial 3	
	A	*I*	*A*	*I*	*A*	*I*	*A*	*I*	*A*	*I*	*A*	*I*
0.08	100	100	100	100	100	100	NM		NM		NM	
0.15	100	100	100	100	100	100	1	1	1	1	1	1
0.22	100	80-90	100	80-90	100	80-90	1	2	1	2	1	2
0.30							2	3			2	2
0.37							3	3	2	3	3	3
0.45							3	3	3	3	3	3
0.52							3	3	3	3	3	3

Uy ($m\ s^{-1}$)	No Movement (% Time)			Aggregate < 3 (% Time)			Aggregate > 4 (% Time)		
	T1	T2	T3	T1	T2	T3	T1	T2	T3
0.08	100	100	100	0	0	0	100	0	0
0.15	0	0	0	57.8	26.8	66.8	42.3	73.2	33.3
0.22	0	0	0	83.3	31.4	83.3	16.8	68.6	16.7
0.30	0	0	0	76.7	N/A	~ 100	23.3	N/A	~0
0.37	0	0	0	N/A	N/A		N/A	N/A	
0.45	0	0	0	N/A	N/A		N/A	N/A	
0.52	0	0	0	N/A	N/A		N/A	N/A	

Note:

Mode of transport
NM = No Movement
Int. = Intermittent Motion
1 = Continuous Rolling/Sliding/Brushing
2 = Mixture of Sliding/Brushing & Suspension
3 = Suspension

N/A - Not Applicable
A = Aggregate
I = Individual piece of alga

APPENDIX F

FURCELLARIA SIZE VIDEO RESULTS

Small Size

Uy ($m\ s^{-1}$)	**Contact (%)**						**Mode of Transport**					
	Trial 1		**Trial 2**		**Trial 3**		**Trial 1**		**Trial 2**		**Trial 3**	
	A	***I***	***A***	***I***	***A***	***I***	***A***	***I***	***A***	***I***	***A***	***I***
0.08	N/A	100	100	100	N/A	100	N/A	Int.	Int.	Int.	N/A	Int.
0.15	100	100	100	N/A	100	100	1	1	1	N/A	1	1
0.22	100	83	100	84	100	86	1	1	1	1	1	1
0.30		34	66	55	84	81		1	2	2	1	2
0.37	N/A	16	54	19	58	42	N/A	1	2	2	2	2
0.45	0	0	42	18	N/A	29	3	3	2	2		2
0.52	0	0	0	0	N/A	10	3	3	3	3		2

Uy ($m\ s^{-1}$)	**No Movement (% Time)**			**Individual (% Time)**			**Aggregate (% Time)**		
	T1	**T2**	**T3**	**T1**	**T2**	**T3**	**T1**	**T2**	**T3**
0.08	89	49	34	6	42	66	0	10	0
0.15	0	0	0	12	0	24	88	100	76
0.22	0	0	0	56	48	64	44	52	36
0.30	0	0	0	86	85	65	14	15	35
0.37	0	0	0	100	93	91	0	7	9
0.45	0	0	0	N/A	83	95	N/A	9	5
0.52	0	0	0	N/A	N/A		N/A	N/A	

Medium Size - Note: the other 2 trials can be found under the Low Abundance Heading

Uy ($m\ s^{-1}$)	Contact (%)						Mode of Transport					
	Trial 1		Trial 2		Trial 3		Trial 1		Trial 2		Trial 3	
	A	*I*	*A*	*I*	*A*	*I*	*A*	*I*	*A*	*I*	*A*	*I*
0.08	100	100	100	100	N/A	100	Int.	Int.	Int.	Int.	N/A	Int.
0.15	100	100	100	100	100	N/A	1	1	1	1	1	N/A
0.22	100	100	100	100	100	N/A	1	1	1	1	1	N/A
0.30	100	80	100	100	100	95	1	1	1	1	1	1
0.37	76	36	86	51	100	72	2	2	2	2	1	2
0.45	0	0		20	70	61	3	3		2	2	2
0.52	0	0	N/A	10	44	24	3	3	N/A	2	2	2

Uy ($m\ s^{-1}$)	No Movement (% Time)			Individual (% Time)			Aggregate (% Time)		
	T1	T2	T3	T1	T2	T3	T1	T2	T3
0.08	38	84	86	11	8	14	51	8	0
0.15	0	0	0	9	16	0	91	84	100
0.22	0	0	0	32	7	0	69	93	100
0.30	0	0	0	61	16	49	39	84	51
0.37	0	0	0	88	74	71	12	26	29
0.45	0	0	0	N/A	99	69	N/A	1	31
0.52	0	0	0	N/A	100	77	N/A	0	23

Large Size

Uy ($m\ s^{-1}$)	Contact (%)						Mode of Transport					
	Trial 1		Trial 2		Trial 3		Trial 1		Trial 2		Trial 3	
	A	*I*	*A*	*I*	*A*	*I*	*A*	*I*	*A*	*I*	*A*	*I*
0.08	100	100	100	100		100	NM		NM			1
0.15	100	100	100	N/A	100	100	1	1	1	N/A	1	1
0.22	100	100	100	100	100	100	1	1	1	1	1	1
0.30	100	100	100	100	100	89	1	1	1	1	1	1
0.37	72	62	100	74	38	30	2	2	1	2	2	2
0.45	74	54	40	25		15	2	2	2	2	2	2
0.52	30	32	N/A	17	N/A	0	2	2	N/A	2	N/A	

Uy ($m\ s^{-1}$)	No Movement (% Time)			Individual (% Time)			Aggregate (% Time)		
	T1	T2	T3	T1	T2	T3	T1	T2	T3
0.08	100	100	4	0	0	100	100	100	0
0.15	0	0	0	4	0	5	96	100	95
0.22	0	0	0	8	34	6	92	66	94
0.30	0	0	0	39	59	34	61	41	66
0.37	0	0	0	44	7	67	56	93	33
0.45	0	0	0	58	93	95	42	8	5
0.52	0	0	0	77	100	100	23	0	0

Note:
Mode of transport
NM = No Movement
Int. = Intermittent Motion
1 = Continuous Rolling/Sliding/Brushing
2 = Mixture of Sliding/Brushing & Suspension
3 = Suspension

N/A - Not Applicable
A = Aggregate
I = Individual piece of alga

APPENDIX G

FURCELLARIA ABUNDANCE VIDEO RESULTS

Low Abundance

Uy ($m\ s^{-1}$)	**Contact (%)**				**Mode of Transport**				**No Movement (% Time)**		**Individual (% Time)**		**Aggregate (% Time)**	
	Trial 1		**Trial 2**		**Trial 1**		**Trial 2**		**T1**	**T2**	**T1**	**T2**	**T1**	**T2**
	A	***I***	***A***	***I***	***A***	***I***	***A***	***I***						
0.08	100	100	100	100	NM		Int.	Int.	100	80	0	19	100	6
0.15	100	100	100	100	1	1	1	1	0	0	14	5	86	96
0.22	100	100	100	N/A	1	1	1	N/A	0	0	8	0	92	100
0.30	100	81	100	65	1	2	2	1	0	0	36	21	64	79
0.37	100	59	73	52	1	2	2	2	0	0	59	44	41	56
0.45	44	32	70	32	2	2	2	2	0	0	77	65	23	35
0.52	N/A	13		19	N/A	2		2	0	0	100	98	0	2

Medium Abundance

Uy ($m\ s^{-1}$)	Contact (%)								Mode of Transport							
	Trial 1		Trial 2		Trial 3		Trial 4		Trial 1		Trial 2		Trial 3		Trial 4	
	A	I	A	I	A	I	A	I	A	I	A	I	A	I	A	I
0.08	100	100	100	100	100	100	100	100	NM		NM		NM		NM	
0.15	100	100	100	100	100	100	100	100	1	1	1	1	1		1	1
0.22	100	100	100	100	100	100	100	100	1	1	1	1	1	1	1	1
0.30	100	100	<100		100	N/A	100	100	1	1	1	2	1		1	
0.37	100			~ 50	100	~80	100	100	1	N/A	2	2	1	1	2	2
0.45	< 100	< 80							1	2	2	2	2	2	2	2
0.52									2	2	2	2	2	2	2	2

Uy ($m\ s^{-1}$)	No Movement (% Time)				Aggregate ≤ 3 pieces (% Time)				Aggregate ≥ 4 pieces (% Time)			
	T1	T2	T3	T4	T1	T2	T3	T4	T1	T2	T3	T4
0.08	100	100	100	100	0	0	0	0	100	100	100	0
0.15	0	0	0	0	13	3	5	17	88	97	95	83
0.22	0	0	0	0	70	86	16	5	30	14	84	95
0.30	0	0	0	0	33	33	2	86	67	67	98	14
0.37	0	0	0	0		6	32	90		94	68	10
0.45	0	0	0	0								
0.52	0	0	0	0								

High Abundance

Uy ($m\ s^{-1}$)	Contact (%)						Mode of Transport					
	Trial 1		Trial 2		Trial 3		Trial 1		Trial 2		Trial 3	
	A	I	A	I	A	I	A	I	A	I	A	I
0.08	100	100	100	100	100	100	NM		NM		NM	
0.15	100	100	100	N/A	100	100	1		1		1	1
0.22	100	100	100	< 100	100	100	1		1	1	1	1
0.30	100	<100	80-100	~ 80	100	<100	1	1	1	2	1	2
0.37	<100	<70	< 80		<100	<100	1	2	2	2	1	2
0.45							2	2	2	2	2	2
0.52							2	2	2	2	2	2

Uy ($m\ s^{-1}$)	No Movement (% Time)			Aggregate < 3 pieces (% Time)			Aggregate > 4 pieces (% Time)		
	T1	T2	T3	T1	T2	T3	T1	T2	T3
0.08	100	100	100	0	0	0	100	100	100
0.15	0	0	0	15	0	5	85	100	95
0.22	0	0	0	6	21	13	95	79	87
0.30	0	0	0	18	46	43	83	54	57
0.37	0	0	0	65	72		35	28	
0.45	0	0	0	94			7		
0.52	0	0	0						

Note:
Mode of transport
NM = No Movement
Int. = Intermittent Motion
1 = Continuous Rolling/Sliding/Brushing
2 = Mixture of Sliding/Brushing & Suspension
3 = Suspension

N/A - Not Applicable
A = Aggregate
I = Individual piece of alga

APPENDIX H
EXPANDED SCALE OF 4 CONTROL TRIALS AND RESPECTIVE SSC FROM FILTER SAMPLES

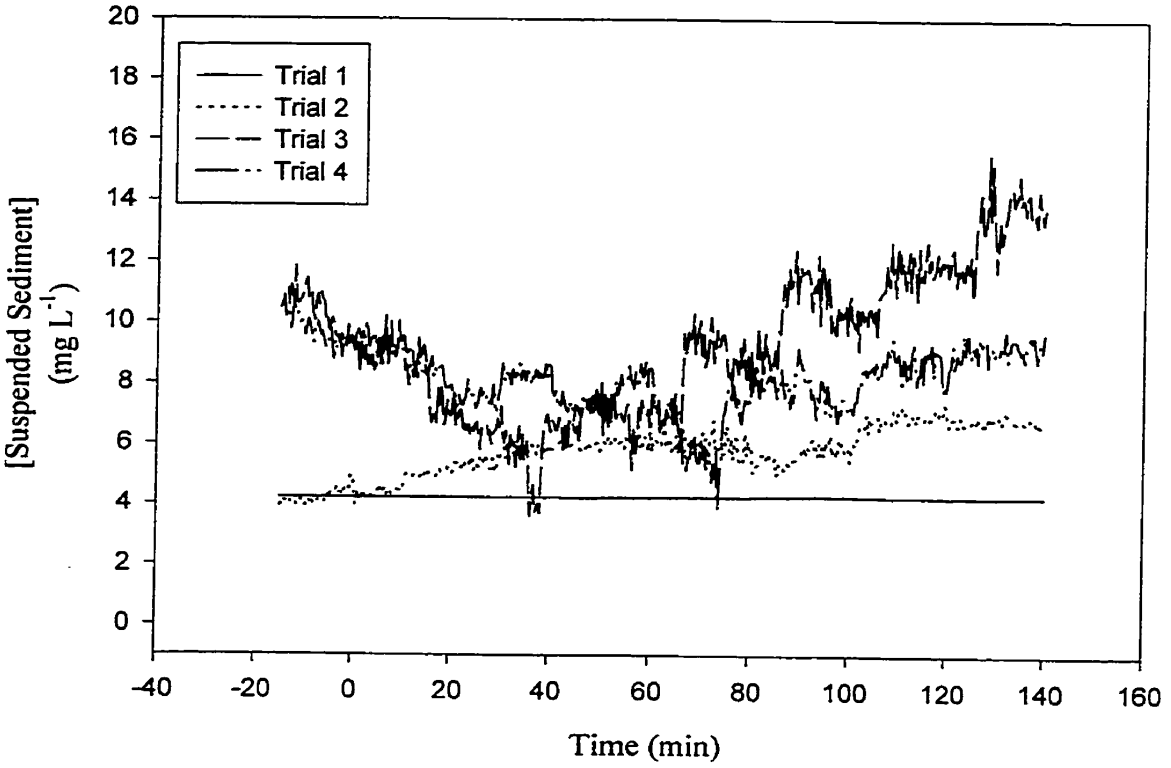

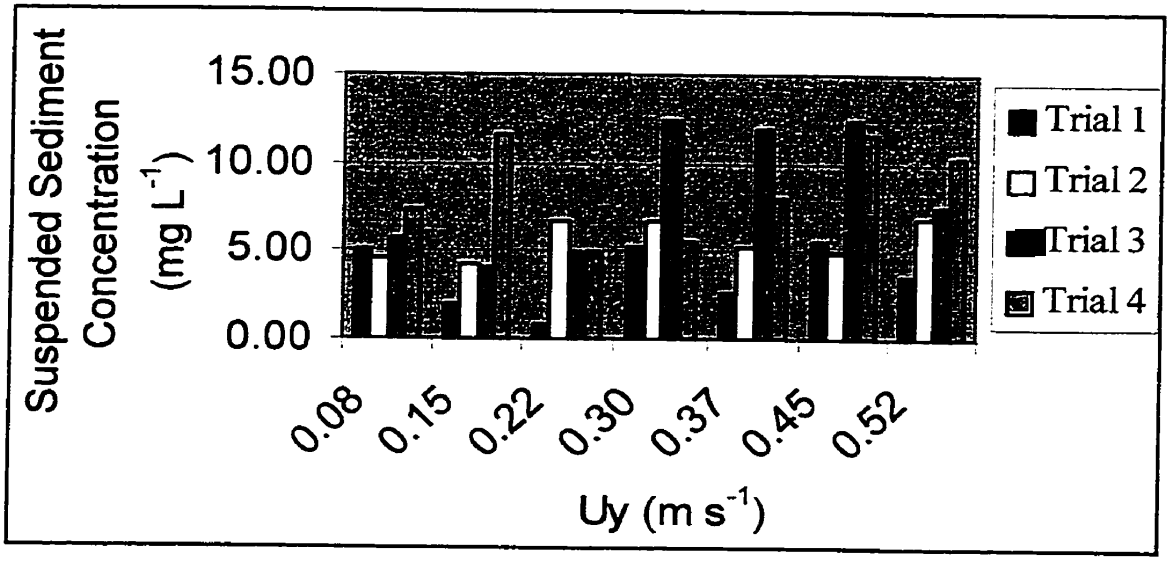

APPENDIX I
CRITICAL EROSION THRESHOLDS

Controls

TRIAL	$U_{y\,crit}$	$U_{*\,crit}$	τ_{crit}
1	7.4×10^{-81}	1.0×10^{-81}	0.0
2	6.2×10^{-4}	8.8×10^{-5}	7.8×10^{-6}
3	0.045	6.4×10^{-3}	0.042
4	Before motor was started	N/A	N/A

Chondrus Small Size

TRIAL	$U_{y\,crit}$	$U_{*\,crit}$	τ_{crit}
1	0.13	0.018	0.34
2	0.077	0.011	0.12
3	0.12	0.016	0.27

Chondrus Medium Size/Low Abundance

TRIAL	$U_{y\,crit}$	$U_{*\,crit}$	τ_{crit}
1	0.11	0.016	0.25
2	0.13	0.019	0.35
3	0.15	0.021	0.45
4	0.11	0.016	0.26
5	0.14	0.020	0.39
6	0.12	0.017	0.30

Chondrus Large Size

TRIAL	$U_{y\,crit}$	$U_{*\,crit}$	τ_{crit}
1	0.14	0.020	0.39
2	0.14	0.20	0.39
3	0.16	0.022	0.51

Chondrus Medium Abundance

TRIAL	$U_{y\,crit}$	$U_{*\,crit}$	τ_{crit}
1	0.10	0.014	0.20
2	0.12	0.017	0.28
3	0.14	0.019	0.38

Chondrus High Abundance

TRIAL	$U_{y\,crit}$	$U_{*\,crit}$	τ_{crit}
1	0.15	0.020	0.43
2	0.14	0.020	0.42
3	0.14	0.020	0.39

Furcellaria Small Size

TRIAL	$U_{y\,crit}$	$U_{*\,crit}$	τ_{crit}
1	0.16	0.022	0.49
2	0.14	0.020	0.40
3	0.16	0.022	0.51

Furcellaria Medium Size/Low Abundance

TRIAL	$U_{y\,crit}$	$U_{*\,crit}$	τ_{crit}
1	0.14	0.019	0.37
2	0.13	0.019	0.37
3	0.17	0.024	0.57
4	0.15	0.021	0.43
5	0.15	0.022	0.48

Furcellaria Large Size

TRIAL	$U_{y\,crit}$	$U_{*\,crit}$	τ_{crit}
1	0.15	0.021	0.44
2	0.13	0.018	0.34
3	0.14	0.020	0.40

Furcellaria Medium Abundance

TRIAL	$U_{y\,crit}$	$U_{*\,crit}$	τ_{crit}
1	0.14	0.020	0.41
2	0.16	0.023	0.52
3	0.15	0.022	0.48

Furcellaria High Abundance

TRIAL	$U_{y\,crit}$	$U_{*\,crit}$	τ_{crit}
1	0.15	0.020	0.43
2	0.14	0.019	0.38
3	0.14	0.019	0.38

APPPENDIX J
CHONDRUS T-RATIOS AND T* VALUES

High Density Bonferroni Critical Value = approximately 2.42

	Slope	Standard Error	T-Ratio
Trial 1	7.89804	0.49838	15.85
Trial 2	9.79367	0.58099	16.86
Trial 3	3.18089	0.28447	11.18

Bonferroni Critical Value = approx. 2.42

t*	Trial 1	Trial 2	Trial 3
Trial 1	0	2.47645	8.22015
Trial 2	2.47645	0	10.22234
Trial 3	8.22015	10.22234	0

Medium Density Bonferroni Critical Value = approx. 2.42

	Slope	Standard Error	T-Ratio
Trial 1	0.86617	0.05095	17.00
Trial 2	1.15785	0.03153	36.72
Trial 3	3.10370	0.24123	12.87

Bonferroni Critical Value = approx. 2.42

t*	Trial 1	Trial 2	Trial 3
Trial 1	0	4.86807	9.07529
Trial 2	4.86807	0	7.99834
Trial 3	9.07529	7.99834	0

Low Density/Medium Size Bonferroni Critical Value = approx. 2.98

	Slope	Standard Error	T-Ratio
Trial 1	0.60388	0.05512	10.96
Trial 2	0.91469	0.02586	35.37
Trial 3	1.57363	0.13739	11.45
Trial 4	1.22165	0.06919	17.66
Trial 5	1.97446	0.06861	28.78
Trial 6	1.39741	0.06162	22.68

Bonferroni Critical Value = approx. 2.98

t*	Trial 1	Trial 2	Trial 3	Trial 4	Trial 5	Trial 6
Trial 1	0	5.10489	6.55084	6.98348	15.57322	9.59813
Trial 2	5.10489	0	4.71336	4.15571	14.45370	7.22350
Trial 3	6.55084	4.71336	0	2.28813	2.61010	1.17031
Trial 4	6.98348	4.15571	2.28813	0	7.72587	1.89700
Trial 5	15.57322	14.45370	2.61010	7.72587	0	6.25738
Trial 6	9.59813	7.22350	1.17031	1.89700	6.25738	0

Small Size Bonferroni Critical Value = approx. 2.42

	Slope	Standard Error	T-Ratio
Trial 1	0.35906	0.0044417	80.84
Trial 2	0.58477	0.06309	9.27
Trial 3	0.51828	0.01882	27.54

Bonferroni Critical Value = approx. 2.42

t*	Trial 1	Trial 2	Trial 3
Trial 1	0	3.56875	8.23394
Trial 2	3.56875	0	4.80208
Trial 3	8.23394	4.80208	0

Large Size Bonferroni Critical Value = approx. 2.42

	Slope	Standard Error	T-Ratio
Trial 1	1.82478	0.07915	23.05
Trial 2	2.17488	0.07470	29.12
Trial 3	4.37949	0.67164	6.52

Bonferroni Critical Value = approx. 2.42

t*	Trial 1	Trial 2	Trial 3
Trial 1	0	3.21683	3.77755
Trial 2	3.21683	0	3.26231
Trial 3	3.77755	3.26231	0

APPENDIX K
FURCELLARIA T-RATIOS AND T* VALUES

High Density Bonferroni Critical Value = approximately 2.42

	Slope	Standard Error	T-Ratio
Trial 1	2.61432	0.06289	41.57
Trial 2	2.94269	0.06477	45.43
Trial 3	3.26788	0.21271	15.36

Bonferroni Critical Value = approx. 2.42

t*	Trial 1	Trial 2	Trial 3
Trial 1	0	3.6373	2.9465
Trial 2	3.6373	0	1.4625
Trial 3	2.9465	1.4625	0

Medium Density Bonferroni Critical Value = approx. 2.67

	Slope	Standard Error	T-Ratio
Trial 1	3.70311	0.24415	15.17
Trial 2	1.32285	0.06519	20.29
Trial 3	3.71135	0.15579	23.82
Trial 4	1.68762	0.05815	29.02

Bonferroni Critical Value = approx. 2.67

t*	Trial 1	Trial 2	Trial 3	Trial 4
Trial 1	0	9.4192	0.02845	8.0305
Trial 2	9.4192	0	14.1432	4.1756
Trial 3	0.02845	14.1432	0	12.1610
Trial 4	8.0305	4.1756	12.1610	0

Low Density/Medium Size Bonferroni Critical Value = approx. 2.84

	Slope	Standard Error	T-Ratio
Trial 1	0.46789	0.02450	19.10
Trial 2	0.70100	0.06522	10.75
Trial 3	1.53995	0.17783	8.66
Trial 4	0.99271	0.04658	21.31
Trial 5	1.44573	0.07178	20.14

Bonferroni Critical Value = approx. 2.84

t*	Trial 1	Trial 2	Trial 3	Trial 4	Trial 5
Trial 1	0	3.3459	5.9722	9.9718	12.8924
Trial 2	3.3459	0	4.4292	3.6397	7.6788
Trial 3	5.9722	4.4292	0	2.9769	0.4913
Trial 4	9.9718	3.6397	2.9769	0	5.2942
Trial 5	12.8924	7.6788	0.4913	5.2942	0

Small Size Bonferroni Critical Value = approx. 2.42

	Slope	Standard Error	T-Ratio
Trial 1	0.24071	0.0083245	28.92
Trial 2	0.26417	0.0077073	34.28
Trial 3	0.51028	0.01199	42.56

Bonferroni Critical Value = approx. 2.42

t*	Trial 1	Trial 2	Trial 3
Trial 1	0	2.0679	18.4681
Trial 2	2.0679	0	17.2666
Trial 3	18.4681	17.2666	0

Large Size Bonferroni Critical Value = approx. 2.42

	Slope	Standard Error	T-Ratio
Trial 1	4.94159	0.21550	22.93
Trial 2	1.55650	0.12242	12.71
Trial 3	1.55179	0.23607	6.57

Bonferroni Critical Value = approx. 2.42

t*	Trial 1	Trial 2	Trial 3
Trial 1	0	13.6581	10.6051
Trial 2	13.6581	0	0.01771
Trial 3	0.01771	0.01771	0

APPENDIX L
2-WAY ANOVA COMPARISON RESULTS FOR THE AVERAGE EROSION RATES OF THE *CHONDRUS* AND *FURCELLARIA* TREATMENTS

Chondrus Size

Comparison	**P-value**
All sizes	0.034
Small vs. medium	0.063
Medium vs. large	0.089
Small vs. large	0.073

Chondrus Abundance

Comparison	**P-value**
All abundances	0.028
Low vs. medium abundance	0.213
Medium vs. high abundance	0.069
Low vs. high abundance	0.069

Furcellaria Size

Comparison	**P-value**
All sizes	0.001
Small vs. medium	0.004
Medium vs. large	0.013
Small vs. large	0.008

Furcellaria Abundance

Comparison	**P-value**
All abundances	0.001
Low vs. medium abundance	0.009
Medium vs. high abundance	0.151
Low vs. high abundance	0.009

APPENDIX M
1-WAY ANOVA COMPARISON RESULTS FOR FINIAL SSC, OVERALL SLOPE AND TAU_{CRIT} FOR THE *CHONDRUS* AND *FURCELLARIA* TREATMENTS

Chondrus Size

	Comparison	**P-value**
Final SSC	All sizes	0.037
Final SSC	Small vs. medium size	0.086
Final SSC	Medium vs. large size	0.072
Final SSC	Small vs. large size	0.085
Overall Slope	All sizes	0.012
Overall Slope	Small vs. medium size	0.030
Overall Slope	Medium vs. large size	0.039
Overall Slope	Small vs. large size	0.045
Tau_{crit}	All sizes	0.071
Tau_{crit}	Small vs. medium size	0.197
Tau_{crit}	Medium vs. large size	0.114
Tau_{crit}	Small vs. large size	0.071

Chondrus Abundance

	Comparison	**P-value**
Final SSC	All abundances	0.005
Final SSC	Low vs. medium abundance	0.508
Final SSC	Medium vs. high abundance	0.073
Final SSC	Low vs. high abundance	0.005
Overall Slope	All abundances	0.003
Overall Slope	Low vs. medium abundance	0.457
Overall Slope	Medium vs. high abundance	0.066
Overall Slope	Low vs. high abundance	0.004
Tau_{crit}	All abundances	0.151
Tau_{crit}	Low vs. medium abundance	0.446
Tau_{crit}	Medium vs. high abundance	0.077
Tau_{crit}	Low vs. high abundance	0.135

Furcellaria Size

	Comparison	P-value
Final SSC	All sizes	0.082
Final SSC	Small vs. medium size	0.074
Final SSC	Medium vs. large size	0.137
Final SSC	Small vs. large size	0.127
Overall Slope	All sizes	0.058
Overall Slope	Small vs. medium size	0.051
Overall Slope	Medium vs. large size	0.106
Overall Slope	Small vs. large size	0.107
Tau_{crit}	All sizes	0.430
Tau_{crit}	Small vs. medium size	0.627
Tau_{crit}	Medium vs. large size	0.389
Tau_{crit}	Small vs. large size	0.173

Furcellaria Abundance

	Comparison	P-value
Final SSC	All abundances	0.018
Final SSC	Low vs. medium abundance	0.035
Final SSC	Medium vs. high abundance	0.734
Final SSC	Low vs. high abundance	0.001
Overall Slope	All abundances	0.017
Overall Slope	Low vs. medium abundance	0.036
Overall Slope	Medium vs. high abundance	0.683
Overall Slope	Low vs. high abundance	0.001
Tau_{crit}	All abundances	0.573
Tau_{crit}	Low vs. medium abundance	0.709
Tau_{crit}	Medium vs. high abundance	0.208
Tau_{crit}	Low vs. high abundance	0.520